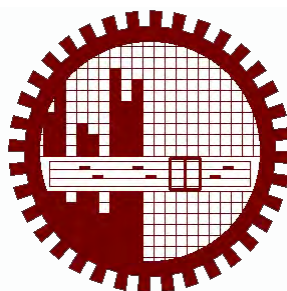


**DEVELOPMENT AND VALIDATION OF A DUAL FILTRATION
TECHNIQUE TO CONTROL THE SIZE DISTRIBUTION OF GIANT
LIPID VESICLES**

by

Tawfika Nasrin

MASTER OF PHILOSOPHY IN PHYSICS



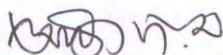
Department of Physics

BANGLADESH UNIVERSITY OF ENGINEERING AND TECHNOLOGY

December, 2021


The thesis titled “DEVELOPMENT AND VALIDATION OF A DUAL FILTRATION TECHNIQUE TO CONTROL THE SIZE DISTRIBUTION OF GIANT LIPID VESICLES” submitted by Tawfika Nasrin, Roll No. 0419143001F, Session: April/2019, has been accepted as satisfactory in partial fulfillment of the requirement for the degree of MASTER OF PHILOSOPHY IN PHYSICS on 18 December, 2021.

BOARD OF EXAMINERS



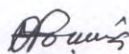
Dr. Mohammad Abu Sayem Karal
(Supervisor)
Professor
Department of Physics, BUET, Dhaka

Chairman



Dr. Md. Rafi Uddin
Professor and Head
Department of Physics, BUET, Dhaka-1000

Member (Ex-Officio)



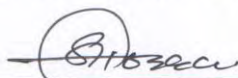
Dr. Md. Forhad Mina
Professor
Department of Physics, BUET, Dhaka-1000

Member



Dr. Mohammad Khurshed Alam
Associate Professor
Department of Physics, BUET, Dhaka-1000

Member

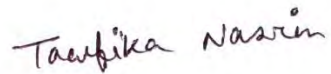


Dr. Khandker Saadat Hossain
Professor
Department of Physics
University of Dhaka, Dhaka-1000

Member (External)

CANDIDATE'S DECLARATION

It is hereby declared that this thesis or any part of it has not been submitted elsewhere for the award of any degree or diploma.



Tawfika Nasrin

Tawfika Nasrin

Roll No. 0419143001

Session: April, 2019

Dedicated
To
My Beloved Parents
And Teachers

Acknowledgement

Firstly, I would like to convey my utmost appreciation to my respected supervisor Professor Dr. Mohammad Abu Sayem Karal, Department of Physics, Bangladesh University of Engineering and Technology (BUET), Dhaka for giving me the chance for doing research on membrane biophysics. His constant encouragement inspired me to be a better researcher and hard-working person. It was a great experience to be a part of his research team.

I convey my gratitude to Professor Dr. Md. Rafi Uddin, Head of the Department of Physics, BUET for his great support to move through the academic course during this degree program. I am thankful to all other respected teachers of the Department of Physics for their kind co-operation.

I acknowledge all my lab mates, especially Marzuk Ahmed, Shareef Ahammed, Md. Kabir Ahamed, Nadia Akter Mokta, Sabrina Sharmin, Malay Kumar Sarkar, Salma Akter, Sharif Hasan, Urbi Shyamolima Orchi and Md. Towhiduzzaman for their continuous encouragement and support.

I am also thankful to the authority of the Department of Physics, BUET for providing me the logistic supports for this thesis work. Sincere acknowledgement to the CASR, BUET for granting funds to carry out this research.

Finally, I would like to express my appreciation to my beloved parents and family members who always supported and encouraged me in my work and inspired me to do my best.

Abstract

A new purification technique is developed for obtaining the distribution of giant unilamellar vesicles (GUVs) within a specific range of sizes using dual filtration. The GUVs were prepared using the natural swelling method. For filtration, different combinations of polycarbonate membranes were utilized in filter holders. In this experiment, the combinations of membranes were selected with three pairs of pore sizes, such as, (i) 12 and 10 μm , (ii) 12 and 8 μm , and (iii) 10 and 8 μm . By these filtration arrangements, obtained GUVs size distributions were in the ranges of 6–26 μm , 5–38 μm , and 5–30 μm , respectively. The size distribution range for the dual filtration technique was found lower, the mode was smaller, and also the skewness became smaller (narrow size distribution) than for the single filtration technique. By continuing this process of purification for a second time, the GUVs size distribution became even narrower. After using an extra filtration with dual filtration, two different size distributions of GUVs were obtained at a time. This experimental observation suggests that different specific size distributions of GUVs can be obtained easily, even if GUVs are prepared by different other methods. Using this technique, the water-soluble fluorescent probe, calcein, has been removed from the suspension of GUVs successfully.

Contents

Abstract	vi
Contents	vii
List of Figures	x
List of Tables	xvii
List of Symbols and Abbreviation	xviii

CHAPTER 1

INTRODUCTION 1-5

1.1 Background	1
1.2 Aims and Objectives	4
1.3 Outline of Thesis	5

CHAPTER 2

LITERATURE REVIEW AND THEORETICAL ASPECTS 6-26

2.1 Literature Review	6
2.2 Applications of Purified GUVs	22
2.3 Lipid Bilayer and Vesicles	24

CHAPTER 3

MATERIALS AND METHOD **27-39**

3.1 Materials	27
3.2 Instruments Used for the Synthesis and Observation of GUVs	27
3.3 Synthesis of Lipid Membranes of GUVs	27
3.4 Dual Filtration Technique for the Purification of GUVs	28
3.5 Accessories for Dual Filtration Technique	30
3.6 Dual Filtration Technique	32
3.7 Collection of purified GUV suspension	35
3.8 Single Filtration Technique	36
3.9 Purification of GUVs Using an Extra Filtration with Dual Filtration	37
3.10 Observations of GUV	37
3.11 Statistical Analysis using Lognormal Distribution	39

CHAPTER 4

RESULTS AND DISCUSSION **40-69**

4.1 Dual Filtration with a Combination of 12 and 10 μm Pores Polycarbonate Membranes	40
4.2 Single Filtration with 12 μm Pores Polycarbonate Membrane	47
4.3 Single Filtration with 10 μm Pores Polycarbonate Membrane	50
4.4 Dual Filtration with the Combinations of 12 and 8 μm , and 10 and 8 μm Pores Polycarbonate Membranes	53

4.5 Purification of GUVs Containing Water-Soluble Fluorescent Probe, Calcein, Using Dual Filtration Technique	57
4.6 Effects of Flow Rate on the Average Size of GUVs in Dual Filtration Technique	60
4.7 Fraction of Required Sizes GUVs in Filter Holder 2 Compared to the Total Number of GUVs Before Filtration	61
4.8 Effects of Repeating Dual Filtration on The Size Distribution of GUVs	62
4.9 Purification of GUVs Using an Extra Filtration with Dual Filtration	66

CHAPTER 5

70-72

CONCLUSIONS

Conclusions	70
References	73-82

APPENDIX

Published Journal	83-84
-------------------	-------

List of Figures

Fig. 2.1 Simplified illustration of the main ideas of the different processes for the preparation of GUVs. 7

Fig. 2.2 (A) The equipment for the membrane filtering method. (B) The equipment for the membrane filtering method added a stopcock. 10

Fig. 2.3 Phase-contrast images and size distribution histograms of GUV suspension in different conditions. The bars in the images correspond to 50 μm . 11

Fig. 2.4 An experimental system of non-electromechanical technique to purify GUVs. 12

Fig. 2.5 (A), (B) represents the phase contrast image and size distribution histogram before purification, and (C), (D) shows the phase contrast image and size distribution histogram after purification. Purification was performed for 45 minutes with a flow rate of 1.5 mL/min. The bar in the image is correspondent to 30 μm . 13

Fig. 2.6 (A) shows the phase contrast image and (B) shows the size distribution histogram of GUVs solution after the first purification. (C) shows the phase contrast image and (D) shows the size distribution histogram of GUVs solution after the second purification. Both purifications were performed for 45 minutes with a flow rate of 2 mL/min. The bar in images correspondence to 30 μm . 14

Fig. 2.7 Effects of filtration on the distribution of the size of GUVs incorporating different X at $C = 162 \text{ mM}$. 16

Fig. 2.8 Effects of filtration on the distribution of the size of GUVs incorporating different C at $X = 0.40$. 17

- Fig. 2.9** Schematic representation of purification of giant vesicles by 18
microfiltration.
- Fig. 2.10** Confocal images of GVs (a, b) and size distribution of the population 19
(c).
- Fig. 2.11** Schematic diagram of vesicle extrusion-dialysis. 20
- Fig. 2.12** For oleate vesicles (A) and (B) show a phase-contrast image of 21
vesicles and size distribution histogram after extrusion. (C) and (D) show the
phase contrast image and size distribution of extruded vesicles that are gone
through dialysis.
- Fig. 2.13** Effect of agarose gel electrophoresis on bovine brain coated vesicles. 22
- Fig. 2.14** Lipid molecule and molecular structure of lipids. 25
- Fig. 2.15** (a) Lipid bilayer (3D view), (b) schematic diagram of lipid bilayer (2D) 25
view.
- Fig. 3.1** Schematic diagram of Dual Filtration Technique. 29
- Fig. 3.2** Polypropylene syringes. 30
- Fig. 3.3** Pipe for buffer flow. 30
- Fig. 3.4** Different types of fittings. 31
- Fig. 3.5** Polypropylene filter holder. 31
- Fig. 3.6** Filter paper. 31

Fig. 3.7 Stop cock.	32
Fig. 3.8 Peristaltic pump.	32
Fig. 3.9 Experimental set-up of dual filtration technique.	33
Fig. 3.10 A schematic representation of experimental set-up of dual filtration technique.	35
Fig. 3.11 A step-wise schematic representation of collecting the purified GUV suspension from the space under the filter holders.	35
Fig. 3.12 Experimental set-up of single filtration technique.	36
Fig. 3.13 Experimental set-up of dual filtration with using an extra filtration.	37
Fig. 3.14 GUV suspension in handmade microchamber.	38
Fig. 3.15 Inverted phase contrast fluorescence microscope.	38
Fig. 3.16 Lognormal and normal distributions.	39
Fig. 4.1 Effects of dual filtration with 12 and 10 μm (case i) pores polycarbonate membranes on the size and distribution of 40%DOPG/60%DOPC-GUVs in the first independent experiment. The purification was performed at a flow rate of 1 mL/min for 1 h. (A), (C), and (E) show the phase-contrast image of unpurified GUVs, GUVs obtained from filter holder 1, and GUVs obtained under filter holder 2 respectively. (B), (D), and (F) represent the corresponding size distribution histograms of (A), (C), and (E) respectively. The bar in the images (A, C, E) corresponds to a length of 50 μm . The solid line of (B), (D) and (F)	43

corresponds to fitting with Eq 4.1.

Fig. 4.2 Effects of dual filtration with 12 and 10 μm (case i) pores polycarbonate membranes on the size and distribution of 40%DOPG/60%DOPC-GUVs in the second independent experiment. The purification was performed at a flow rate of 1 mL/min for 1 h. (A), (C), and (E) show the phase-contrast image of unpurified GUVs, GUVs obtained from filter holder 1, and GUVs obtained under filter holder 2 respectively. (B), (D), and (F) represent the corresponding size distribution histograms of (A), (C), and (E) respectively. The bar in the images (A, C, E) corresponds to a length of 30 μm . The solid line of (B), (D) and (F) corresponds to fitting with Eq 4.1. 45

Fig. 4.3 Effects of single filtration (using 12 μm pores polycarbonate membrane filter paper) on the size distribution of 40%DOPG/60%DOPC-GUVs in the first independent experiment. (A), (B) represents the size distribution histogram for the unpurified and purified GUVs respectively. The purification was performed at a flow rate of 1 mL/min for 1 h. The solid line of figures corresponds to fitting with Eq 4.1. 48

Fig. 4.4 Effects of single filtration (using 12 μm pores polycarbonate membrane filter paper) on the size distribution of 40%DOPG/60%DOPC-GUVs in the second independent experiment. (A), (B) represents the size distribution histogram for the unpurified and purified GUVs respectively. The purification was performed at a flow rate of 1 mL/min for 1 h. 49

Fig. 4.5 Effects of single filtration (using 10 μm pores polycarbonate membrane filter paper) on the size distribution of 40%DOPG/60%DOPC-GUVs in the first independent experiment. (A), (B) represents the size distribution histogram for the unpurified and purified GUVs respectively. The purification was performed at a flow rate of 1 mL/min for 1 h. 51

Fig. 4.6 Effects of single filtration (using 10 μm pores polycarbonate membrane filter paper) on the size distribution of 40%DOPG/60%DOPC-GUVs in the second independent experiment. (A), (B) represents the size distribution histogram for the unpurified and purified GUVs respectively. The purification was performed at a flow rate of 1 mL/min for 1 h. 52

Fig. 4.7 Effects of dual filtration with 12 and 8 μm (case ii), and 10 and 8 μm (case iii) pores polycarbonate membranes on the size and distribution of 40%DOPG/60%DOPC-GUVs in the first independent experiment. The purification was performed at a flow rate of 1 mL/min for 1 h. (A), (B) represents the phase-contrast image and corresponding size distribution histogram under filter holder 2 respectively for case (ii), and (C), (D) represents the phase-contrast image and corresponding size distribution histogram under filter holder 2 respectively for case (iii). The bar in the images (A, C) corresponds to a length of 50 μm . 54

Fig. 4.8 Effects of dual filtration with 12 and 8 μm (case ii), and 10 and 8 μm (case iii) pores polycarbonate membranes on the size and distribution of 40%DOPG/60%DOPC-GUVs in the second independent experiment. (A), (B) represents the phase-contrast image and corresponding size distribution histogram under filter holder 2 respectively for case (ii), and (C), (D) represents the phase-contrast image and corresponding size distribution histogram under filter holder 2 respectively for case (iii). The purification was performed at a flow rate of 1 mL/min for 1 h. The bar in the images (A, C) corresponds to a length of 30 μm . 55

Fig. 4.9 Purification of 40%DOPG/60%DOPC-GUVs containing calcein using the dual filtration technique in the first independent experiment. The purification was performed at a flow rate of 1 mL/min for 1 h. (A) and (B) represents the unpurified and purified GUV suspensions respectively. (C), (D) represents the phase-contrast images of unpurified and purified (collected under filter holder 2) GUVs respectively, and (E) represents the size distribution histograms of purified 58

GUVs. The bar in the images (C, D) corresponds to a length of 50 μm .

Fig. 4.10 Purification of 40%DOPG/60%DOPC-GUVs containing calcein using the dual filtration technique in the second independent experiment. The purification was performed at a flow rate of 1 mL/min for 1 h. (A) represents the phase-contrast image of purified GUVs and (B) represents the corresponding size distribution histogram. The bar in the image (A) corresponds to a length of 30 μm .

Fig. 4.11 Flow rate dependent average size of purified 40%DOPG/60%DOPC-GUVs using dual filtration technique. The average values and standard deviations for different flow rates were calculated for 3-4 independent experiments.

Fig. 4.12 Effects of repeated purification on the 40%DOPG/60% DOPC-GUVs (for case (i), first independent experiment). The purification was performed at a flow rate of 1 mL/min for 1 h. (A) and (B) represent the phase contrast image and the corresponding size distribution histogram of GUVs in filter holder 2 after the first purification. (C) and (D) represent the phase contrast image and the corresponding size distribution histogram of GUVs in filter holder 2 after the second purification. The bar in the images (A, C) corresponds to a length of 50 μm .

Fig. 4.13 Effects of repeated purification on the 40%DOPG/60% DOPC-GUVs (for case (i), second independent experiment). The purification was performed at a flow rate of 1 mL/min for 1 h. (A) and (B) represent the phase contrast image and the corresponding size distribution histogram of GUVs in filter holder 2 after the first purification. (C) and (D) show the phase contrast image and the corresponding size distribution histogram of GUVs in filter holder 2 after the second purification. The bar in the images (A, C) corresponds to a length of 20 μm .

Fig. 4.14 (A) Experimental set-up for the Purification of GUVs using an extra 67
filtration with dual filtration technique. (B) and (C) represent the size distribution
histogram of GUVs under filter holders 2 and 3 respectively. The purification
was performed at a flow rate of 1 mL/min for 1 h.

List of Tables

Table 4.1 The average size of GUVs, skewness and mode of the distribution for different combinations of the polycarbonate membrane	47
Table 4.2 Fraction of required sized GUVs under filter holder 2 compared to the total number of GUVs before filtration for different combinations of polycarbonate membranes.	62

List of Symbols and Abbreviation

GUVs	-	Giant Unilamellar Vesicles
LUVs	-	Large Unilamellar Vesicles
SUVs	-	Small Unilamellar Vesicles
GVs	-	Giant Vesicles
w/o	-	water in oil
w/o/w	-	water in oil in water
POPC	-	1-palmitoyl-2-oleoyl- <i>sn</i> -glycero-3-phosphocholine
POPG	-	Phosphatidylethanolamine-phosphatidylglycerol
DOPC	-	1, 2-dioleoyl- <i>sn</i> -glycero-3-phosphocholine
DOPG	-	1, 2-dioleoyl- <i>sn</i> -glycero-3-phospho-(1- <i>rac</i> -glycerol)
EGTA	-	Ethyleneglycol- <i>N,N,N',N'</i> ,-tetraacetic Acid
BSA	-	Bovine Serum Albumin
PIPES	-	1,4-Piperazinediethanesulfonic Acid

CHAPTER 1

INTRODUCTION

1.1 Background

The cell in a living organism is the structural, functional and biological unit which is known as the building block of life. Cell contains cytoplasmic fluid enclosed by a membrane. Biomembrane acts as a pickily porous barrier. This barrier isolates the cell from the outer surroundings. It consists of a phospholipid bilayer where proteins are attached integrally and peripherally. These proteins act as transportation and communication pumps of a membrane that control the passage of different ions. These tend the cell to create electrical and chemical gradients. Proteins are altered with the existence of an annular lipid shell to enormous membrane regularity nature of lipid bilayer, incorporate with lipid molecules attached precisely to the outside area of membrane proteins which are integrative attached [1]. Cholesterol, glycoproteins, and glycolipids are submerged in the bilayer of biomembrane. A biological membrane is permeable to some hydrophobic molecules (e.g., proteins, amino acids, carbohydrates, DNA, RNA, and ions) which have very small characteristics of polarity and to some very small molecules like oxygen, carbon-dioxide and water. Membrane proteins control the passing of these molecules inside the membrane, or these molecules can be transported by active transport. Under different physiological conditions, the cell keeps sodium and potassium ions along the cell membrane to accredit membrane potential, which is very essential for different cellular functions [1].

The cell membrane consists of lipids and proteins and that's why it is called a lipo-protein membrane. Membrane lipids are generally fatty acid-based and they are two types – phospholipids and sterols (generally cholesterol) [2]. The vital element of the cell membrane is phospholipids, in which two out of three groups of hydroxyls (of glycerol) are combined with carboxyl groups of fatty acids and the other one is combined with phosphoric acid. This kind of lipid is named phosphatide. Phosphoric acid is mostly associated with an organic group. Steroids, which are another kind of complex lipid, are significantly different from simple lipids by their chemical structure [3]. A steroid maintains one 5- membered and three

6- membered carbon rings. If an alcohol group is linked to one of the carbon rings, then that steroid is called sterols. Cholesterol is one of the examples of sterols. Sterols are extensively allocated in the fungi, plants, and animals' plasma membrane, but it is not found in bacteria [3]. Bilayers generally consist of a head and a tail which is amphiphilic phospholipids. The head is made of a hydrophilic phosphate group, and the tail is made of two fatty acid chains which are hydrophobic. This kind of head group can adjust the non-verbal communication of a bilayer surface and act as signals for other molecules in the cell membrane. The tails can dictate the phase of the bilayer membrane and can influence its dynamics [4]. Cholesterol other than phospholipids has been found in animal cells and supports to indurate the bilayer and lessen its porosity and also supports to control the action of some fundamental membrane proteins. At lower temperatures, the lipid bilayer remains in a state named solid gel phase, but at a higher temperature, phase transformation happens to a fluid state [5]. Vesicles are models of cells, which are used for studying the function of complex biomembranes [6]. The word "vesicle" originates from "*vesicula*" which means a tiny sac. The outer layer of the vesicle is called the membrane [7].

Based on the layer, vesicles are mainly of two types; one is unilamellar, and the other is multilamellar. According to size, unilamellar vesicles are three types- (i) Small Unilamellar Vesicles (SUVs), (ii) Large Unilamellar Vesicles (LUVs) and (iii) Giant Unilamellar Vesicles (GUVs). The vesicles with 20-200 nm sizes are called SUVs, while the vesicles with 100-1000 nm are known as LUVs. On the other hand, bigger sized vesicles such as 1-80 μm , are known as GUVs and these are cell-sized vesicles. These vesicles are considered a promising tool for their wide range of industrial and medical applications [8-10]. The cell size vesicles such as GUVs have been widely used to investigate the elasticity of membranes [11], deformation [12-13], and poration [14-15]. Although intravenous drug delivery generally uses vesicles with sizes smaller than 1 μm , some clinical applications such as inhaled liposomal drug delivery use larger vesicles of sizes several microns [16-18]. One of the main advantages of using GUVs over nanometer-size vesicles is their visibility in optical microscopy. For example, it is possible to observe the static and dynamic changes of GUVs induced by peptides, toxins and, nanoparticles [19-20].

Vesicles can be prepared by various well-established methods like spontaneous or natural swelling method or gentle hydration method [21], electroformation or electroswellling method [22], lipid stabilized water in oil emulsion method, surfactant stabilized emulsion method [23] etc. Also, GUVs can be prepared by the fusion of SUVs or LUVs [24], lipid stabilized water in oil in water (w/o/w) double emulsion [25], originated from an initially planar bilayer [26]. Among the various methods for preparing different sizes GUVs [27], the natural swelling and electroformation methods are highly popular for synthesizing oil-free GUVs. During synthesis, many small vesicles, some lipid aggregates and a small fraction of multilamellar vesicles (MLVs) are generally formed in the suspension of GUVs, which are hindering the interaction between membrane-active agents and lipid vesicles. Such lipid aggregates and MLVs are removed by the high-speed centrifugation of GUV suspension during preparation and left smaller vesicles [21, 28-30]. Therefore, it is necessary to purify the GUVs. To purify the GUVs, a number of distinctive methods are available. One of the techniques is dialysis. It needs special equipment (dialysis bag), and it is a time-consuming technique [31]. It also requires a large volume of external solution to flow the buffer for several hours. Centrifugation is a very fast process for purification since it takes only 10–15 minutes [32]. It is an easy method, but it requires a high concentration of sucrose and glucose inside and outside of GUVs.

To obtain oil-free GUVs, membrane filtering with micrometer pores polycarbonate membrane [29] and microfiltration [33] methods are generally used. Those methods can purify the GUVs by eliminating the non-entrapped solute such as nanometer-sized vesicles from the suspension. Though the microfiltration method is very easy and fast, its recovery rate is very low [33]. Gravity-based non-electromechanical membrane filtering technique [34] shows similar performance to membrane filtering method. These methods/techniques provide a wide range of size distribution of purified GUVs. As an example, if a polycarbonate membrane with 10 μm pores is used for purification, the obtained size distribution of GUVs would be 8–70 μm [29, 33-34]. To our knowledge, so far, all the reported purification techniques produce a wide range of size distribution of GUVs rather than narrow size distribution.

The extrusion-dialysis method [35] was developed for preparing the monodisperse vesicles with an overall duration process of ~ 24 h. Such a long period would hamper the stability of spherical-shaped vesicles. It is very important to mention that, in many experiments, specific sizes GUVs are necessary. For example, the ‘single GUV method’ [19-20] requires similar sizes GUVs, where a ‘single GUV’ is induced by various types of membrane-active agents and calculates the corresponding kinetic constant of pore formation and membrane permeation [11, 30]. Moreover, similar-sized GUVs are also essential for the investigation of lipid heterogeneities [36], vesicle growth and shape changes [37], permeabilization of membranes by pulsed electric fields [38], peptide-induced pore sizes determination in the membranes [39], the effect of peptides in membranes [40], electric tension-induced pore formation for obtaining the kinetics of poration [41]. Therefore, the specific size distribution of purified GUVs is indispensable for various experiments. To fulfill the target, a new purification technique is developed with dual filtration for getting a specific size range of vesicles, and also this technique is not the time-consuming one.

1.2 Aims and Objectives

The aims and specific objectives of the study are as follows:

- (i) Modification of the membrane filtering technique for obtaining the specific size distribution of GUVs.
- (ii) Investigation of the effects of filtering using a combination of polycarbonate membranes on the size and distribution of GUVs.
- (iii) Investigation of the effects of flow rate on the average size of GUVs purified using a combination of polycarbonate membranes.
- (iv) Purification of GUVs containing water-soluble fluorescent probes using different combinations of polycarbonate membranes.
- (v) Observation of the significances of repeated purification on the distribution of the size of GUVs.

1.3 Outline of Thesis

There are five chapters in this thesis.

In chapter one, a general introduction of a biological membrane, vesicles, and different purification techniques of GUVs are discussed. The aims and objectives of this study are also included here.

In chapter two, the literature review of different purification techniques and their results are described.

In chapter three, the materials and method of the research are presented. The experimental setup of the dual filtration technique for the purification of GUVs is also discussed here.

In chapter four, the effects of dual filtration in various combinations on the size distribution of GUVs and the effects of flow rate on the average size of GUVs are discussed. The result of the repetition of dual filtration is also discussed in this chapter.

In chapter five, the overall conclusion is presented.

CHAPTER 2

LITERATURE REVIEW AND THEORETICAL ASPECTS

2.1 Literature Review

Walde *et al.* [27] discussed different procedures for the formation of giant vesicles (GVs) and their applications. Fig. 2.1 represents the simplified illustration of the main ideas of the different processes for the preparation of GUVs. GV resembles the mimic of all biological cells and have been very popular for investigating different aspects of biological membranes such as the reconstruction of proteins of the membrane [30], investigation of lipid heterogeneities [36], permeabilization of the membrane [38], budding of membrane and membrane fission [42, 43]. GV has been widely used to investigate the elasticity of membranes [44], rupture formation [45], and phase separation [46]. Another interesting appliance is gene-related experiments within the vesicles [47]. The author group discussed the key concepts of eight different methods for the preparation of GUVs that are currently used. In method 1, the preparation of GUVs by the hydrating of lipid film was discussed. They classified this procedure into two parts- 1(a) and 1(b). In 1(a), they discussed the instinctive swelling or natural swelling method or mild hydration method which was first reported by Reeves and Dowben [21, 48]. This method requires the precise hydration of dehydrated lipids placed on rigid surfaces. When the bilayer is in a state called liquid disorder, hydration has been performed [49]. The process of hydration of the dehydrated film is initially conducted by applying nitrogen gas which is water-permeated, which is known as pre-hydration, after that, by hydration with the appropriate water-logged solution [21]. In 1(b), they discussed the method named electroformation or electroswellling method developed by Angelova and Dimitrov [50]. In this method, lipids are accumulated by water-logged solutions having pre-developed SUVs or LUVs [51]. Accumulation can also be composed of the w/o emulsion system [52]. By regulating the effective voltage of the electric field, the formation of giant vesicles in aqueous suspension can be possible [51]. This method is now widely popular for the preparation of GUVs to investigate the mechanical properties of membranes [53], study the dynamics of the lipid membranes [54], lipid order and membrane fluidity [55], etc.

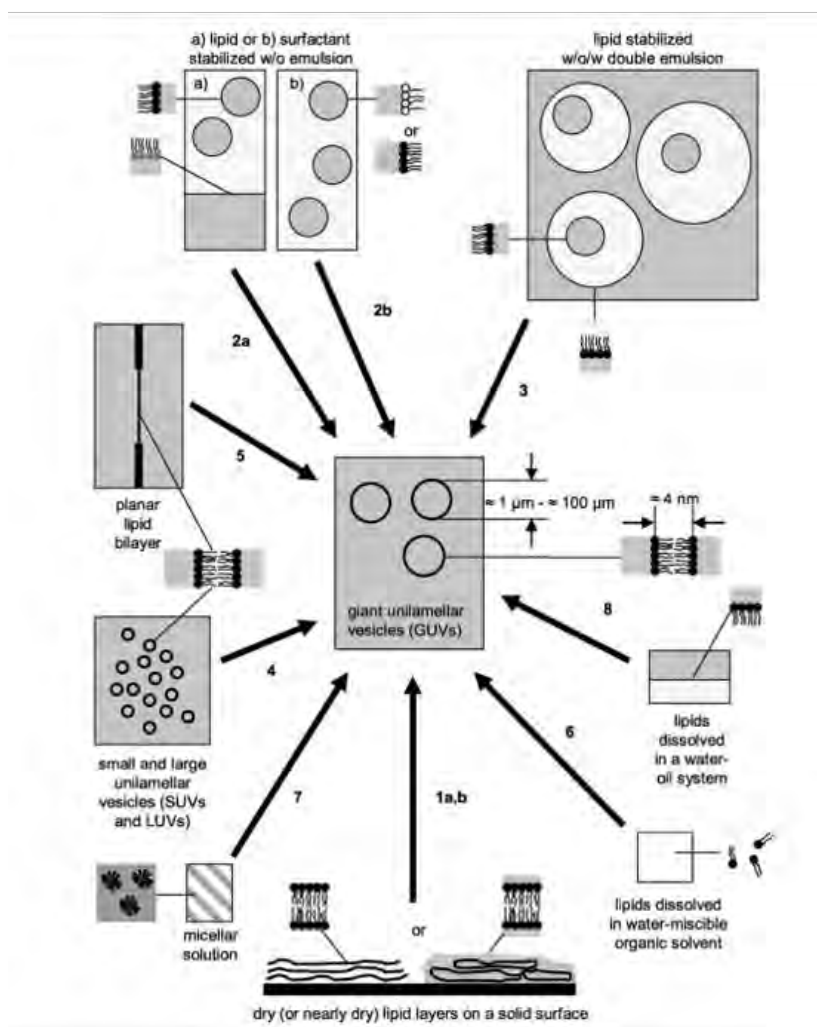


Fig. 2.1 Simplified illustration of the main ideas of the different processes for the preparation of GUVs [27].

In method 2, they discussed two different methods which are 2(a): water in oil (w/o) emulsion transfer method which is originally described by Pautot *et al.* as “inverted-emulsion method [3] and 2(b): surfactant stabilitated water in oil emulsion process [23] for the preparation of GUVs. The initial state of method 2(a) is made by bilayer forming lipid and oil and, the state is called w/o emulsion [3]. After that, this emulsion flows onto a system (two-phase) containing an aqueous state (as a lower phase) and top phase of oil which contains a bilayer forming lipid. This system is pre-incubated for an instant before the

w/o emulsion is added so that they can form a monolayer. The driblets of water of the top phase w/o emulsion approach to shifting from the w/o emulsion to the o/w edge. Lastly, moved to the lower water-logged phase where the formation of giant vesicles happened. Centrifugal force can be applied if the instinctive water driblet procedure is interrupted. The size of the starting water driblet of the w/o emulsion influences the size of the giant vesicles [3]. Tan *et al.* [56] described that from an initiatory w/o emulsion stabilitated with a phospholipid, formation of a giant vesicle is possible, which they discussed in this paper as method 2(b). Surfactant-stabilitated w/o emulsion prepared by microchannel emulsification was applied as an initial stage of this method [56]. In this case, stabilization of water driblets w/o emulsion with proper surfactant solution is made. The water droplets are settled by shifting the emulsion system to nitrogen (liquid). The transition of surfactant solution with the bilayer framing lipid is made (water droplets remain frozen) and giant vesicles can be found after the interchange of oil with a water-logged solution which contains small vesicles prepared from the lipids.

In method 3, they discussed the lipid-stabilitated w/o/w double emulsion process for the preparation of GUVs. The starting system of this method is lipid-stabilitated w/o/w double emulsions [25]. In this method, a water droplet is confined in a droplet of oil which is also in an external aqueous state. Lipid molecules cover every inner water droplet (hydrophilic head group faces the internal aqueous part of the droplet and lipophilic side faces the oil droplet). Oil droplet is covered by lipid molecules which hydrophilic head groups direct the external aqueous phase. The volatile oil is removed by the microfluidic technique [56], and this results in the production of giant vesicles. The size of the giant vesicle is regulated by the internal water droplet size of the w/o/w emulsion [57]. The GUVs prepared by this method can be used to study pH-responsive polymersomes [57].

They discussed the preparation of GUVs by fusion of small vesicles in method 4. It is a difficult method and a large number of small vesicles are needed to form a GUV. Sometimes fusion is persuaded by the freezing-thawing cycle in a dense electrolyte mixture [24] and sometimes occurs through the interactions of LUVs with hydrocarbon in a glass surface [58]. In method 5, they explained the formation of GUVs from an initially planar bilayer. At first, the planar bilayer is formed in a double-well chamber between two aqueous solutions

[26]. Vesicle formation is then persuaded by a jet-blowing technique [59]. This method is not completely developed yet.

In method 6, vesicles formation from lipids incorporated in water-miscible solvent is discussed. The basis of this procedure is relevant to the “ethanol-injection method” and the process used for the preparation of the “ethosomes” [60]. The mechanism of giant vesicle formation is not completely clear yet. The formation of vesicles from micellar lipid solutions is discussed in method 7. This method is relevant to the “detergent depletion method” which is used for the formation of the submicrometer-sized vesicles [61]. In method 8, they discussed the formation of vesicles from lipids dissolved in a w/o phase. This method is related to method 3, described by Moscho *et al.* [62]. The initial state of this method is an o/w (oil in water) two-state system. The oil phase contains lipids that are heavier than the water-logged solution and makes the lower phase. Lipids deposit at the water-oil interphase. Vaporization of the oil tends to the preparation of heterogeneous giant vesicles [62]. Vesicles prepared by this method are used for the study of giant vesicles as microcreators [63].

Tamba *et al.* [29] developed a new purification technique for the filtration of GUVs and named it a membrane filtering method. They prepared charged 50%DOPC/50%DOPG-GUVs by the natural swelling method [21, 40]. In this apparatus, a nucleopore polycarbonate membrane having 12 μm diameter pores is placed in a polypropylene filter holder. The upper side of the filter holder is connected to a 10 mL plastic syringe and the lower side is attached with a polypropylene tube (5 mm internal diameter and 11 cm in length). Another end of the polypropylene tube is attached with a second 10 mL plastic syringe. Fig. 2.2 shows the set-up of the membrane filtering method.

The size distribution of GUVs formed by the natural or spontaneous swelling method is almost 2-70 μm which are heterogeneous in size. A buffer solution is added with the unpurified GUV suspension by using a double-headed peristaltic pump, and they performed two rounds of filtration of the suspension at 2mL/min flow rate for 30 minutes each and obtained almost homogeneous sized GUVs with a diameter of 10-30 μm .

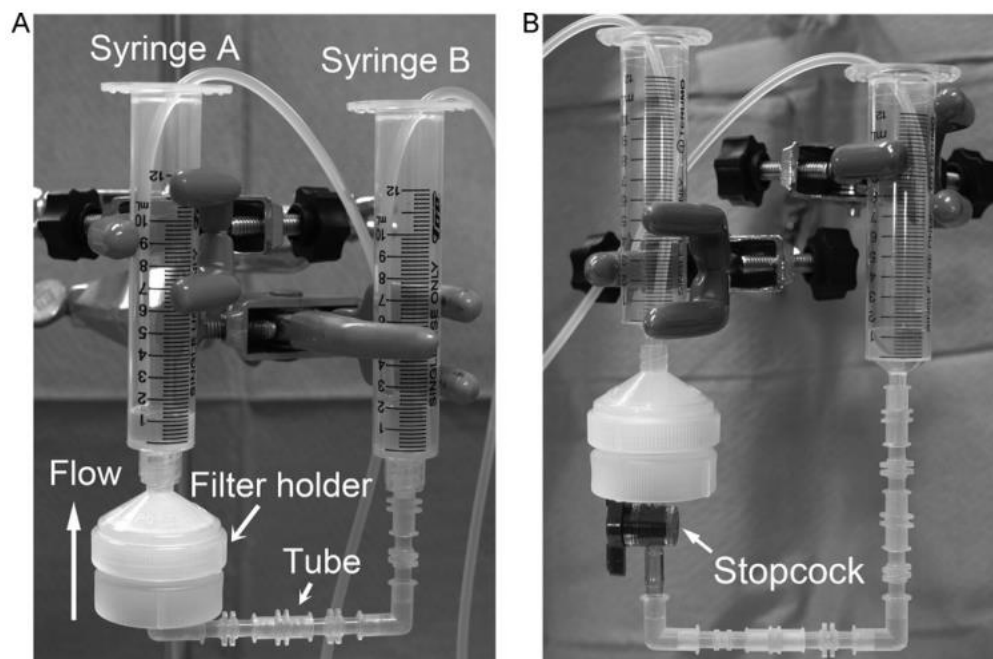


Fig. 2.2 (A) The equipment for the membrane filtering method. (B) The equipment for the membrane filtering method added a stopcock [29].

From Fig. 2.3, we can see the outcomes of purifying the GUV suspension on the size distribution of the GUVs. (A) shows a phase-contrast image and (B) shows a size distribution histogram of GUV suspension before purification. Here, we can see that the population of GUVs whose diameter is less than $10\ \mu\text{m}$ is very large. (C) shows a phase-contrast image and (D) shows a size distribution histogram after the first purification (flow rate $2\ \text{mL}/\text{min}$ for $30\ \text{min}$). After the first purification, the fraction of the GUVs with a diameter less than $10\ \mu\text{m}$ becomes small. The fraction of the vesicles with a diameter less than $10\ \mu\text{m}$ is $13 \pm 1\%$. And it gives a large population of GUVs with a diameter of $10\text{-}30\ \mu\text{m}$. A phase-contrast image is shown by (E) and (F) shows a size distribution histogram after the second purification (flow rate $2\ \text{mL}/\text{min}$ for $30\ \text{min}$). After the second purification, the fraction of GUVs with a diameter lesser than $10\ \mu\text{m}$ becomes $4 \pm 1\%$ and it gives a very sharpened distribution of GUVs around $10\text{-}30\ \mu\text{m}$. This method is also applicable for the purification of GUVs from water-soluble fluorescent probes.

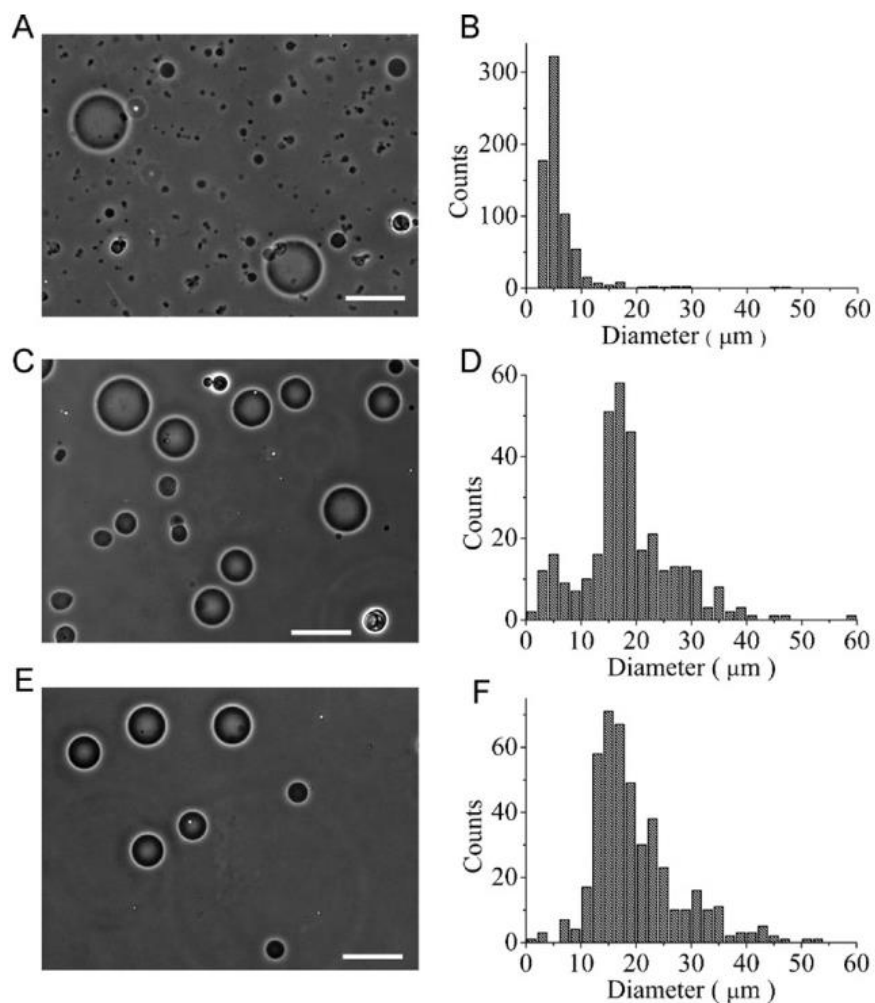


Fig. 2.3 Phase-contrast images and size distribution histograms of GUV suspension in different conditions. The bars in the images correspond to 50 μm [29].

Karal *et al.* [34] developed a non-electromechanical purification method to purify the giant unilamellar vesicles as shown in Fig. 2.4. The main difference between this technique and the membrane filtering technique is the use of a peristaltic pump [29]. In this method, the gravitational force is utilized to maintain the flow rate of buffer instead of peristaltic pump which makes the technique very low cost.

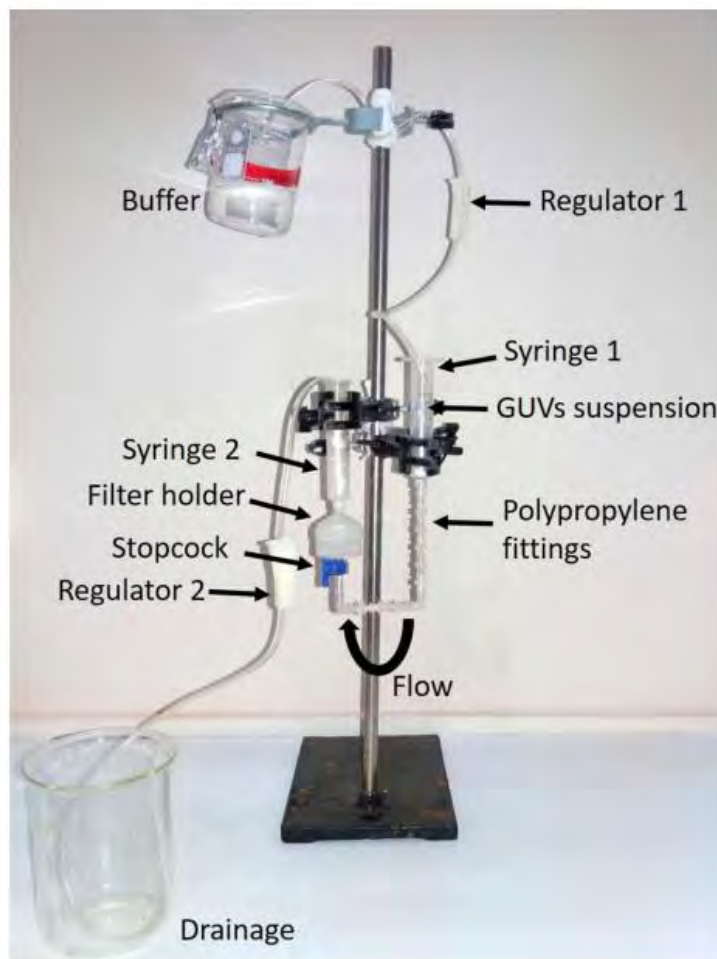


Fig. 2.4 An experimental system of non-electromechanical technique to purify GUVs [34].

The apparatus consists of a 10 μm diameter pores nucleopore polycarbonate membrane clamped in a polypropylene filter holder. The uppermost side of the filter holder is attached with a plastic syringe 2 of 10 mL and the lower side is attached with 9 polypropylene fittings which make a tube. Another side of the tube is attached with syringe 1 of the identical measurement. A glass beaker containing buffer is clamped at a specific elevation from where the buffer is continually streaming throughout a plastic tube (internal diameter is 3 mm) due to gravity. The GUVs suspension in buffer was added in syringe 1. A roller clamp regulator is used for controlling the flow rate.

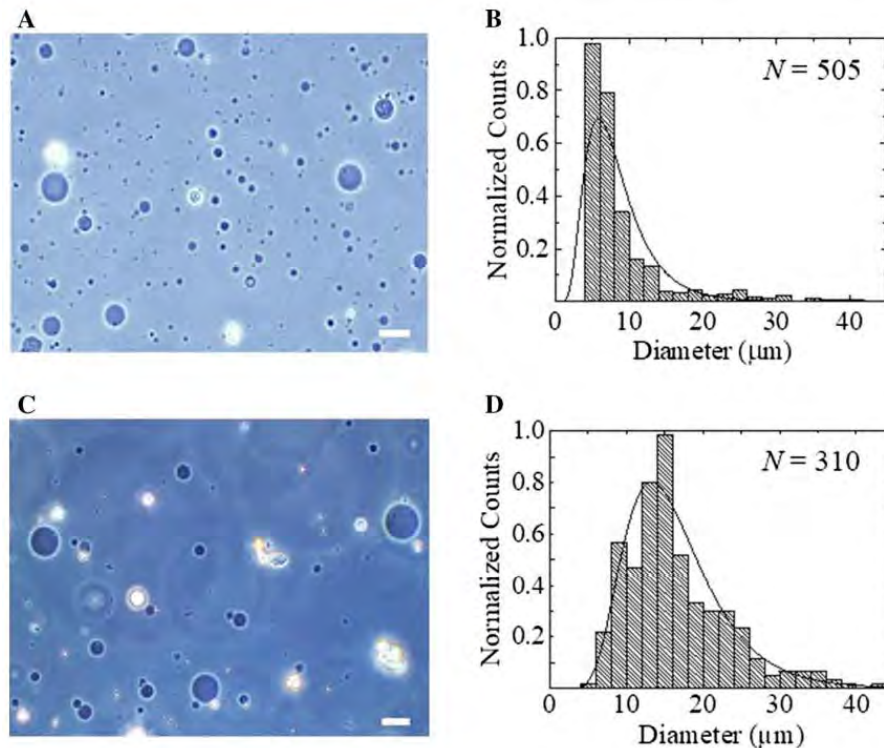


Fig. 2.5 (A), (B) represents the phase contrast image and size distribution histogram before purification, and (C), (D) shows the phase contrast image and size distribution histogram after purification. Purification was performed for 45 minutes with a flow rate of 1.5 mL/min. The bar in the images is correspondent to 30 μm [34].

Fig. 2.5 represents the effect of purification on the average size and size distribution of the giant unilamellar vesicles. (A) shows the phase contrast image of GUVs before purification. There is a very small number of GUVs larger than diameter 10 μm and a large number of GUVs smaller than diameter 10 μm . (C) shows the image of GUVs after purification. After purification, the population of GUVs with a diameter smaller than 10 μm is reduced and the GUVs with a diameter of 10-30 μm are increased because of the elimination of smaller vesicles. (B) and (D) represents the size distribution histogram of (A) and (C) respectively. A log-normal distribution can define this kind of distribution [64] as follows:

$$f(d) = \frac{1}{d} \times \frac{1}{\sigma\sqrt{2\pi}} \exp\left(-\frac{(\ln d - \mu)^2}{2\sigma^2}\right) \quad (2.1)$$

Here, $f(d)$ represents the normalized counts of GUVs having diameter d , μ is the mean, and σ^2 is the variance of the lognormal distribution. These are evaluated from the real distribution. Thus, the average value of the distribution is as follows:

$$d_{ave} = \exp\left(\mu + \frac{1}{2}\sigma^2\right) \quad (2.2)$$

From Fig. 2.6, however, we can see that after the second purification (C), a great amount of homogeneous GUVs is found to have a diameter of 10-30 μm by eliminating the vesicles whose diameter is less than 10 μm than the first purification. The density of the GUVs greater than 10 μm and in the range 10-30 μm is elevated over the consequence of the first-time purification. Here they used 40% DOPG/60% DOPC lipid for the preparation of GUVs by natural swelling method [21].

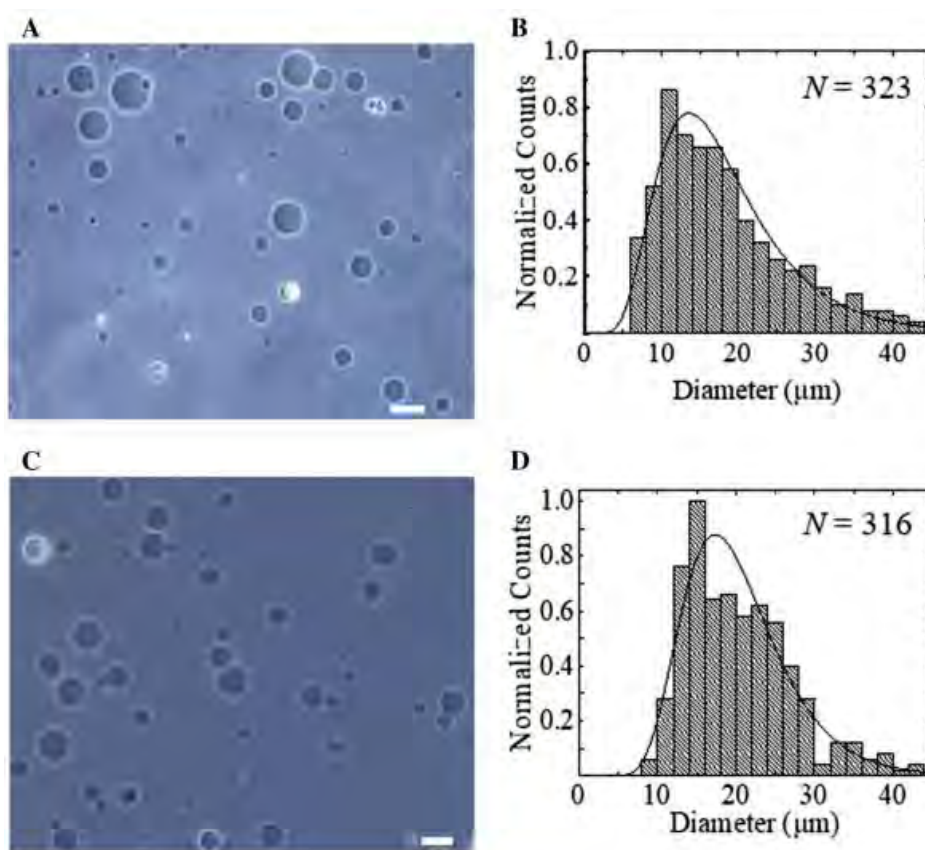


Fig. 2.6 (A) shows the phase contrast image and (B) shows the size distribution histogram of GUVs solution after the first purification. (C) shows the phase contrast image and (D) shows the size distribution histogram of GUVs solution after the second purification. Both purifications were performed for 45 minutes with a flow rate of 2 mL/min. The bar in the images is correspondence to 30 μm [34].

Ahmed *et al.* [65] investigated the effects of filtration of charged GUVs within a buffer incorporating different salt concentrations using their size distribution. In this work, vesicles were prepared by the natural swelling method [21] and then purified by the gravity-based membrane-filtering technique [34]. GUVs were formed by varying the mole fraction (X) of DOPG in the membrane and as well as by varying the concentration of salt (C) in the buffer solution. They introduced two important parameters for theoretically calculating the average size of purified giant unilamellar vesicles. These parameters are γ , multiplication factor for the mean (μ) and η for standard deviation (σ) of the lognormal distribution. The equation for the average value of purified GUVs [66] is -

$$D_{ave}^{pur} = D_{ave}^{unp} \left[\mu(\gamma - 1) + \frac{1}{2} \sigma^2(\eta^2 - 1) \right] \quad (2.3)$$

In Fig. 2.7, (a, c, e) show the effect of filtration on the distribution of the size of unpurified GUVs and (b, d, f) for purified GUVs at $C = 162$ mM. $X = 0.25$ for (a, b), $X = 0.55$ for (c, d) and $X = 0.90$ for (e, f). The finest fitted theoretical curve is shown by the blue line in (a, c, e) and red line (b, d, f). The histograms are fitted with the equation (2.1). From this equation, the average values of the GUVs can be measured.

In Fig. 2.8, (a, c, e) and (b, d, f) show the effect of filtration on the distribution size of unpurified GUVs and purified GUVs, respectively, at $X = 0.40$. $C = 62$ mM for (a, b), $C = 312$ mM for (c, d), and $C = 362$ mM for (e, f). The finest fitted theoretical curve is shown by the blue line in (a, c, e) and red line (b, d, f). The histograms are fitted with the equation (2.1), from this equation the average values of the GUVs can be measured. Thus, we can say that the average size of the purified GUVs is elevated with the elevation of mole fraction (X), and with the increase of concentration of salt (C) in buffer solutions, it is decreased.

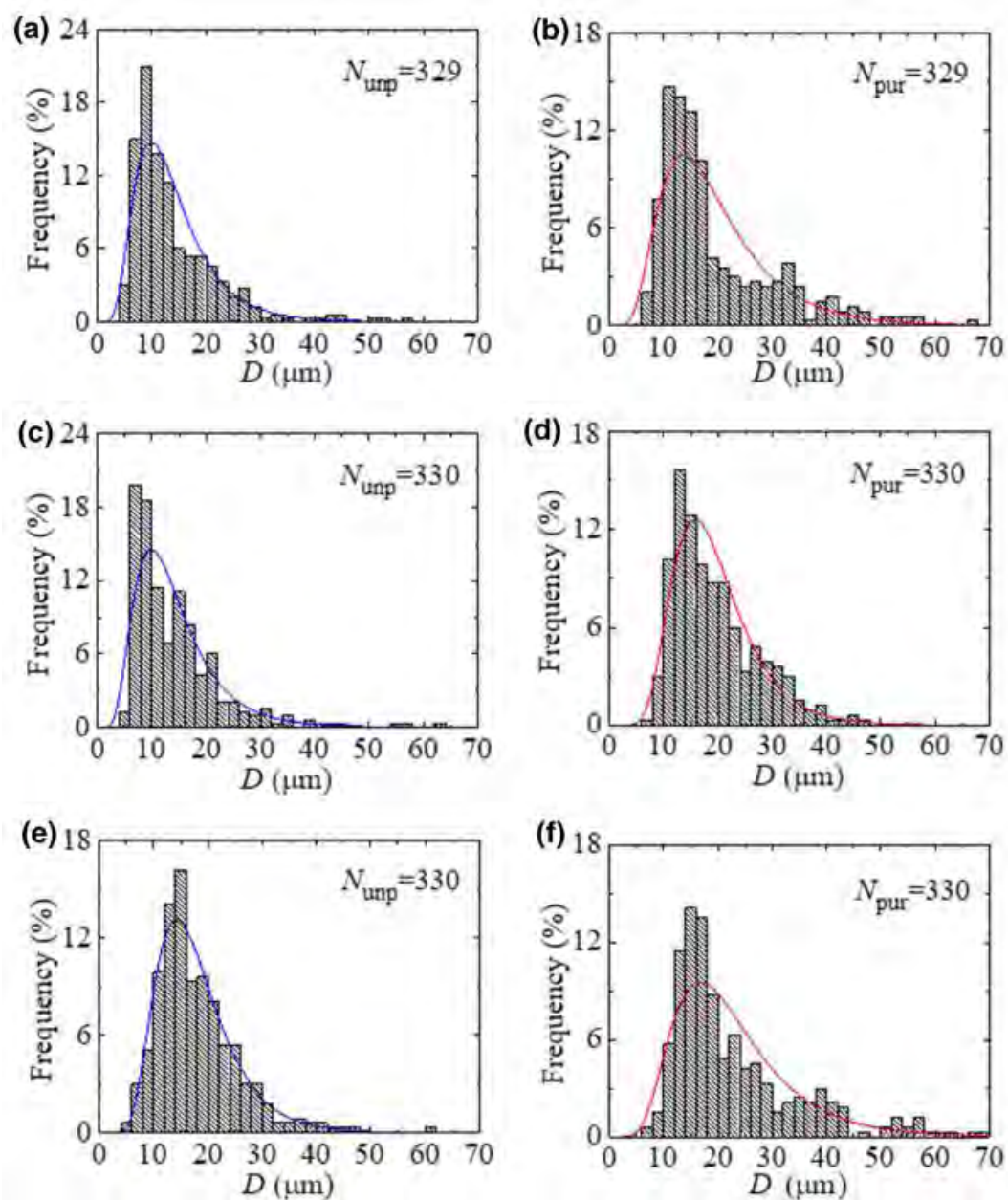


Fig. 2.7 Effects of filtration on the distribution of the size of GUVs incorporating different X at $C = 162$ mM [65].

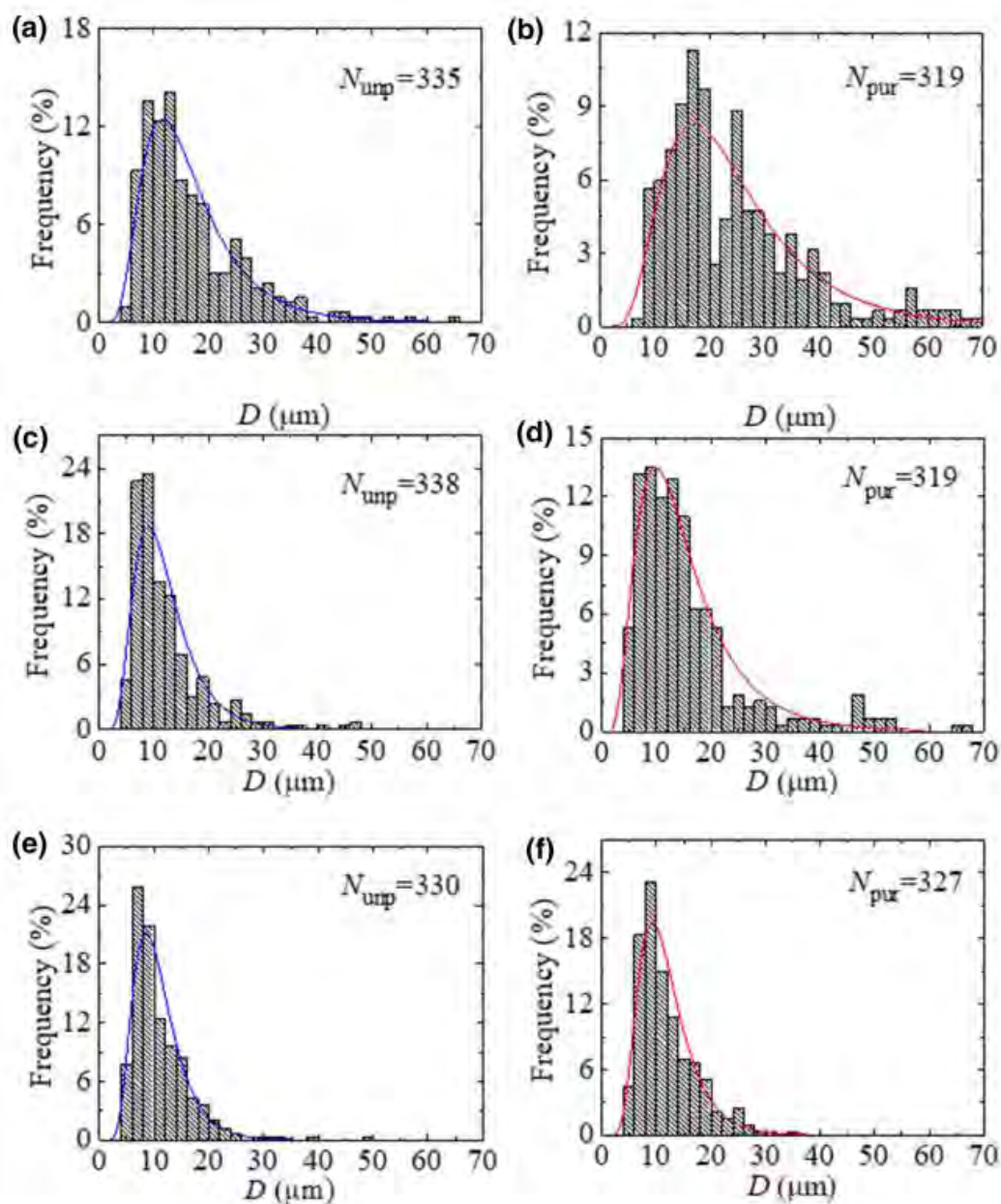


Fig. 2.8 Effects of filtration on the distribution of the size of GUVs incorporating different C at $X = 0.40$ [65].

Fayolle *et al.* [33] developed microfiltration for the purification of giant vesicles (GVs). During the preparation of GV, many non-entrapped solutes are formed. These non-entrapped solutes should be eliminated for various applications of GV. Fig. 2.9 shows the schematic representation of the membrane filtering technique. They used a nylon membrane with an average of $0.2 \mu\text{m}$ sized pore inside a filter holder connected with a vacuum

Erlenmeyer flask. There is also a pump connected to the flask with a pressure regulator to generate a pressure difference. The optimum pressure difference is 400-600 mbar and the lipid concentration is 50-100 μM . If the lipid concentration is increased, clogging would happen.

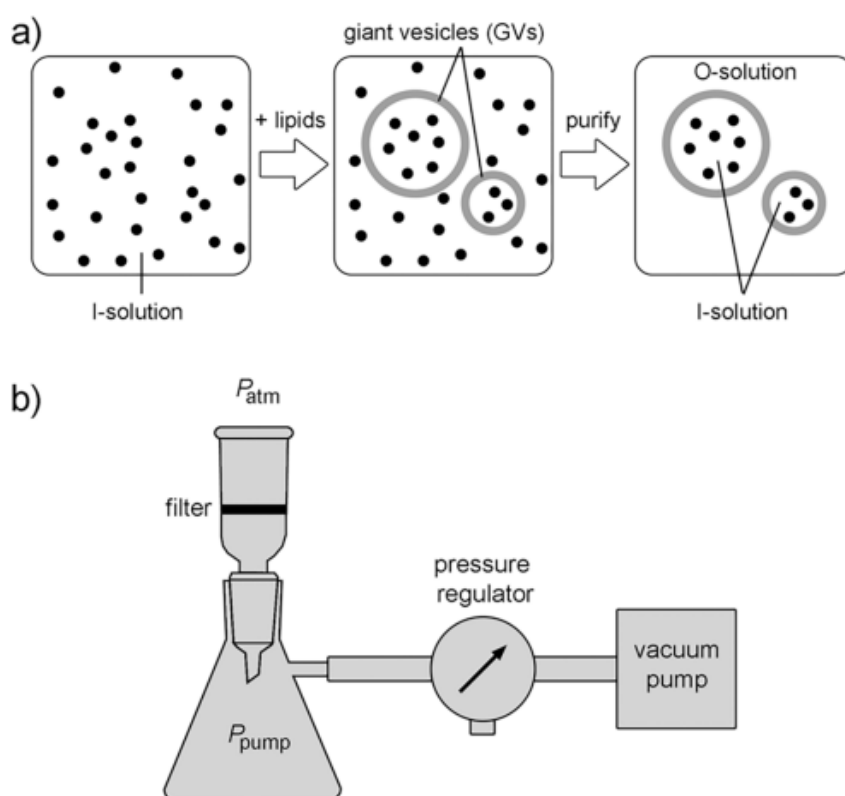


Fig. 2.9 Schematic representation of purification of giant vesicles by microfiltration [33].

Fig. 2.10 represents (a) confocal image of GV before microfiltration, (b) confocal image of GV after microfiltration, and (c) size distribution of the two populations. The grey area stands for the GUVs population before microfiltration and the black line represents the population after microfiltration. It is a simple, cheap, and very low-time-consuming (<10 min) technique, but the GV recovery rate is very low (<50%). Another drawback of this method is if size distribution measurement is the main target, it needs more than one round of filtration which increases the time period as well as increases lipid loss. In this case, GUV is prepared by the natural swelling method [21].

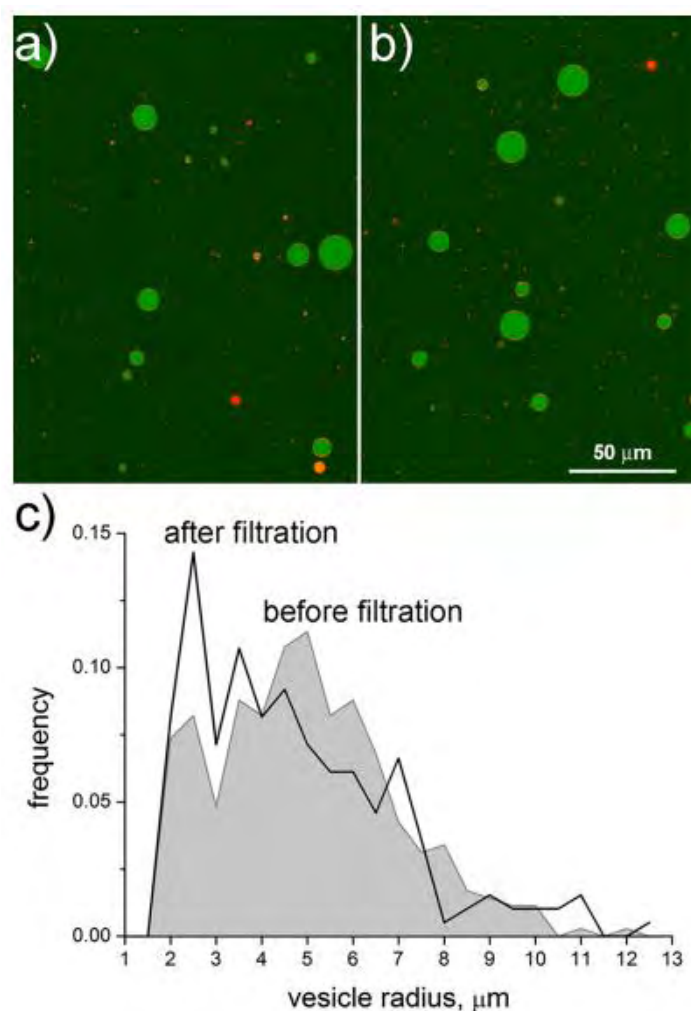


Fig. 2.10 Confocal images of GVVs (a, b) and size distribution of the population (c) [33].

Zhu *et al.* [35] established a method for the preparation of large monodisperse multilamellar vesicles. The size of the vesicle is the most important parameter for both research and practical application. By combining extrusion [67] and large pore dialysis [68] the author group prepared oleate vesicles by resuspending a dried film of oleic acid in 0.2 M Na-bicine containing 2 mM 8-hydroxypyrene-1,3,6-trisulfonic acid trisodium salt at pH 8.5, to a final concentration of 10 mM oleic acid in the buffer. The vesicles that are prepared in such a method are called polydisperse multilamellar vesicles. They extruded these polydisperse vesicles through a 5 μm diameter pore polycarbonate membrane which eliminates the

vesicles which are larger than $5\ \mu\text{m}$ in diameter. Then these extruded vesicles are gone through at least 6 rounds of dialysis having $3\ \mu\text{m}$ diameter pore polycarbonate membrane which eliminates the vesicles smaller than $3\ \mu\text{m}$ and leaving monodisperse vesicles with an average diameter of $\sim 4\ \mu\text{m}$. Fig. 2.11 represents the schematic diagram of the extrusion-dialysis process.

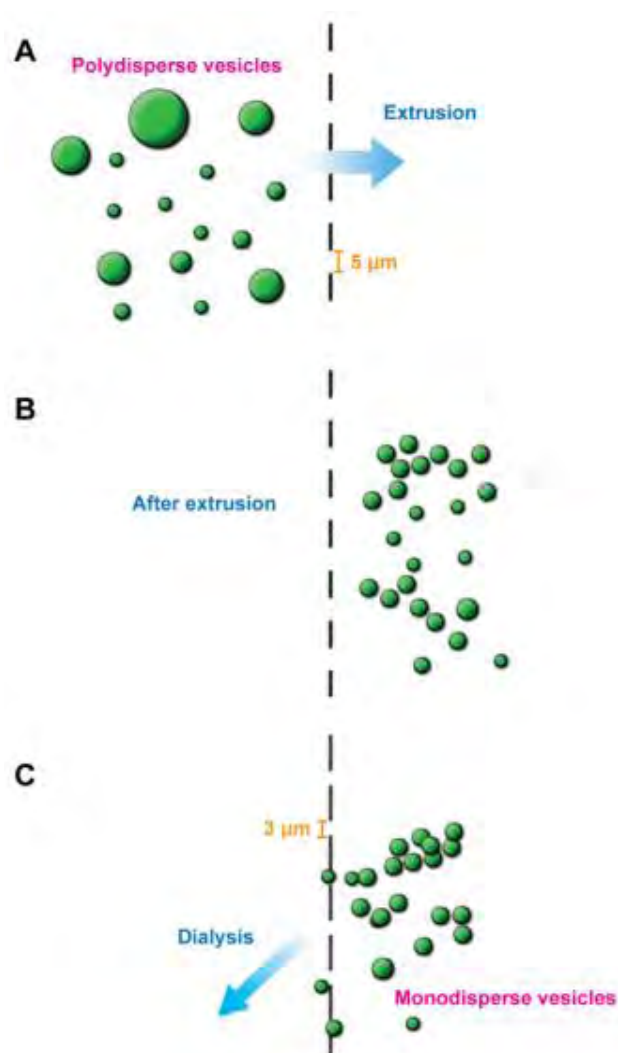


Fig. 2.11 Schematic diagram of vesicle extrusion-dialysis [35].

Fig. 2.12 shows the phase contrast image and size distribution histogram. From (A), we can see that after extrusion, there remain vesicles that are smaller than $5\ \mu\text{m}$ only. After dialysis,

these extruded vesicles by 3 μm pore polycarbonate membrane, vesicles smaller than 3 μm are eliminated, and the average size of the remaining vesicle is ~ 4 μm . They used the same method for the POPC vesicles and got a similar result. The extrusion-dialysis procedure is independent of the vesicle preparation.

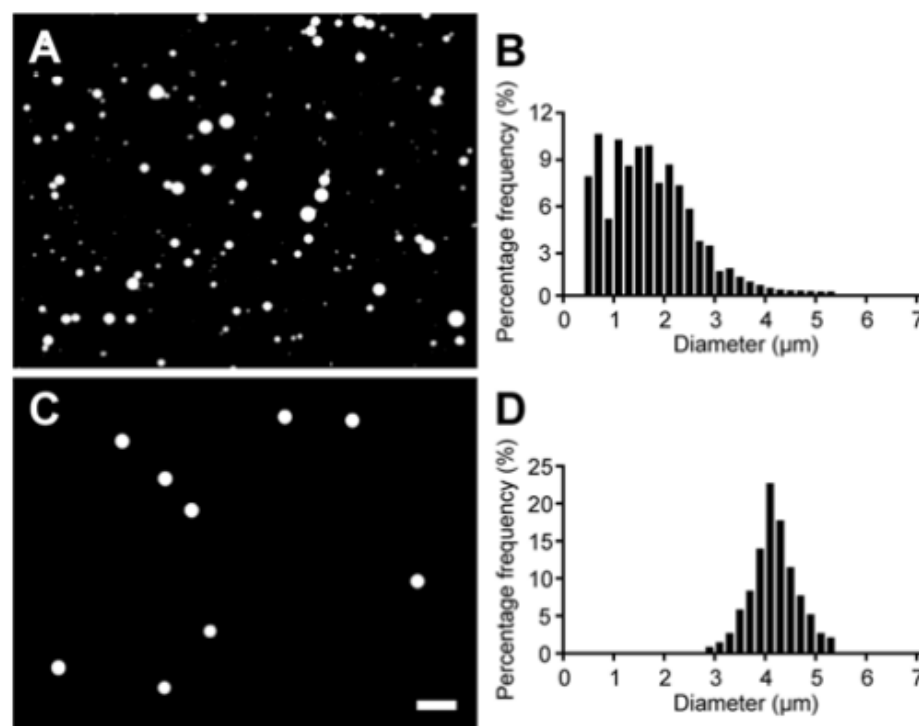


Fig. 2.12 For oleate vesicles, (A) and (B) show a phase-contrast image of vesicles and size distribution histogram after extrusion. (C) and (D) show the phase contrast image and size distribution of extruded vesicles that are gone through dialysis [35].

Rubenstein *et al.* [69] discussed a new technique for the purification of the coated vesicles by electrophoresis using an agarose gel. Coated vesicles furnish a basic mechanism for the transfer of membranes and membrane-related molecules among a variety of intracellular compartments in higher cells. Conventional preparation of coated vesicles contains contaminant smooth vesicles and empty coats. These can be detached by agarose gel electrophoresis. Typically, electrophoresis is carried out for 24 h at 5 $^{\circ}\text{C}$ using 0.75 V/cm.

They performed this electrophoresis on bovine brain-coated vesicles. Fig. 2.13 shows the effect of electrophoresis on bovine brain-coated vesicles in 0.3% agarose. The vesicles they got after the agarose gel electrophoresis are almost 97% pure. This purification reduces the lipid to protein ratio. It also revealed that the ATPase, which was considered to be a part of coated vesicle membrane [70] is actually an impurity.

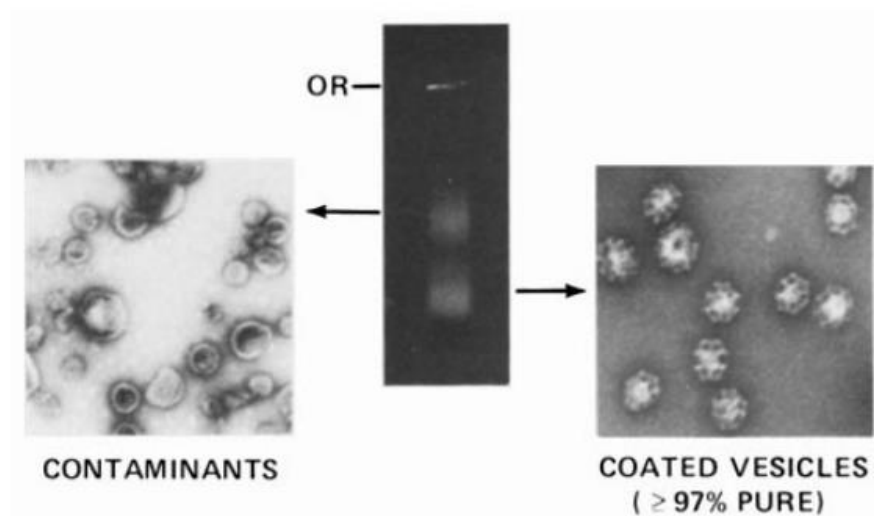


Fig. 2.13. Effect of agarose gel electrophoresis on bovine brain coated vesicles [69].

2.2 Applications of Purified GUVs

Because of cell mimicking characteristics of GUVs, the purified GUVs are currently extensively used in numerous disciplines of biomembrane physics, biomembrane chemistry, and, in the area of synthesis of mimicking of cell study. One of the most common applications of GUV is that they can be used as a simple model system for analyzing the specific physicochemical characteristics of biomembranes. For the studying of reconstituting membrane components in GUVs where mimicking of the biological membrane is the main target, thin unilamellar walls and specific sizes and shapes of GUVs are often required. Since the study of a biological cell is tremendously complex, giant unilamellar vesicles give

precise tactics to study membrane interrelation activities such as fusion of membrane, localizationism of protein in the plasma membrane, analysis of ion channels, etc.

Another interesting, as well as difficult sector of implementation of GUVs, is the scrutiny that pursues the fabricating the systems that have a certain fundamental characteristic of biological cells. GUVs are compartment-like structures. These compartments are encumbered with a variety of molecules to permit various chemical interactions to happen in the vesicles for regulating the sustenance of the structure of the vesicle and also for its growth and reproduction. In the time of preparation of GUVs by different methods, many SUVs, LUVs, lipid aggregates, non-entrapped solutes are also prepared. For various research purposes, oil-free GUVs are required as well as the GUVs have to be free from these aggregates and SUVs and LUVs. So, purification is needed. If LUVs were used instead of GUVs, average observations are possible using different experimental tools such as dynamic light scattering, fluorescence spectrometer, etc. whether the interactions happened inside of the vesicles or on the outside surface of every individual vesicle, LUVs could not provide better results [71].

Some applications/uses of GUVs are highly considered in the scientific community such as the use of GUVs permits an uninterrupted imaging and accountable investigation of the generation of pore or poration in phospholipid membrane [45], imaging as well as investigation of the poration in phospholipid membranes induced by the peptide, Magainine-2 [30], investigation of the order of lipid and regularity of membrane [55], studying of the growth of vesicle and change in shape [72], studying of the permeabilization of membranes of the vesicle by applying an electric field (pulsed) [38]. The GUVs are used for the investigation of the impact of oxidative stress on the vesicles [73], studying of the impact on the structure and size of the vesicles after applying the millimeter electromagnetic waves [74], investigation of protein-lipid bilayer interactions [75], investigation of gene-related experiments within every single vesicle [47], research on the reaction of lipid bilayers with virus-like particles for understanding virus-membrane interaction [76], studying the osmotic impacts to mimic the procedures happening at the time of the hypo-hydration of cells [77].

Though the investigation is in a very preliminary state yet, some positive reports are reported in the condition of embedding the liposomes to DNA microchips [78] or to microwells [79] to develop a “liposome-microchip”. This may be very helpful for advancing immunoassays supported by liposomes [79]. Since the size of GUVs is large, it is suitable for the application regarding the field of biosensors. These biosensors could be used for the observation of the toxin’s permeabilization by divulging the omnipresence of bacteria producing lysins [80-81]. GUVs can be used to detect several types of xenobiotics [82]. Investigation and study of the diversity of the lateral lipid in the membranes for the lipid domain formation in the biological membrane [83]. GUVs are used as a mimic for the study of the development of cristae in mitochondria [84] and studying of the reconstructed cytoskeleton [85], used as the model of cytoplasm incorporating polymers [86]. Other applications of GUVs are studying the reconstructed membrane proteins inside the vesicle membranes [87], used as biomimetic systems for researching definite stages of the exocytosis process [88], assembles of networks of GUVs which are interrelated via lipid tubes [89], investigation on the morphology and vesicle size due to the impact of enzymes being activated on the lipids, investigation of budding, and fission is [90], investigation of GUVs as microreactors [91], investigation of several molecule reactions within GUVs [92], and many more.

For the above-mentioned applications or uses, there is a need for the production of a large number of similar-sized GUVs which is generally not possible, but purification can be a helping tool to obtain it.

2.3 Lipid Bilayer and Vesicles

The membrane of a biological cell constitutes a lipid bilayer. It also includes cholesterol that lie among phospholipids for continuing their regularity at different temperatures [2]. Lipids are the building blocks of the structure and function of living cells. The lipid molecules are arranged in such a way that the hydrophilic part remains in contact with water, while the hydrophobic tails project inward [93]. Fig. 2.14 shows the illustration of lipid molecules [53].

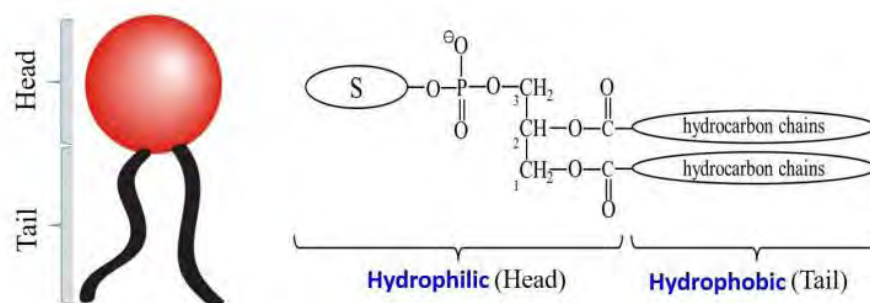


Fig. 2.14 Lipid molecule and molecular structure of lipids [53].

Fig. 2.15 represents a lipid bilayer that consists of two layers. It is a very fine membrane of flat sheets which is polar in nature and makes a ceaseless boundary throughout the cell that holds many more molecules, proteins, and ions in their required places and prevents their diffusion where not needed. Lipid bilayers are impermeable to hydrophilic molecules [94]. Bilayers generally consist of amphiphilic phospholipids having a head of hydrophilic phosphate and a tail containing a pair of fatty acid chains which is hydrophobic.

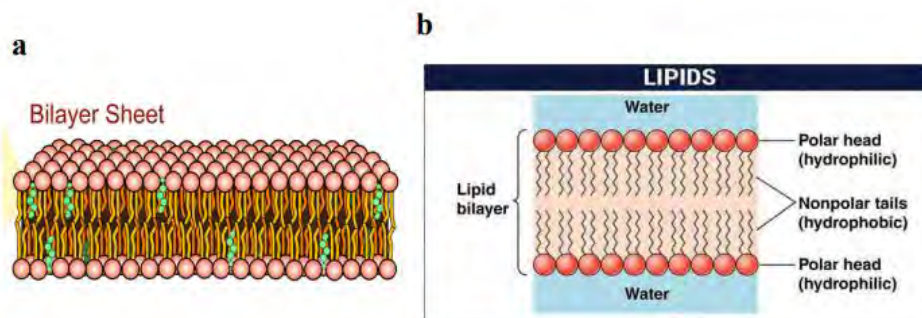


Fig. 2.15 (a) Lipid bilayer (3D view), (b) schematic diagram of lipid bilayer (2D view) [53]

Vesicles are a particular type of aqueous compartment. The outer layer of each vesicle is called a membrane which is embodied in one or several numbers of fine layers made of amphiphilic molecules. These amphiphiles carry hydrophilic and lipophilic parts. The hydrophilic portions adjacent to the aqueous media and the lipophilic sides involve the

formation of the inner side of every layer [7]. Depending on the layer number, vesicles are two types- (i) Unilamellar vesicle (only one lipid bilayer) and (ii) Multilamellar vesicle (more than one lipid bilayer). Unilamellar vesicles are three types which are as follows:

- (i) Small Unilamellar Vesicles (SUV) of sizes up to 100 nm
- (ii) Large Unilamellar Vesicles (LUV) of size range 100-1000 nm
- (iii) Giant Unilamellar Vesicles (GUV) of size range 1-80 μm .

CHAPTER 3

MATERIALS AND METHOD

3.1 Materials

1, 2-dioleoyl-*sn*-glycero-3-phosphocholine (DOPC) and 1, 2-dioleoyl-*sn*-glycero-3-phosphoglycerol (sodium salt) (DOPG) were purchased from Avanti Polar Lipid Inc. (Alabaster, AL). Piperazine-1, 4-bis (2-ethanesulfonic acid) (PIPES), Bovine serum albumin (BSA), O, O'-bis (2-aminoethyl) ethyleneglycol-*N,N,N',N'*-tetraacetic acid (EGTA), Glucose, Sucrose, Chloroform and Calcein were purchased from Sigma-Aldrich, Germany.

3.2 Instruments Used for the Synthesis and Observation of GUVs

The following instruments were used for the synthesis and observation of GUVs.

- 1) Drying oven (Ecocell)
- 2) Nitrogen gas cylinder with multistage regulator
- 3) pH meter (BT675 Boeco, Germany)
- 4) Vortex mixture (Stuart SA8, UK)
- 5) Incubator (Phoenix TIN-IN35, Germany)
- 6) Analytical balance (Radwag, Poland)
- 7) Freezer (Siemens, Germany)
- 8) Rotary vacuum pump (Pfeiffer, Germany)
- 9) Centrifuge machine (NUVE NF 800R, Turkey)
- 10) Inverted phase contrast fluorescence microscope (Olympus IX73, Japan).

3.3 Synthesis of Lipid Membranes of GUVs

40%DOPG/60%DOPC-GUVs (% indicates mole %) were synthesized by the natural swelling method [21]. At first, 1 mM DOPG (80 μ L) and DOPC (120 μ L) in chloroform were taken into a 4.5 mL glass vial and dried with a gentle flow of nitrogen gas to produce a thin and homogeneous lipid film. The residual chloroform in the film was removed by placing the vial in a vacuum desiccator overnight (12 hours). An amount of 20 μ L MilliQ water was added to the vial and then pre-hydrated at 45°C for 8 minutes. After pre-

hydration, the sample was incubated with 1 mL of buffer (10 mM PIPES, pH 7.0, 150 mM NaCl, 1 mM EGTA containing 0.10 M sucrose) for 3 hours at 37°C to produce unpurified GUV suspension. For preparing the water-soluble fluorescent probe, calcein, containing GUVs, vesicles were synthesized in the buffer containing 1 mM calcein in the inside of vesicles. Calcein solution was prepared beforehand of a total of 15 mL containing 9.34 mg calcein and 1.5 mL of 0.10 M pipes and 1.5 mL of 0.10 M sucrose which act as an internal solution. Then GUVs were purified by dual filtration technique. An amount of 300 μ L purified GUVs suspensions were transferred into a U-shaped hand-made microchamber which was coated with 0.10% (w/v) BSA, dissolved in a buffer containing 0.10 M glucose. The GUVs were observed using an inverted phase-contrast microscope (Olympus IX-73, Japan) with a 20 \times objective at 25 ± 1 °C.

3.4 Dual Filtration Technique for the Purification of GUVs

For the various applications of GUVs, the specific size of GUVs is necessary. For example, the ‘single GUV method’ [19-20] requires similar sizes GUVs, where a ‘single GUV’ is induced by various types of membrane-active agents and calculates the corresponding kinetic constant of pore formation and membrane permeation [11, 30]. Moreover, similar size GUVs are also essential for the experiment of peptide-induced pore sizes determination in the membranes [39] and for the investigation of the electric tension-induced pore formation in membranes for obtaining the kinetics of poration [41]. Therefore, the specific size distribution of purified GUVs is indispensable for various experiments. To fulfill the target, a new purification technique with dual filtration is developed for getting a specific size range of vesicles. Fig. 3.1 shows the schematic diagram of what happens with the suspension of giant vesicles upon the first and the second filtration. In this technique, instead of using a single polycarbonate membrane, a combination of such membranes with different size pores is used. The reason for using the dual filtration technique is to get a specific size distribution of vesicles rather than a wide range size distribution. In dual filtration, three combinations of polycarbonate membranes were utilized in filter holder 1 and filter holder 2. For example, case (i) polycarbonate membrane with 12 μ m pores in the filter holder 1 and polycarbonate membrane with 10 μ m pores in the filter holder 2.

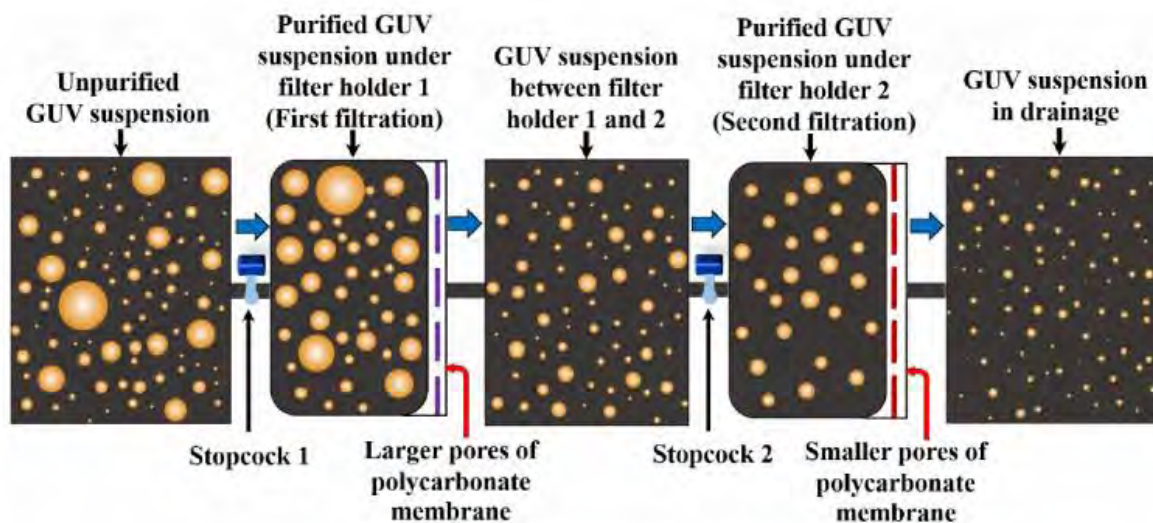


Fig. 3.1 Schematic diagram of Dual Filtration Technique.

For case (ii), the corresponding polycarbonate membranes with pores were $12\ \mu\text{m}$ and $8\ \mu\text{m}$, and for case (iii), the polycarbonate membranes with pores were $10\ \mu\text{m}$ and $8\ \mu\text{m}$. In each case, a polycarbonate membrane with higher pores was placed in filter holder 1, and smaller pores in filter holder 2 as illustrated in Fig. 3.1. Each arrangement provided a specific size distribution of vesicles. The purified GUV suspension was collected under filter holder 2 as shown in Fig. 3.1. In contrast, in a single filtration, only one polycarbonate membrane with pores $12\ \mu\text{m}$ or $10\ \mu\text{m}$ or $8\ \mu\text{m}$ was implemented in filter holder 1. It is to be noted that the successive part such as filter holder 2 was absent in the single filtration. The purified GUV suspension was collected under filter holder 1. Hence, the technique provided a wide range of size distribution of vesicles as depicted in Fig. 3.1. The experimental results are presented in a set of size distribution histograms, and the distributions are analyzed by a lognormal distribution. The average size of GUVs was calculated. The skewness and mode of distribution at various conditions, effects of flow rates on the average size of GUVs with this technique were also calculated. Extra filtration was added with dual filtration technique and size distribution of GUVs collected from different filter holders was calculated. Effects of repeating the dual filtration on the size distribution of GUVs were also observed.

3.5 Accessories for Dual Filtration Technique

Syringe: Two plastic (polypropylene) syringes (JMI Syringes and Medical Devices Ltd. Bangladesh) of 10 mL containing GUVs suspension during the purification were clamped in a stand at a fixed height. Fig. 3.2 represents the polypropylene syringes.



Fig. 3.2 Polypropylene syringes.

Pipe for buffer flow: Fig. 3.3 shows the pipe for buffer flow. This is a tube made of plastic whose internal diameter is 3 mm (JMI Syringes and Medical Devices Ltd. Bangladesh). It is used for transferring the external solution to the first syringe from a buffer-filled glass beaker and another one from the second syringe drainage for eliminating the smaller vesicles.



Fig. 3.3 Pipe for buffer flow.

Fittings for the purification system: This system is made of three types of polypropylene fittings (Luer fittings VRFE6, VRFC6, VRSC6; AS-ONE, Japan) of internal diameter 3 mm. Fig. 3.4 represents three types of polypropylene fittings.



Fig. 3.4 Different types of fittings.

Filter holder: It is a polypropylene filter holder (Swinnex, $\phi = 25$ mm, Millipore Co., Billerica, MA) (Fig. 3.5) where different μm diameter pores nucleopore poly-carbonate membranes (Whatman® Nucleopore™ Track-Etched Membranes, UK) were clasped inside during double filtration.



Fig. 3.5 Polypropylene filter holder.

Filter paper: 12 μm , 10 μm and 8 μm diameter pores nucleopore poly-carbonate membranes (Whatman® Nucleopore™ Track-Etched Membranes, UK) were used for the investigation. Fig. 3.6 represents the filter paper of 10 μm diameter pores filter paper.



Fig. 3.6 Filter paper.

Stop cock: 1-way polycarbonate stopcock (Luer stopcock VXB1055, AS-ONE, Japan) was

used in the purification which was connected to one specific end of the filter holder. Fig. 3.7 represents a stop cock.



Fig. 3.7 Stop cock.

Peristaltic pump: Fig. 3.8 shows a peristaltic pump having compacted two heads (CPP-SP2, Shenchen, China). The range of flow rate of this pump is 0.0024-190 ml/min.



Fig. 3.8 Peristaltic pump.

3.6 Dual Filtration Technique

An experimental setup for a dual filtration technique for the purification of GUVs is illustrated in Fig. 3.9. The arrangement steps followed for the purification is discussed here. The incubated unpurified GUV suspension was centrifuged at $13,000\times g$ (here g is the acceleration due to gravity) for 20 minutes at 20°C using a refrigerated centrifuge machine (NF 800R, NUVE, Turkey). The function of the centrifugation is to remove the multilamellar vesicles (MLVs) and lipid aggregates as these elements sedimented at the bottom of eppendorf tubes [30, 28-29]. After centrifugation, an amount of 2.6–2.8 mL supernatant (unpurified GUV suspension) was collected for the purification experiment. Therefore, most of the lipid aggregates and MLVs were left at the bottom of eppendorf tubes

as supernatant after centrifugation. Then the unpurified GUV suspension in buffer (10 mM PIPES, pH 7.0, 150 mM NaCl, mM EGTA containing 0.10 M glucose) was added to a 10 mL syringe 1 (JMI Syringes and Medical Devices Ltd. Bangladesh) where the buffer containing 0.10 M glucose was continuously flowing by a peristaltic pump (CPP-SP2, Shenchen, China) through a plastic tube of inner diameter 3 mm.

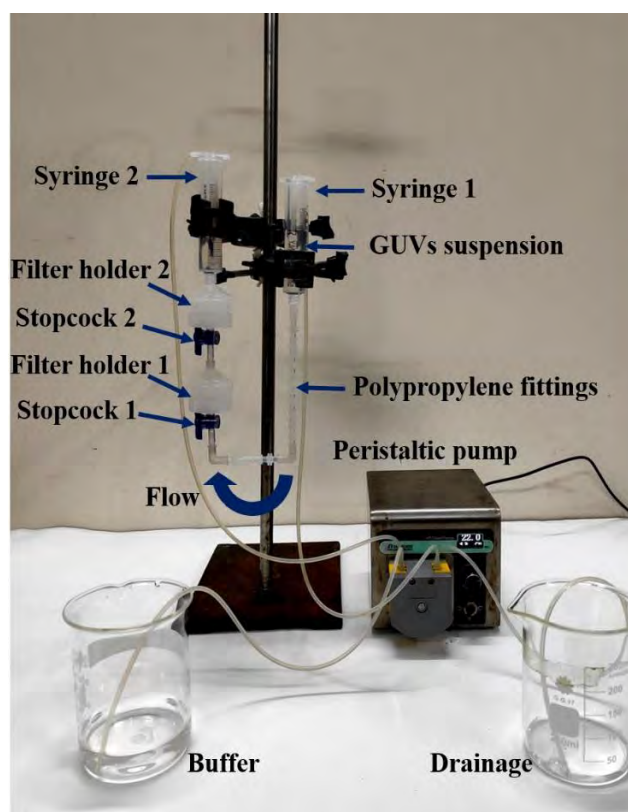


Fig. 3.9 Experimental set-up of dual filtration technique.

The syringe 1 was connected to the bottom of filter holder 1 (Swinnex, $\phi = 25$ mm, Millipore Co., Billerica, MA) through a tube prepared with three different types of polypropylene fittings (Luer fittings VRFE6, VRFC6, VRSC6; AS-ONE, Japan) having inner diameter 3 mm. The tube contains a total number of 18 fittings. The upper end of filter holder 1 was connected to the bottom of filter holder 2, and the upper end of filter holder 2 was connected to a 10 mL plastic syringe 2 (of the same company). The polycarbonate membranes (Whatman1 Nuclepore™ Track-Etched Membranes, UK) were set inside the filter holders. The arrangement of that membranes was followed in descending order of pore

sizes in filter holders 1 and 2, respectively. Three combinations of polycarbonate membranes in filter holder 1 and filter holder 2 according to corresponding pore sizes such as case (i) holder 1: 12 μm and holder 2: 10 μm , case (ii) holder 1: 12 μm and holder 2: 8 μm , and case (iii) holder 1: 10 μm and holder 2: 8 μm were arranged. One important thing is that prior to the flow of buffer containing 0.10 M glucose into syringe 1, it was necessary to remove air bubbles from the polypropylene tube and the filter holders. If the bubbles were present, it hindered the purification process. For that reason, before starting the experiment, 5–6 mL buffer (containing 0.10 M glucose) was poured into syringe 1. A pasteur pipette was inserted into the tube passing through that syringe 1. Then push and pull the pasteur pipette several times so that air bubbles came to the pipette and are removed. Complete removal was confirmed by checking the similar height of buffer in syringes 1 and 2. The flow rate of 1 mL/min was controlled by the peristaltic pump. The GUV suspension passed through the pores of the polycarbonate membrane to syringe 2. A 1-way polycarbonate stopcock (Luer stopcock VXB1055, AS-ONE, Japan) was inserted between filter holder 1 and the polypropylene tube, and also between filter holder 1 and 2 as shown in Fig. 3.9. After filtering the GUV suspension for 1 h, the stopcock was closed along with stopping the peristaltic pump, and the solution collected under filter holder 2 was used as purified GUV suspension for dual filtration. The time duration of about 1 h was necessary to purify the GUV suspension. Otherwise, a large population of smaller vesicles of sizes less than 3 μm remained in the purified GUV suspension. In addition, for the complete removal of the fluorescent probe (calcein) from the GUV suspension, it was also necessary to run the purification process for about 1 h. Although microfiltration [40] required a shorter time (~ 10 min) for purification, the recovery rate was relatively low ($< 50\%$). A schematic representation of the experimental setup of dual filtration is provided in Fig 3.10. The illustration is labeled by several graphical lines such as unpurified GUV suspension, GUV suspension in the first filtration, and GUV suspension in the second filtration. The stopcock 1 and 2, filter holder 1 and 2, polycarbonate membrane with larger and smaller pores, and polypropylene tube are also labeled in the illustration.

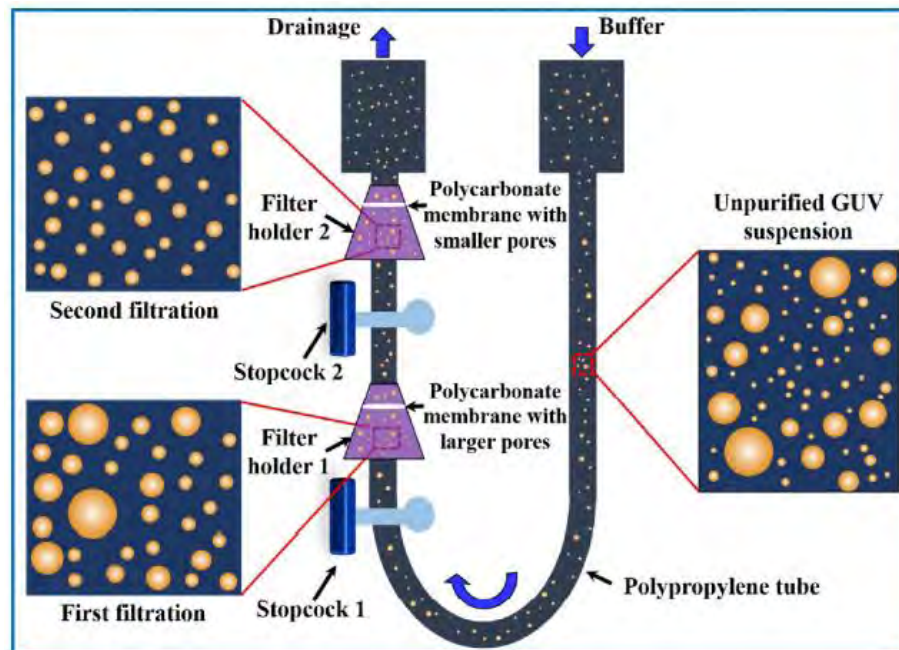


Fig. 3.10 A schematic representation of experimental set-up of dual filtration technique.

3.7 Collection of Purified GUV Suspension

The steps followed for the collection of purified GUV suspension from the space under filter holder 1 and filter holder 2, are illustrated in Fig. 3.11. It is to be remembered that the sample collected from filter holder 1 was used as a purified GUV suspension for single filtration, while the sample collected from filter holder 2 was used as a purified GUV suspension for dual filtration.

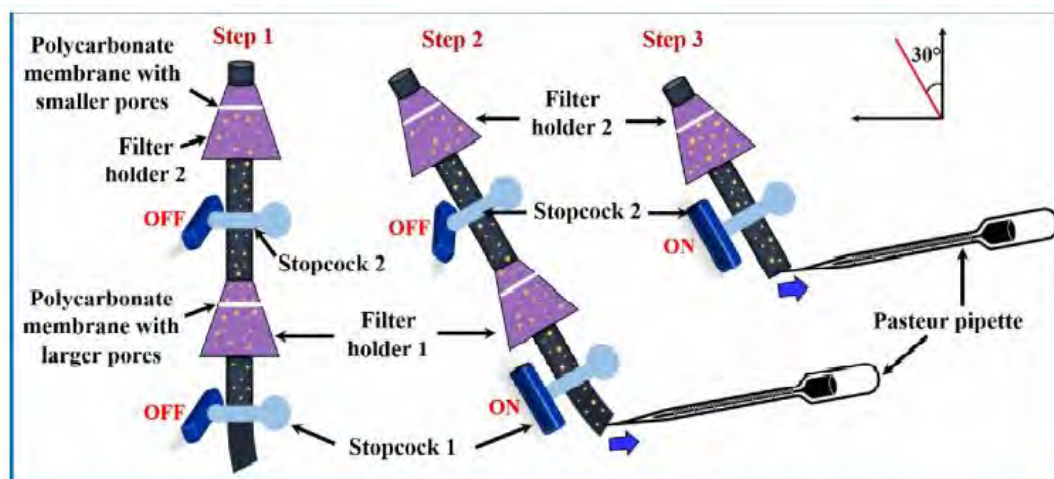


Fig. 3.11 A step-wise schematic representation of collecting the purified GUV suspension from the space under the filter holders.

In step 1, both the stopcocks were closed as the purification process was completed. The filter holder and stopcock combination were kept at an inclined position (30-degree angle) and inserted a pasteur pipette at the bottom of stopcock 1, and collected the purified GUV suspension slowly (by sucking) from the space under filter holder 1 by opening the stopcock 1 (step 2 of Fig. 3.11). In step 3, filter holder 1 with polypropylene tube was removed from the lower end of stopcock 2. Then collected the purified GUV suspension for dual filtration by opening the stopcock 2 and sucking the purified solution slowly. The purified solutions were held onto 4 eppendorf tubes for further experiment.

3.8 Single Filtration Technique

As a comparison of dual filtration with single filtration, the experimental set-up for the second is provided in Fig. 3.12. In this technique, only one filter holder with a polycarbonate membrane was used. In this case, the tube contains a total number of 9 fittings. The polycarbonate membranes were used in the filter holder with pore sizes 12 or 10 or 8 μm . The process of collecting the purified GUV suspension for single filtration is depicted in step 2 of Fig. 3.11.

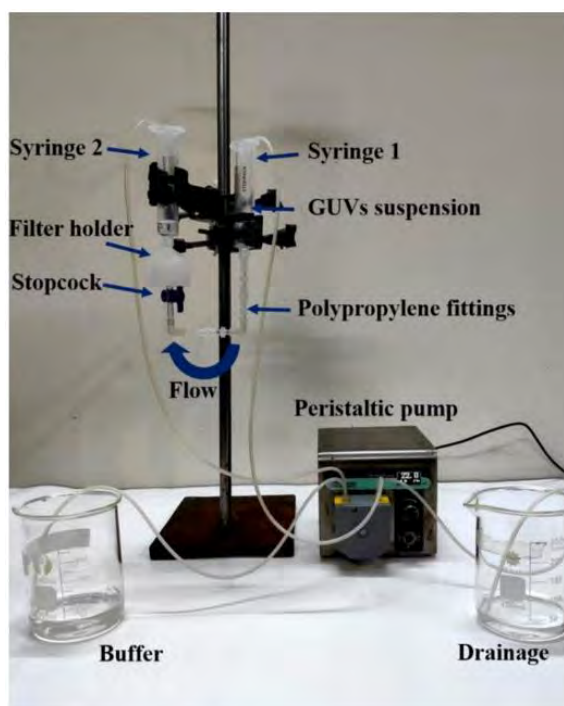


Fig. 3.12 Experimental set-up of single filtration technique.

3.9 Purification of GUVs Using an Extra Filtration with Dual Filtration

Fig. 3.13 represents the purification of GUVs using extra filtration with dual filtration. Here, polycarbonate membranes of 12, 10, and 8 μm pores were used in filter holders 1, 2, and 3, respectively. The process of collecting the purified GUV suspension for this technique is similar to that described in Fig. 3.11.

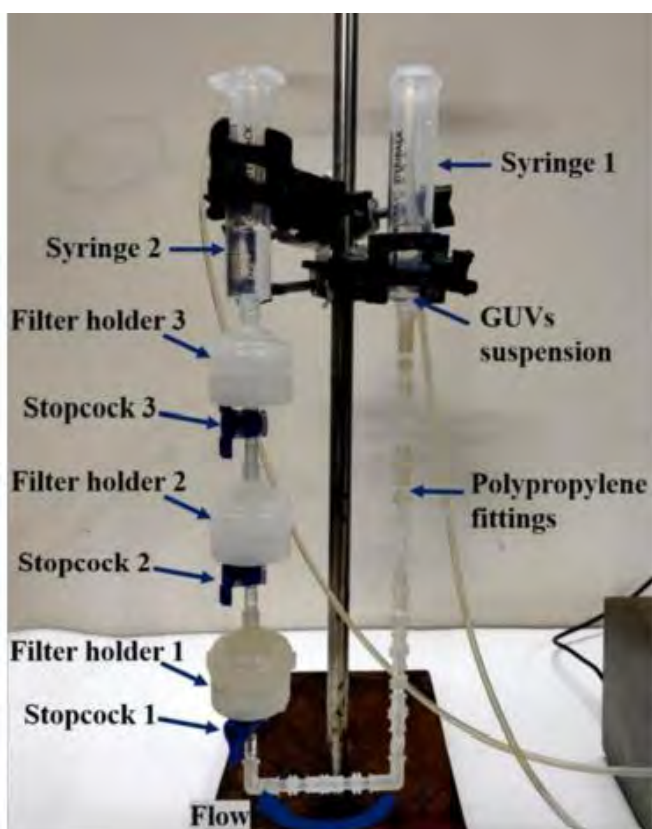


Fig. 3.13 Experimental set-up of dual filtration with using an extra filtration.

3.10 Observations of GUV

After finishing the purification, an amount of 300 μL GUV suspension was taken into a handmade microchamber (Fig. 3.14) for microscopic observation. The inside of the microchamber was coated with 0.10% (w/v) BSA dissolved in buffer (containing 0.10 M glucose) to restrict the interaction between the glass surface and GUVs. For observing the purified GUVs in suspension, buffer incorporating sucrose (0.10 M) was used as an internal solution, while buffer incorporating glucose (0.10 M) was used as an external solution of

GUVs.



Fig. 3.14 GUV suspension in handmade microchamber.

The phase-contrast fluorescence microscope is worthy for observing uncolored samples along with translucent samples. It uses the variance amidst light rays dispersing continuously originated from the source and light rays deviated by the sample while light travel through it to make bright/dark contrast to images of translucent samples. A phase-contrast objective and a condenser for observations are attached with the microscope. Samples could be formed to resemble dark while the background is bright (positive contrast) or the sample appears bright with a dark background (negative contrast). An inverted phase-contrast microscope (Olympus IX-73, Japan) with a 20x objective at 25 ± 1 °C is used for the observation of GUVs and a digital camera (Model: DP22, Olympus) is used for recording the images (Fig. 3.15).



Fig. 3.15 Inverted phase contrast fluorescence microscope.

3.11 Statistical Analysis using Lognormal Distribution

Lognormal distributions are generally used for the representation of various events having a wide field of information or data. Sometimes negative values of some specific phenomena are physically impossible. In this case, lognormal distribution plays an important role. In probability theory, the lognormal distribution is a successive regularity distribution of an arbitrary variable whose logarithm is distributed normally. Thus, if an arbitrary variable X is distributed log-normally, then, $Y = \ln(X)$ has a normal distribution. Similarly, if Y has normal distribution, the exponential function of it $X = \exp(Y)$ has a log-normal distribution [95-96]. An arbitrary variable having log-normal distribution has just positive real values. It is an appropriate and applicable model for quantification to array radar data, geology, incomes, biological and physical lifetimes, stock market prices, geography etc. [97].

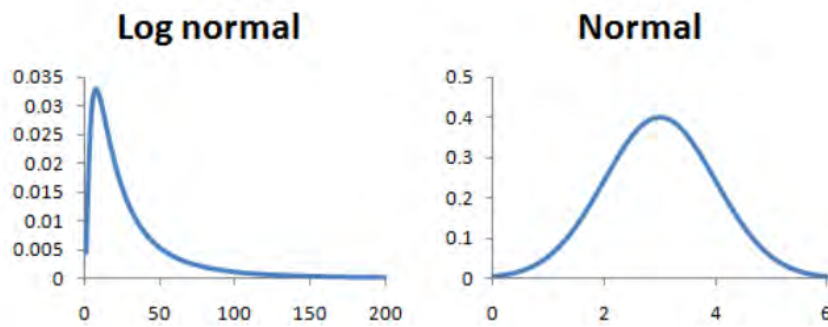


Fig. 3.16 Lognormal and normal distributions.

The size distribution histograms were analyzed with the lognormal distribution. The lognormal distribution is defined [64, 95-96] as follows:

$$f(d) = \frac{1}{d} \times \frac{1}{\sigma\sqrt{2\pi}} \exp\left(-\frac{(\ln d - \mu)^2}{2\sigma^2}\right) \quad (3.1)$$

Here, $f(d)$ represents the GUVs normalized counts having d diameter. μ represents the mean and σ^2 is the variance of the lognormal distribution. Thus, the average value of the distribution is as follows:

$$d_{ave} = \exp\left(\mu + \frac{1}{2}\sigma^2\right) \quad (3.2)$$

CHAPTER 4

RESULTS AND DISCUSSION

In the dual filtration technique, instead of using a single polycarbonate membrane, a combination of such membranes with different size pores is used. The reason we used the dual filtration technique is to get a specific size distribution of vesicles rather than a wide range of size distribution. In this technique, three types of polycarbonate membranes were used for the purification of GUVs. These are 12 μm pores polycarbonate membrane filter paper, 10 μm pores polycarbonate membrane filter paper, and 8 μm pores polycarbonate membrane filter paper. GUVs were prepared by the natural swelling method [21]. In dual filtration, three combinations of polycarbonate membranes were used in filter holder 1 and filter holder 2. For example, case (i) polycarbonate membrane with 12 μm pores in filter holder 1 and polycarbonate membrane with 10 μm pores in filter holder 2. For case (ii) the corresponding polycarbonate membranes with pores were 12 μm and 8 μm , and for case (iii) the polycarbonate membranes with pores were 10 μm and 8 μm . In each case, a polycarbonate membrane with higher pores was used in filter holder 1, and smaller pores in filter holder 2. Each arrangement provided a specific size distribution of vesicles. The purified GUV suspension was collected under the filter holder 2. In contrast, in a single filtration, only one polycarbonate membrane with pores of 12 μm or 10 μm or 8 μm was implemented in filter holder 1. It is to be noted that filter holder 2 was absent in the single filtration and in this method purified GUV suspension was collected under filter holder 1. Hence, the technique provided a wide range of size distribution of vesicles as depicted. The experimental results are presented in a set of size distribution histograms, and the distributions are analyzed by a statistical lognormal distribution. We calculated the average size of GUVs, the skewness, and the mode of distribution at various conditions.

4.1 Dual Filtration with a Combination of 12 and 10 μm Pores Polycarbonate Membranes

The effects of dual filtration with different optical microscopic images, size distributions, and a corresponding analysis of unpurified and purified GUVs has been demonstrated. The

unpurified GUV suspension was added into the 60 mL buffer containing 0.10 M glucose that was continuously flowing from syringe 1 to filter holder 1 by a peristaltic pump as described in Fig. 3.9 of chapter 3. Hence, the volume ratio of purified GUV suspension and buffer B was 1:22. For getting the image of unpurified GUV suspension, an amount of 20 μL unpurified GUV suspension was diluted with 280 μL buffer containing 0.10 M glucose solution in the microchamber, which provided the volume ratio of unpurified GUV suspension and buffer as 1:14. To investigate the effects of dual filtration with a combination of polycarbonate membranes on the size and distribution of GUVs, 12 μm pores polycarbonate membrane was used in filter holder 1, and 10 μm pores polycarbonate membrane was used in filter holder 2 (case i) as described in Fig. 3.9 of chapter 3. Fig. 4.1(A) shows a phase-contrast image of unpurified GUV suspension with different sizes of vesicles. Fig. 4.1(B) shows the corresponding histogram of the size (i.e., diameter, D) distribution of 300 GUVs (i.e., number of measured GUVs, $N = 300$), where the range of size of GUVs was 3.7–38.7 μm . Fig. 4.1(C) shows the phase-contrast image of GUVs obtained under filter holder 1. Fig. 4.1(D) shows the corresponding size distribution histogram of a similar amount of N , where the range of size of GUVs was 9.2–45.0 μm . Again, Fig. 4.1(E) shows the phase contrast image of GUVs obtained under filter holder 2 and Fig. 4.1(F) shows the corresponding size distribution histogram of similar N , where the range of size of GUVs was 6.6–26.2 μm . These results clearly indicate that a wide range of size distribution was observed when GUVs were collected under filter holder 1 since it was the first step of the dual filtration technique. In contrast, the size distribution became narrow under filter holder 2. It means that GUVs were filtered for both 12 μm and 10 μm pores polycarbonate membranes, which reduces the size of the vesicles.

The size distribution histograms were analyzed with the well-known lognormal distribution [66], which was also previously used for fitting the size distribution of GUVs [64, 98]. The lognormal distribution is described as follows:

$$f(D) = \frac{1}{D\sigma\sqrt{2\pi}} \exp\left(-\frac{(\ln D - \mu)^2}{2\sigma^2}\right) \quad (4.1)$$

where, $f(D)$ indicates the normalized counts of GUVs with diameter D , μ is the mean and σ^2 is the variance. Then the average value of the distribution [64] is as follows:

$$d_{ave} = \exp\left(\mu + \frac{1}{2}\sigma^2\right) \quad (4.2)$$

In the lognormal distribution, the skewness measures the asymmetry of the probability distribution about its mean position. The skewness of the distribution [64] is as follows:

$$\chi = [\exp(\sigma^2) + 2]\sqrt{\exp(\sigma^2) - 1} \quad (4.3)$$

Generally, the mode is the value that is most likely obtained in the samples. In lognormal distribution, it is expressed as follows [64]:

$$X = \exp(\mu - \sigma^2) \quad (4.4)$$

All the histograms of Fig 4.1 were fitted with Eq 4.1, and then the average value (d_{ave}), skewness (χ), and mode (X) of the distribution were obtained using Eqs 4.2, 4.3 and, 4.4, respectively. The coefficient of determination, R^2 , was used to evaluate the best fitting of the theoretical equation to the experimental data. In the first independent experiment, the values of d_{ave1} , were 9.9 μm for unpurified GUVs, 21.4 μm for purified GUVs under filter holder 1 and 11.1 μm for purified GUVs under filter holder 2. The values of corresponding skewness χ_1 were 1.52, 1.05 and 0.55. Similarly, the values of the corresponding mode, X_1 were 7.3, 18.2 and 10.6 μm .

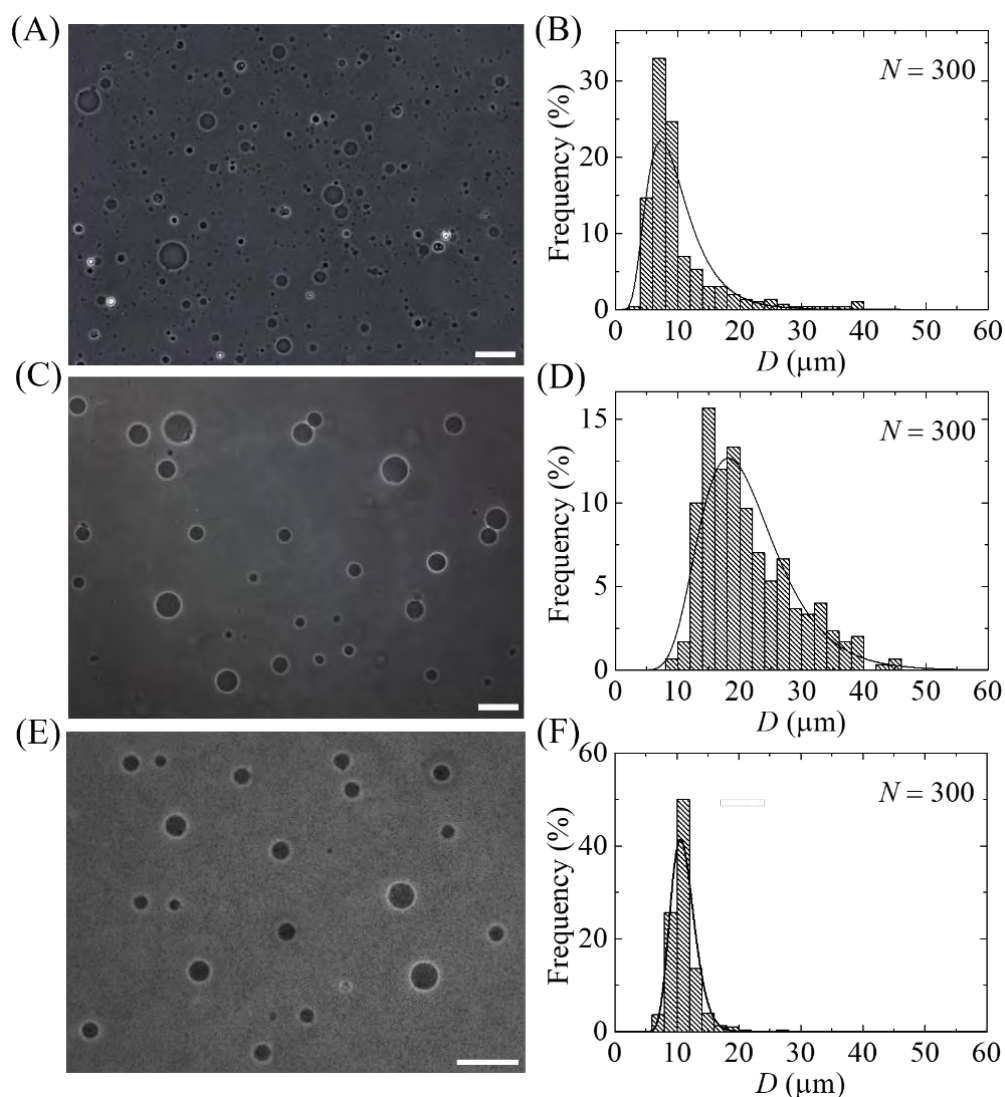


Fig. 4.1 Effects of dual filtration with 12 and 10 μm (case i) pores polycarbonate membranes on the size and distribution of 40%DOPG/60%DOPC-GUVs in the first independent experiment. The purification was performed at a flow rate of 1 mL/min for 1 h. (A), (C), and (E) show the phase-contrast image of unpurified GUVs, GUVs obtained from filter holder 1, and GUVs obtained under filter holder 2 respectively. (B), (D), and (F) represent the corresponding size distribution histograms of (A), (C), and (E) respectively. The bar in the images (A, C, E) corresponds to a length of 50 μm . The solid line of (B), (D) and (F) corresponds to fitting with Eq 4.1.

Fig. 4.2 represents the effects of dual filtration with 12 and 10 μm (case i) pores polycarbonate membranes on the size and distribution of 40%DOPG/60%DOPC-GUVs for the second independent experiment. Fig. 4.2(A) and Fig. 4.2(B) show the phase-contrast images and the corresponding size distribution histogram of unpurified GUVs. Fig. 4.2(C) and Fig. 4.2(D) show the phase contrast image and the corresponding size distribution histogram of GUVs in filter holder 1. Fig. 4.2(E) and Fig. 4.2(F) show the phase contrast image and the corresponding size distribution histogram of GUVs in filter holder 2. The ranges of the size of GUVs were obtained 3.3–58.7 μm in Fig. 4.2(B), 5.2–65.0 μm in Fig. 4.2(D) and 6.6–20.2 μm in Fig. 4.2(F). These results demonstrated that a wider range of size distribution was observed when GUVs were collected under filter holder 1 compared to filter holder 2. The number of independent experiments was three, i.e., $n = 3$. The histograms of Fig 4.2 were fitted with Eq 4.1, and then the average size, skewness and mode of the distribution were obtained using Eqs 4.2, 4.3 and 4.4, respectively. In the second independent experiment, the values of $d_{\text{ave}2}$ were obtained 11.5 μm for unpurified GUVs, 24.2 μm for purified GUVs under filter holder 1 and 10.9 μm for purified GUVs under filter holder 2. The values of the corresponding skewness χ_2 were obtained at 1.73, 1.35 and 0.61. Similarly, the values of the corresponding mode were obtained X_2 were 7.9, 18.9 and 10.2 μm in the second independent experiment. These results were very similar to those obtained in the first independent experiment. A similar result was also found for third independent experiments.

From both Fig. 4.1 and 4.2, it has been seen that the size distribution becomes narrower after double filtration. Though Fig. 4.1(B) and Fig. 4.2(B) show the narrow size distribution, these are the size distribution of unpurified GUVs. It contains many smaller vesicles, large vesicles, lipid aggregates which should be removed for the specific experiments of GUV and the size range of GUVs is large. That's why Fig. 4.1(B) and Fig. 4.2(B) are not our desired ones. Fig. 4.1(D) and Fig. 4.2(D) represent the size distribution of GUVs under filter holder 1, which were purified by 12 μm pores of polycarbonate membrane filter paper. The GUVs which were filtrated by 12 μm pores polycarbonate membrane filter paper, underwent the second filtration by 10 μm pores polycarbonate membrane filter paper. These purified GUVs were collected under filter holder 2, which gave the narrower size distribution i.e., the size range of GUVs became less.

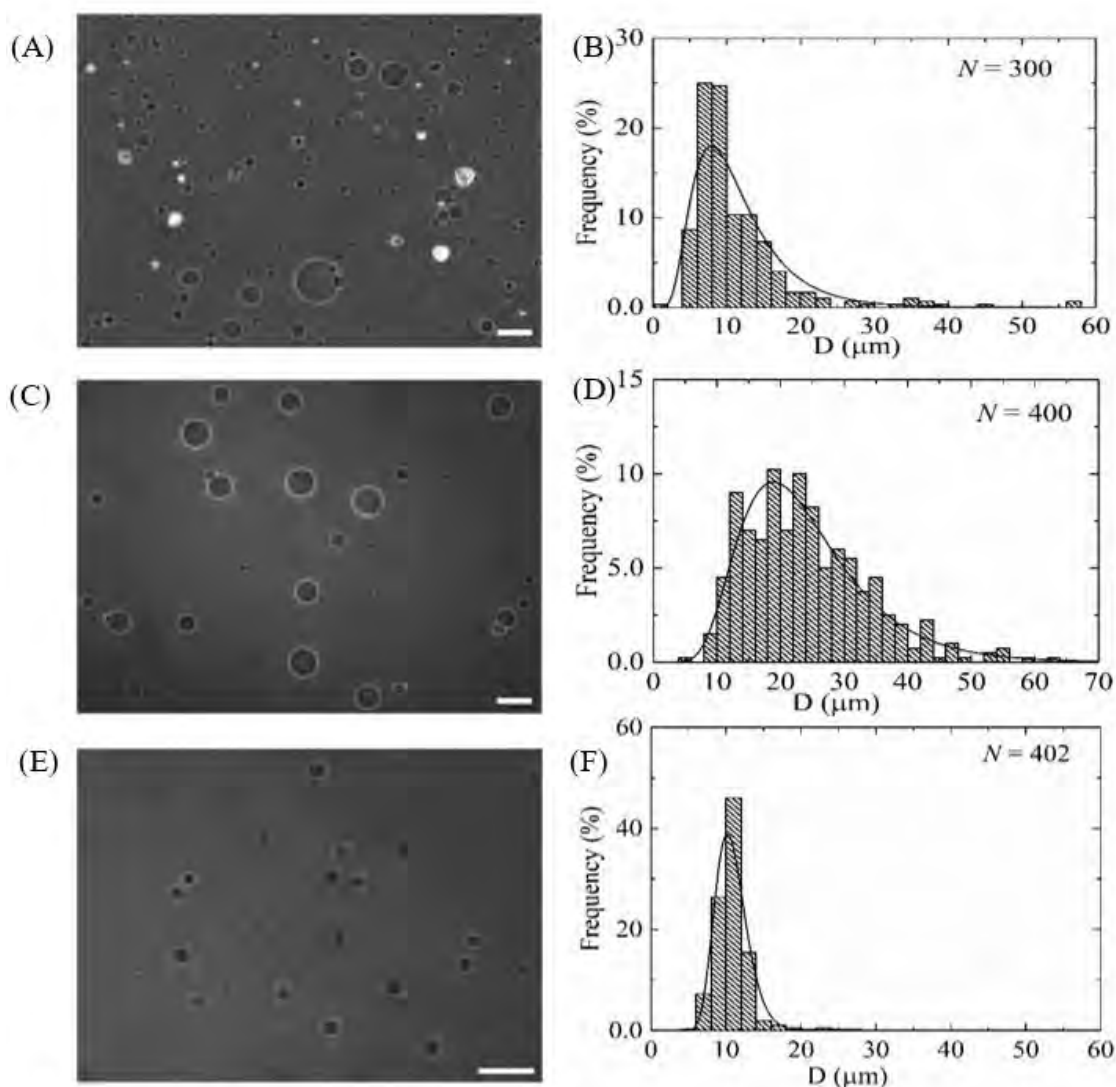


Fig. 4.2 Effects of dual filtration with 12 and 10 μm (case i) pores polycarbonate membranes on the size and distribution of 40%DOPG/60%DOPC-GUVs in the second independent experiment. The purification was performed at a flow rate of 1 mL/min for 1 h. (A), (C), and (E) show the phase-contrast image of unpurified GUVs, GUVs obtained from filter holder 1, and GUVs obtained under filter holder 2 respectively. (B), (D), and (F) represent the corresponding size distribution histograms of (A), (C), and (E) respectively. The bar in the images (A, C, E) corresponds to a length of 30 μm . The solid line of (B), (D) and (F) corresponds to fitting with Eq 4.1.

To quantify the change of GUV's size under various conditions such as unpurified GUVs, GUVs under filter holder 1, and GUVs under filter holder 2, it was necessary to measure the average size of GUVs. Skewness measurement was included to study the asymmetry of the probability distribution of the size of vesicles about their mean position. Interestingly, for all those experiments, there was a presence of some bigger size GUVs than the pores in filter holder 1, and some smaller size GUVs than the pores in filter holder 2 (Figs 4.1(F), 4.2(F)). The reason behind that the membrane of GUVs is elastic and hence, at higher pressure, some spherical GUVs alter to prolata to cylindrical-shaped vesicles [12, 99], which was passed through the pores of the polycarbonate membrane in filter holder 1. On the other hand, due to obstruction of smaller vesicles [29, 34] at the pores in filter holder 2, all the GUVs which are smaller than pore sizes would not pass through.

The reproducibility is checked by performing a similar experiment three times (i.e., $n = 3$). The arithmetic mean of the average values of the distribution, $D_{ave} = (d_{ave1} + d_{ave2} + d_{ave3})/3$, from three independent experiments were obtained $10.5 \pm 0.8 \mu\text{m}$ for unpurified GUVs, $23.0 \pm 1.5 \mu\text{m}$ for purified GUVs under filter holder 1, and $11.5 \pm 1.0 \mu\text{m}$ for purified GUVs under filter holder 2, where the values after \pm indicates standard deviation. The average values of skewness were obtained 1.73 ± 0.25 for unpurified GUVs, 1.21 ± 0.15 for purified GUVs under filter holder 1 and 0.94 ± 0.60 for purified GUVs under filter holder 2. In a similar way, the average values of mode were obtained $7.3 \pm 0.8 \mu\text{m}$ for unpurified GUVs, $18.7 \pm 0.5 \mu\text{m}$ for purified GUVs under filter holder 1 and $9.9 \pm 0.8 \mu\text{m}$ for purified GUVs under filter holder 2. These results suggest that the asymmetry in distribution became less for the samples collected from filter holder 2. The less the asymmetry means the probability of finding GUVs of similar size is higher. In addition, the mode of the distribution of GUVs under filter holder 2 is much smaller than in filter holder 1. The average size of GUVs, the skewness, and mode of distribution using the combination of $12 \mu\text{m}$ and $10 \mu\text{m}$ pores polycarbonate membranes are provided in Table 4.1.

Table 4.1 The average size of GUVs, skewness and mode of the distribution for different combinations of the polycarbonate membrane

Flow rate (mL/min)	Arrangement of polycarbonate membranes with μm pores in dual filtration		Average size of GUVs (μm) in filter holder 2	Skewness χ	Mode X (μm)
	Filter holder 1	Filter holder 2			
1.0	12	10	11.5 ± 1.0	0.94 ± 0.60	9.9 ± 0.8
	12	8	11.5 ± 0.02	1.64 ± 0.60	8.3 ± 1.5
	10	8	9.0 ± 0.03	0.81 ± 0.01	8.1 ± 0.01

4.2 Single Filtration with a 12 μm Pores Polycarbonate Membrane

An experiment was performed by using a single filtration technique with the polycarbonate membrane of pore size of 12 μm . The details of single filtration are described in the methodology section 3.8. The size distribution histograms of unpurified and purified GUVs are shown in Fig. 4.3 (A) and (B), respectively. The range of sizes for purified GUVs was 6–60 μm . Both the histograms were fitted using Eq 4.1, and the average sizes of the distribution were 16.0 μm for unpurified GUVs and 23.5 μm for purified GUVs. The skewness of the distribution of unpurified GUVs was 1.86 and purified GUV suspension was 1.23. The average size of purified GUVs is greater than the unpurified ones because, a large number of smaller vesicles than the pore size (in this case, the pore size of

polycarbonate membrane filter paper is $12\ \mu\text{m}$) is eliminated during the purification process. This makes the greater average size of the purified GUVs than unpurified GUVs.

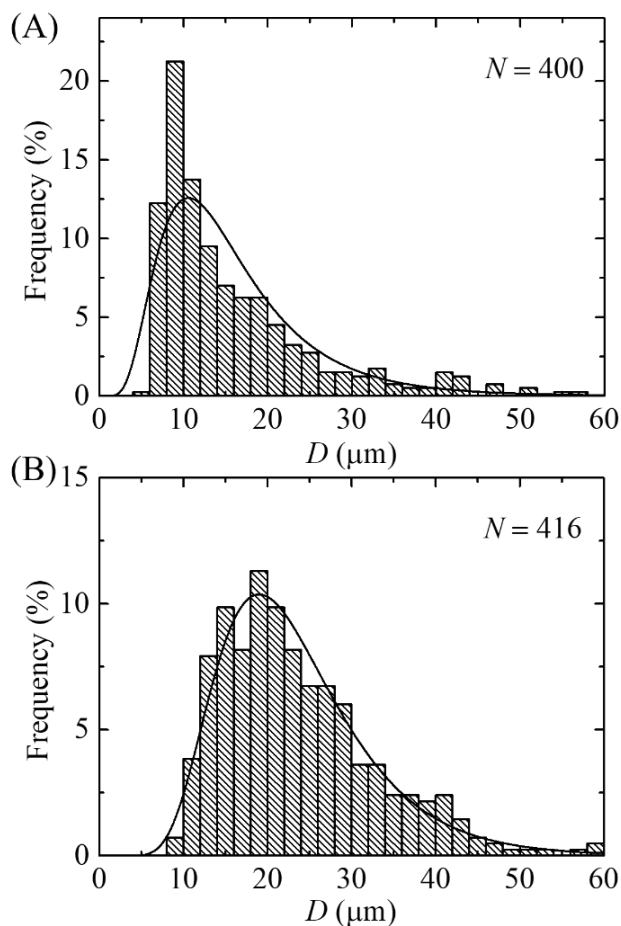


Fig. 4.3 Effects of single filtration (using $12\ \mu\text{m}$ pores polycarbonate membrane filter paper) on the size distribution of 40%DOPG/60%DOPC-GUVs in the first independent experiment. (A), (B) represents the size distribution histogram for the unpurified and purified GUVs respectively. The purification was performed at a flow rate of $1\ \text{mL}/\text{min}$ for 1 h. The solid line of figures corresponds to fitting with Eq 4.1.

Another experiment was performed by using a single filtration technique with $12\ \mu\text{m}$ pores polycarbonate membrane under the same condition. The size distribution histograms of unpurified and purified GUVs are shown in Fig. 4.4 (A) and (B), respectively. Both the

histograms were fitted using Eq 4.1. The range of sizes for purified GUVs was 7–59 μm and the average sizes of the distribution were 12.02 μm for unpurified GUVs and 22.08 μm for purified GUVs. The skewness of the distribution of unpurified GUVs was 1.58 and purified GUV suspension was 1.19.

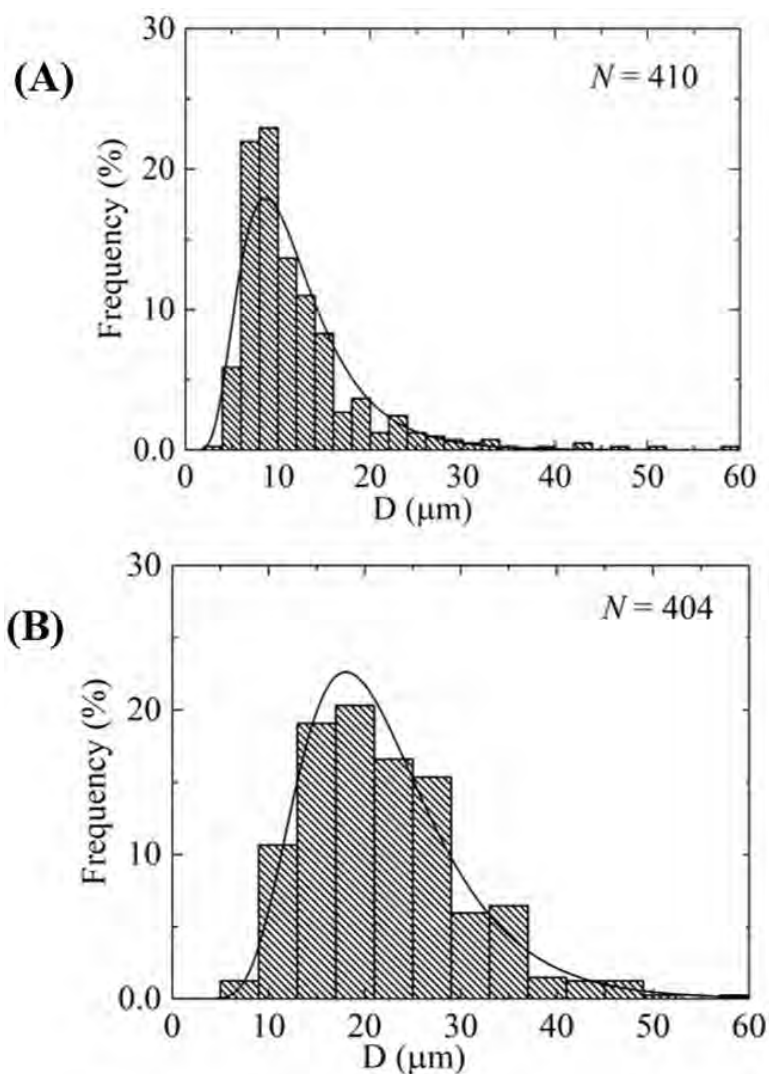


Fig. 4.4 Effects of single filtration (using 12 μm pores polycarbonate membrane filter paper) on the size distribution of 40%DOPG/60%DOPC-GUVs in the second independent experiment. (A), (B) represents the size distribution histogram for the unpurified and purified GUVs respectively. The purification was performed at a flow rate of 1 mL/min for 1 h.

In this condition, one filter holder is used in the set-up of purification, thus it is called single filtration. GUVs were purified by only one polycarbonate membrane filter paper. They underwent one filtration, where 12 μm pores polycarbonate membrane filter paper was inserted in filter holder 1. Theoretically, all of the GUVs smaller than 12 μm should go to the drainage but due to the pore-clogging by smaller vesicles, some smaller vesicles remained in purified GUV suspension. But most of the smaller vesicles, lipid aggregates, non-entrapped solutes were eliminated. Size distribution histogram fitted with lognormal distribution and the distribution is wider. This size distribution is very similar to the distribution obtained under filter holder 1 in case (i) for dual filtration.

Four independent experiments (i.e., $n = 4$) were performed at the same condition and obtained the values of D_{ave} as $12.3 \pm 2.6 \mu\text{m}$ for unpurified and $22.8 \pm 1.3 \mu\text{m}$ for purified GUVs. The average values of skewness were obtained 1.65 ± 0.15 for unpurified GUVs and 1.21 ± 0.12 for purified GUVs. The average values of mode were obtained $8.7 \pm 1.4 \mu\text{m}$ for unpurified GUVs and $18.5 \pm 0.5 \mu\text{m}$ for purified GUVs. The values of GUVs size range, average size, skewness, and mode were much higher in single filtration as compared to that obtained in dual filtration technique, i.e., purified GUVs under filter holder 2. The values of skewness and mode were 1.21 ± 0.12 and $18.5 \pm 0.5 \mu\text{m}$ for single filtration, while the corresponding values were 0.94 ± 0.60 and $9.9 \pm 0.8 \mu\text{m}$ for dual filtration. Moreover, as expected the values obtained in single filtration were very similar to that obtained from filter holder 1 in dual filtration since the pore sizes of the filters were the same.

4.3 Single Filtration with 10 μm Pores Polycarbonate Membrane

An experiment was performed by using a single filtration technique with a 10 μm pores polycarbonate membrane. For the first independent experiment, the size distribution histograms of unpurified and purified GUVs are shown in Fig. 4.5(A) and (B), respectively. The range of sizes for purified GUVs was 6.27–48.34 μm and that for unpurified GUVs was 3.69–75.64 μm . Both the histograms were fitted using Eq 4.1, and the average sizes of the distribution were 10.3 μm for unpurified GUVs and 18.78 μm for purified GUVs. The

skewness of the distribution of unpurified GUVs was 2.0 and that of purified GUV suspension was 1.3. The solid line of figures corresponds to the fitting with Eq 4.1.

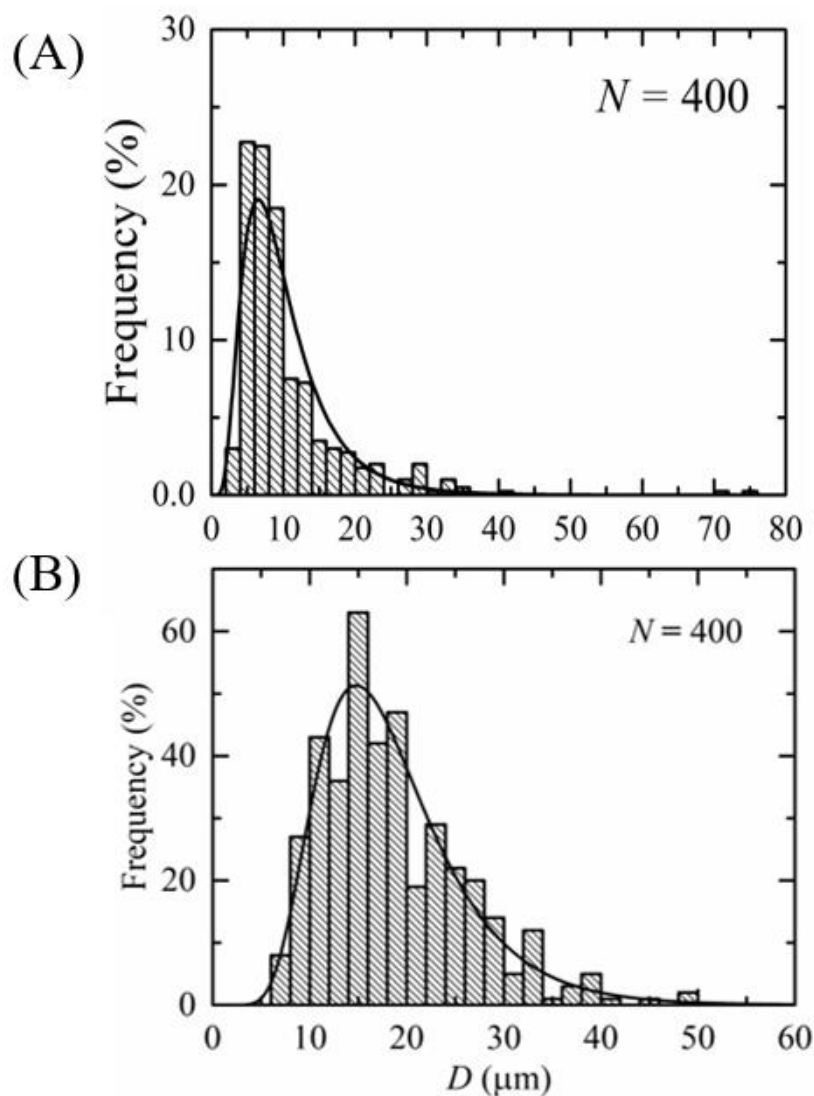


Fig. 4.5 Effects of single filtration (using 10 μm pores polycarbonate membrane filter paper) on the size distribution of 40%DOPG/60%DOPC-GUVs in the first independent experiment. (A), (B) represents the size distribution histogram for the unpurified and purified GUVs respectively. The purification was performed at a flow rate of 1 mL/min for 1 h.

Another experiment was performed by using a single filtration technique with a 10 μm pores polycarbonate membrane under the same condition as was done in section 4.3. The size

distribution histograms of unpurified and purified GUVs are shown in Fig. 4.6 (A) and (B), respectively. Both the histograms were fitted using Eq 4.1. The range of sizes for purified GUVs was 5–49 μm and for unpurified GUVs was 3.69–40.22 μm . The average sizes of the distribution were 10.33 μm for unpurified GUVs and 17.12 μm for purified GUVs. The skewness of the distribution of unpurified GUVs was 1.5 and that of purified GUV suspension was 1.32.

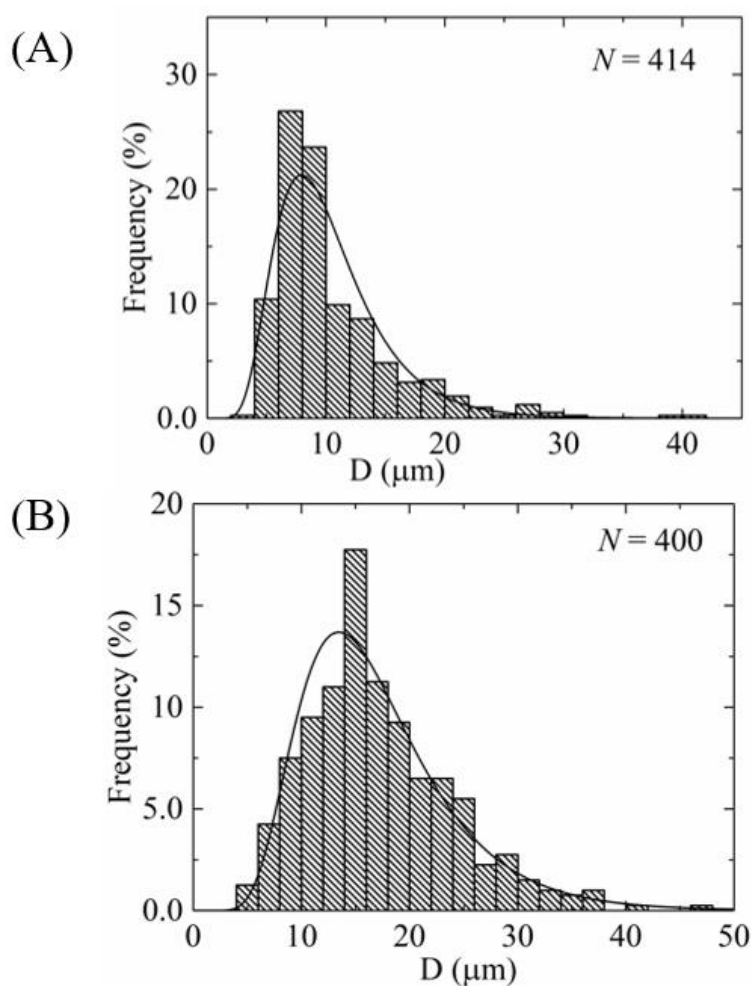


Fig. 4.6 Effects of single filtration (using 10 μm pores polycarbonate membrane filter paper) on the size distribution of 40%DOPG/60%DOPC-GUVs in the second independent experiment. (A), (B) represents the size distribution histogram for the unpurified and purified GUVs respectively. The purification was performed at a flow rate of 1 mL/min for 1 h.

These experiments were performed at the same condition and obtained the values of D_{ave} as $17.95 \pm 0.41 \mu\text{m}$ for unpurified and $10.32 \pm 0.01 \mu\text{m}$ for purified GUVs. The average values of skewness were obtained 1.75 ± 0.12 for unpurified GUVs and 1.31 ± 0.01 for purified GUVs.

4.4 Dual Filtration with the Combinations of 12 and 8 μm , and 10 and 8 μm Pores Polycarbonate Membranes

The size distribution of GUVs using 12 μm pores polycarbonate membrane used in filter holder 1 and 10 μm pores polycarbonate membrane used in filter holder 2 (in case (i)) was described in section 4.1. In case (ii), a membrane with 12 μm pores was used in filter holder 1 and 8 μm pores used in filter holder 2. In case (iii), a membrane with 10 μm pores was used in filter holder 1 and 8 μm pores used in filter holder 2. Here the results of phase-contrast images and size distribution of GUVs for case (ii) and case (iii) are presented. In Fig. 4.7, (A) and (C) show the phase-contrast images of purified GUVs under filter holder 2 for case (ii) and case (iii), respectively.

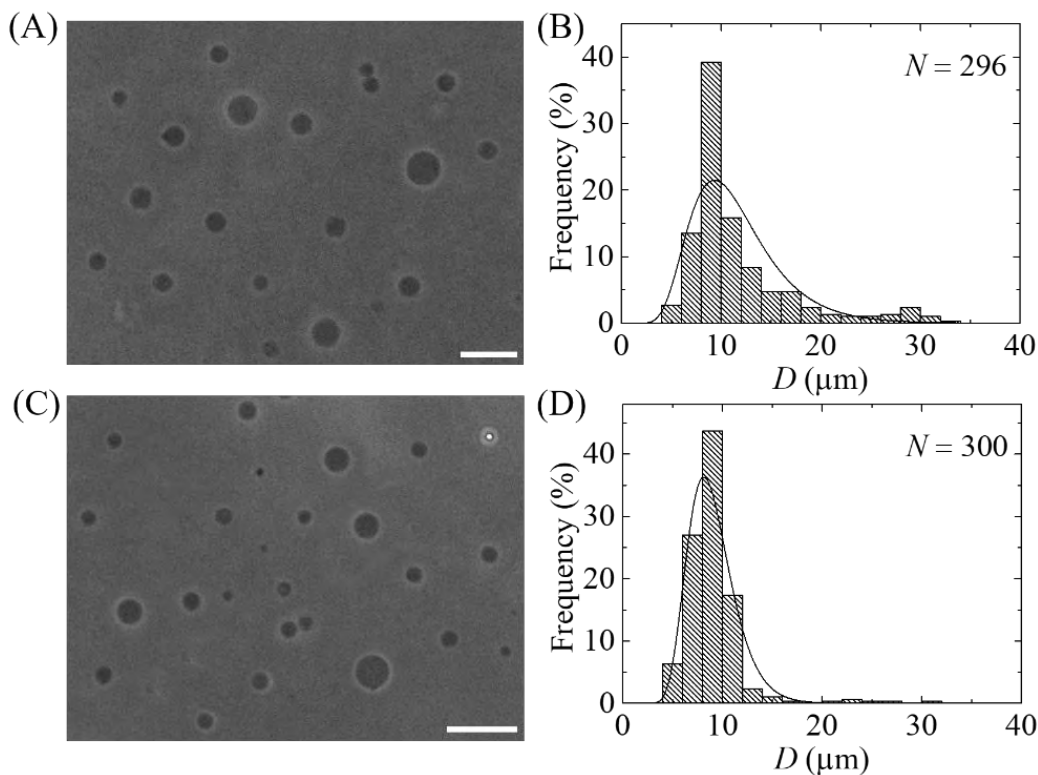


Fig. 4.7 Effects of dual filtration with 12 and 8 μm (case ii), and 10 and 8 μm (case iii) pores polycarbonate membranes on the size and distribution of 40%DOPG/60%DOPC-GUVs in the first independent experiment. The purification was performed at a flow rate of 1 mL/min for 1 h. (A), (B) represents the phase-contrast image and corresponding size distribution histogram under filter holder 2 respectively for case (ii), and (C), (D) represents the phase-contrast image and corresponding size distribution histogram under filter holder 2 respectively for case (iii). The bar in the images (A, C) corresponds to a length of 50 μm .

The corresponding size distribution histograms were presented in (B) and (D). The GUVs size distribution was 5.2–32.4 μm for case (ii), whereas it was 4.4–30.3 μm for case (iii). Both the size distributions were well fitted to Eq 4.1. From the fitted curves, the average value of the distribution was 11.5 μm and the corresponding skewness and mode were 1.23 and 9.3 μm for case (ii). For case (iii), the average value of the distribution was 9.0 μm and the corresponding skewness and mode were 0.82 and 8.1 μm .

Another experiment was performed for both case (ii) and case (iii). In Fig. 4.8, (A) and (C) show the phase-contrast images of purified GUVs under filter holder 2 for case (ii) and case (iii), respectively for the second experiment. The corresponding size distribution histograms were presented in (B) and (D).

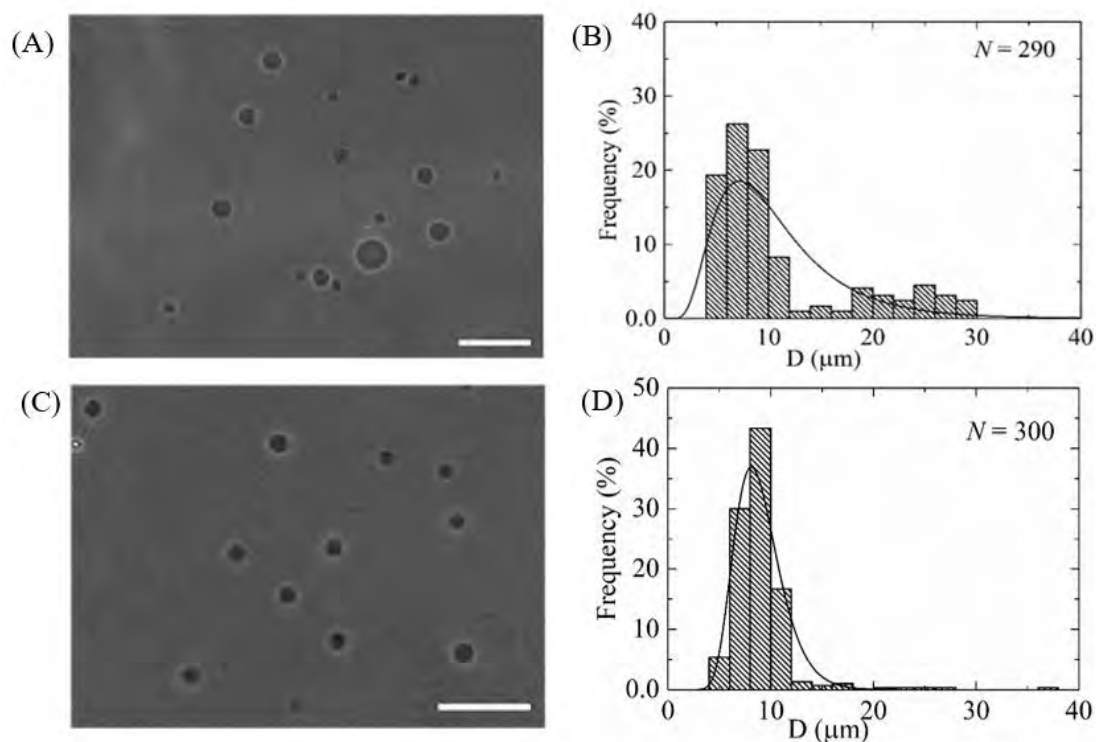


Fig. 4.8 Effects of dual filtration with 12 and 8 μm (case ii), and 10 and 8 μm (case iii) pores polycarbonate membranes on the size and distribution of 40%DOPG/60%DOPC-GUVs in the second independent experiment. The purification was performed at a flow rate of 1 mL/min for 1 h. (A), (B) represents the phase-contrast image and corresponding size distribution histogram under filter holder 2 respectively for case (ii), and (C), (D) represents the phase-contrast image and corresponding size distribution histogram under filter holder 2 respectively for case (iii). The bar in the images (A, C) corresponds to a length of 30 μm .

The GUVs size distribution was 4.4–29.2 μm for case (ii), whereas it was 4.4–37.2 μm for case (iii). The purification was performed at a flow rate of 1 mL/min for 1 h. The bar in the images (A, C) corresponds to a length of 30 μm . The average sizes of GUVs from the second experiment were obtained at 11.6 and 8.97 μm for cases (ii) and (iii), respectively. The corresponding skewness and mode were 2.05 and 7.2 μm for cases (ii). For case (iii), the corresponding skewness and mode were 0.81 and 8.1 μm .

The average sizes of GUVs from $n = 2$ were obtained 11.5 ± 0.02 and 9.0 ± 0.03 μm for case (ii) and (iii), respectively. It is worth mentioning that after two independent experiments, the size distribution was found significantly similar, and thus further experiment was not conducted. The corresponding values of skewness were 1.64 ± 0.6 and 0.81 ± 0.01 . The corresponding values of mode were 8.3 ± 1.5 and 8.1 ± 0.01 μm .

By using three combinations of polycarbonate membrane filter paper, three different size distributions can be obtained by the dual filtration technique. For the latter 2 cases, some vesicles larger and smaller than the pore size were also found. The reason behind that was the same as that described for case (i). Hence, for all three cases of dual filtration, the distribution followed smaller skewness compared to single filtration. The average size of GUVs, the skewness, and mode of distribution using different combinations are provided in Table 4.1. It has been seen that the skewness of size distribution for case (ii) was relatively higher than case (i) and case (iii) (Table 4.1). The higher skewness in case (ii) can be explained in the way that the pore size difference between the filters was higher (i.e., $12-8 = 4$ μm), whereas for other cases it was smaller (i.e., $12-10 = 10-8 = 2$ μm). As a comparison of dual filtration techniques, time duration (i.e., 1 h) was comparable with single membrane filtering [34] and gravity-based purification technique [36]. In the dual filtration technique, for all three cases, the specific size distribution of vesicles was obtained rather than a wide range size distribution as obtained in single filtration.

4.5 Purification of GUVs Containing Water-Soluble Fluorescent Probe, Calcein, Using Dual Filtration Technique

The purification of GUVs encapsulating a water-soluble fluorescent probe, calcein (molecular weight 623, Stokes-Einstein radius 0.74 nm) [100] was also investigated. GUVs were purified using case (i). In this case, 12 μm pores polycarbonate membrane was used in filter holder 1 and 10 μm pores polycarbonate membrane was used in filter holder 2. Before purification, the GUV suspension contained a strong green color due to 1 mM calcein (Fig. 4.9(A)). After centrifugation, the supernatant of unpurified GUV suspension containing calcein was added into the 60 mL buffer containing 0.10 M glucose that was continuously flowing from syringe 1 to filter holder 1 by a peristaltic pump. Hence, the volume ratio of purified GUV suspension and buffer containing 0.10 M glucose was 1:22. While running the process of purification, the green color in syringe 1 buffer was diminishing. After purification, the suspension became colorless, indicating a calcein-free GUV suspension in buffer (with 0.10 M glucose) which can be seen from Fig. 4.9(B). Fig. 4.9(C) shows a fluorescence microscopic image of unpurified GUV suspension.

As the calcein solution appeared in GUV suspension, the GUVs were not clearly observed in Fig. 4.9(C). The fluorescence microscopic image of purified GUV suspension is shown in Fig. 4.9(D), in which the calcein solution is located the inside of GUVs. The outside became dark, which means that the calcein solution was removed from the GUV suspension. The size distribution of purified GUVs (Fig. 4.9(E)) was fitted to Eq 4.1. The average size of distribution was 13.3 μm and the corresponding skewness of distribution was 1.29.

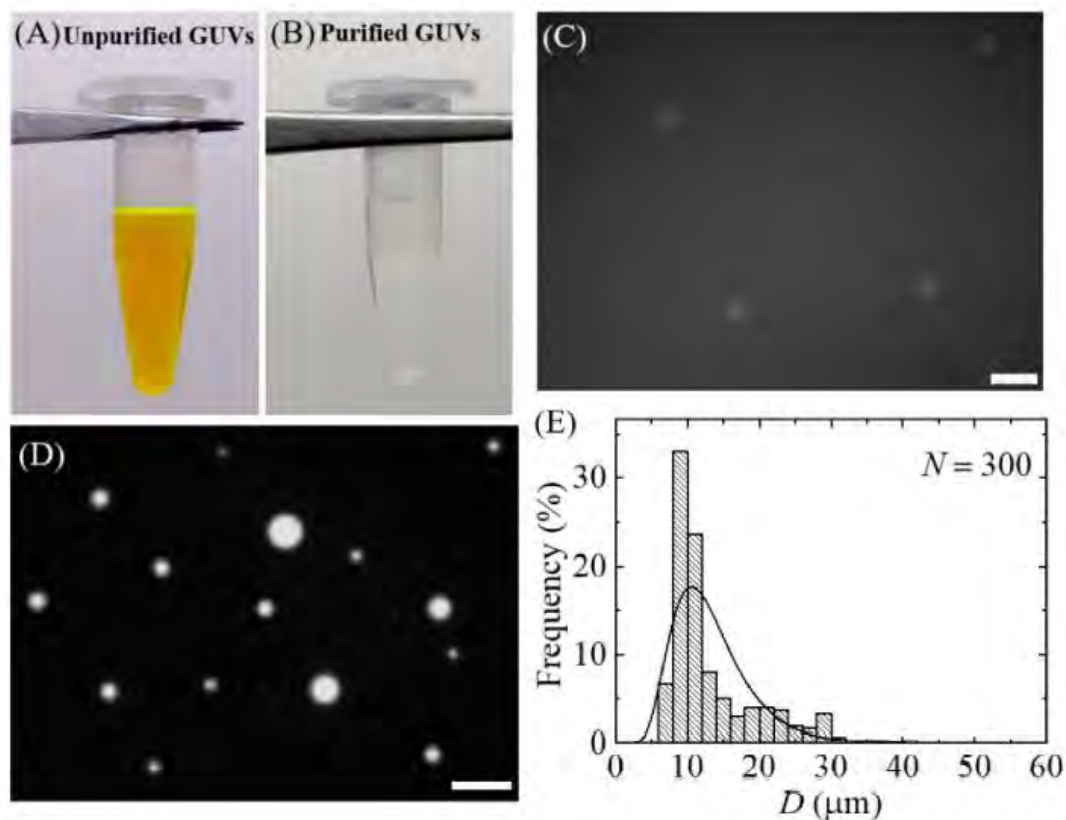


Fig. 4.9 Purification of 40%DOPG/60%DOPC-GUVs containing calcein using the dual filtration technique in the first independent experiment. The purification was performed at a flow rate of 1 mL/min for 1 h. (A) and (B) represents the unpurified and purified GUV suspensions respectively. (C), (D) represents the phase-contrast images of unpurified and purified (collected under filter holder 2) GUVs respectively, and (E) represents the size distribution histograms of purified GUVs. The bar in the images (C, D) corresponds to a length of 50 μm .

Another independent experiment was performed. The average size distribution of purified GUVs was found at 12.72 and the corresponding skewness of distribution was found at 1.67. Fig. 4.10(A) shows the fluorescence microscopic image of purified GUV suspension and

Fig. 4.10(B) represents the corresponding size distribution histogram for the second experiment. Thus, the average size of GUVs and the corresponding skewness for $n = 2$ were $13.0 \pm 0.5 \mu\text{m}$ and 1.24 ± 0.60 respectively. These values were very similar to those obtained in case (i) in section 4.1. These results suggested that the dual filtration technique can be used for the removal of the water-soluble fluorescent probe from the outside of GUV suspension.

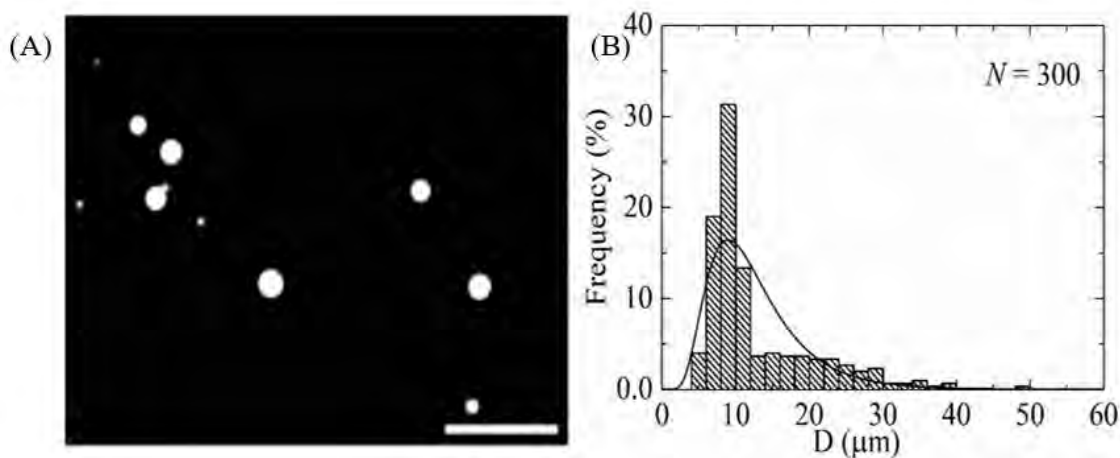


Fig. 4.10 Purification of 40%DOPG/60%DOPC-GUVs containing calcein using the dual filtration technique in the second independent experiment. The purification was performed at a flow rate of 1 mL/min for 1 h. (A) represents the phase-contrast image of purified GUVs and (B) represents the corresponding size distribution histogram. The bar in the image (A) corresponds to a length of 30 μm .

The dual filtration technique was able to purify the GUVs by removing the calcein from the outer suspension of vesicles (Figs. 4.9 and 4.10). Since the Stokes-Einstein radius of calcein is very much smaller (i.e., 0.74 nm) than the size of the pores, therefore, calcein was easily passed through the pores. The paper [29] used single filtration for the removal of the water-soluble fluorescent probe from the GUV suspension. Therefore, the removing ability of the water-soluble fluorescence probe using the dual filtration technique was necessary. The experimental results for removing the water-soluble fluorescence probe were evidence of

removing the smaller vesicles. The GUVs with diameters greater than 3 μm could be measured using an optical microscope without any difficulties. The vesicles with diameters less than 3 μm were not measured. The GUVs with sizes less than 2 μm were not considered as they were too small to visualize [34]. That limitation was also observed by another research group [29].

4.6 Effects of Flow Rate on the Average Size of GUVs in Dual Filtration Technique

The dependence of the average GUV size on the flow rate was investigated using 0.75, 1.0, 1.5 and 2.0 mL/min. In Fig. 4.11, it has been seen that the average size of GUVs increased at least 10% at flow rate 1.0–2.0 mL/min than 0.75 mL/min. This increment may occur due to the passes of some GUVs with diameters higher than the pores of polycarbonate membrane in filter holder 1 due to higher pressure [12, 99]. As the average size for 1.0–2.0 mL/min became the same within the experimental error, those flow rates were considered as suitable for the dual filtration technique. It is to be noted that the investigation was performed for case (i) using 40%DOPG/60%DOPC-GUVs.

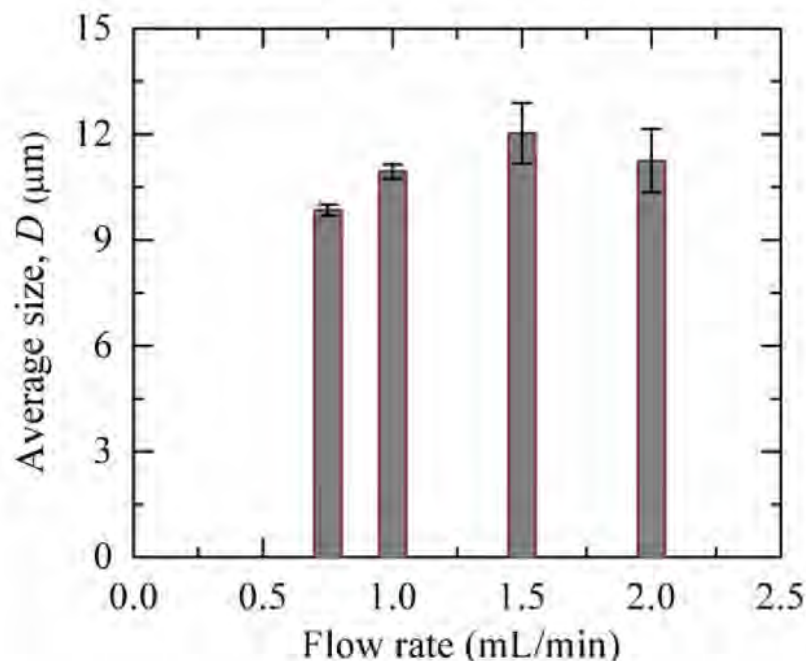


Fig. 4.11 Flow rate dependent average size of purified 40%DOPG/60%DOPC-GUVs using dual filtration technique. The average values and standard deviations for different flow rates were calculated for 3-4 independent experiments.

4.7 Fraction of Required Sizes GUVs in Filter Holder 2 Compared to the Total Number of GUVs Before Filtration

The fraction of required sizes GUVs under filter holder 2 compared to the total number of GUVs before filtration was calculated. It was calculated as the number of GUVs counted within the size of filter pore sizes divided by the total count of GUVs before filtration. For example, in an experiment of the case (i), at first, the total number of 300 GUVs before purification was measured. Then the same number of GUVs was measured under filter holder 2 and counted the GUVs in the range of 10–12 μm . If 150 GUVs were counted, the fraction of required sizes GUVs under filter holder 2 would be $(150/300) \times 100\% = 50\%$. For the second and third repetitions of the case (i), it was 46% and 50%, respectively. Hence, the average fraction of required sizes GUVs under filter holder 2 was $(49 \pm 2) \times 100\%$ for case (i). Similarly, case (ii) and case (iii) were calculated, and presented in Table 4.2.

Table 4.2 Fraction of required sized GUVs under filter holder 2 compared to the total number of GUVs before filtration for different combinations of polycarbonate membranes.

Purification	Flow rate (mL/min)	Arrangement of polycarbonate membranes with μm pores in dual filtration		Fraction of required sized GUVs under filter holder 2 (%)
		Filter holder 1	Filter holder 2	
Purification once	1.0	12	10	49 ± 2
		12	8	42 ± 2
		10	8	30 ± 1
Purification twice	1.0	12	10	83 ± 1
		12	8	74 ± 3
		10	8	58 ± 2

4.8 Effects of Repeating Dual Filtration on The Size Distribution of GUVs

The effects of two times purification on the size distribution of GUVs, i.e., repeat dual filtration of the case (i) using the purified GUV suspension was observed as well. The phase-contrast images and corresponding size distributions of GUVs after first and second purifications are shown in Fig. 4.12. Fig. 4.12(A) and (B) show the phase contrast image and the corresponding size distribution histogram of GUVs in filter holder 2 after the first purification. Fig. 4.12(C) and (D) show the phase contrast image and the corresponding size distribution histogram of GUVs in filter holder 2 after the second purification.

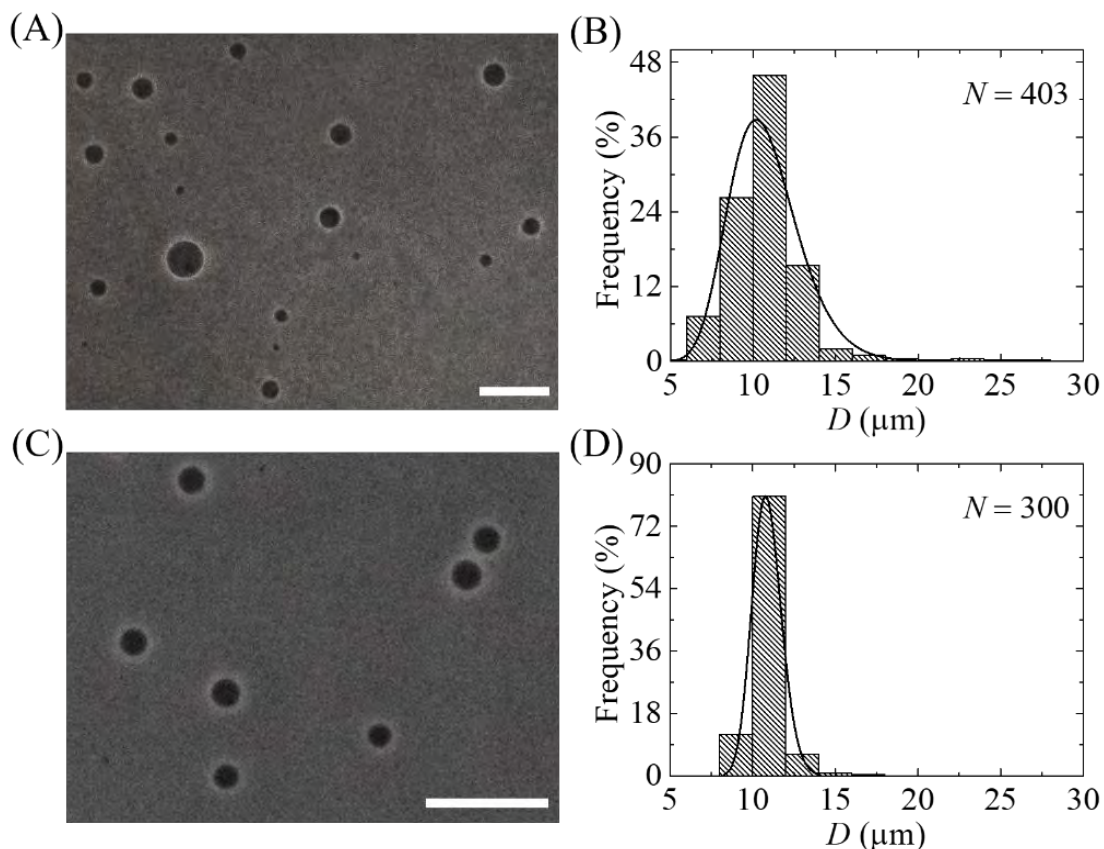


Fig. 4.12 Effects of repeated purification on the 40%DOPG/60% DOPC-GUVs (for case (i), first independent experiment). The purification was performed at a flow rate of 1 mL/min for 1 h. (A) and (B) represent the phase contrast image and the corresponding size distribution histogram of GUVs in filter holder 2 after the first purification. (C) and (D) represent the phase contrast image and the corresponding size distribution histogram of GUVs in filter holder 2 after the second purification. The bar in the images (A, C) corresponds to a length of 50 μm .

In histograms, the ranges of GUVs sizes were 5.9–27.3 μm and 8.1–16.2 μm after first and second purification, respectively. These results indicated that the size distribution of GUVs became narrow after the second purification. We fitted the size distributions using Eq 4.1, and the average values of the size distribution were 10.8 and 12.7 μm for the first and

second purification, respectively. The corresponding values of skewness were 0.61 and 0.22. The corresponding values of mode were 10.2 μm and 10.7 μm .

The second independent experiment was performed for the same condition. The phase-contrast images and corresponding size distributions of GUVs after first and second purifications are shown in Fig. 4.13. In histograms, the ranges of GUVs sizes were 6.6–26.2 μm and 8.5–15.5 μm after first and second purification, respectively. These results indicated that the size distribution of GUVs became narrow after the second purification. We fitted the size distributions using Eq 4.1, and the average values of the size distribution were 11.1 and 10.9 μm for the first and second purification, respectively. The corresponding values of skewness were 0.55 and 0.25. Similarly, the corresponding values of mode were 10.6 μm and 10.8 μm . Fig. 4.13(A) and (B) show the phase contrast image and the corresponding size distribution histogram of GUVs in filter holder 2 after the first purification. Fig. 4.13(C) and (D) show the phase contrast image and the corresponding size distribution histogram of GUVs in filter holder 2 after the second purification.

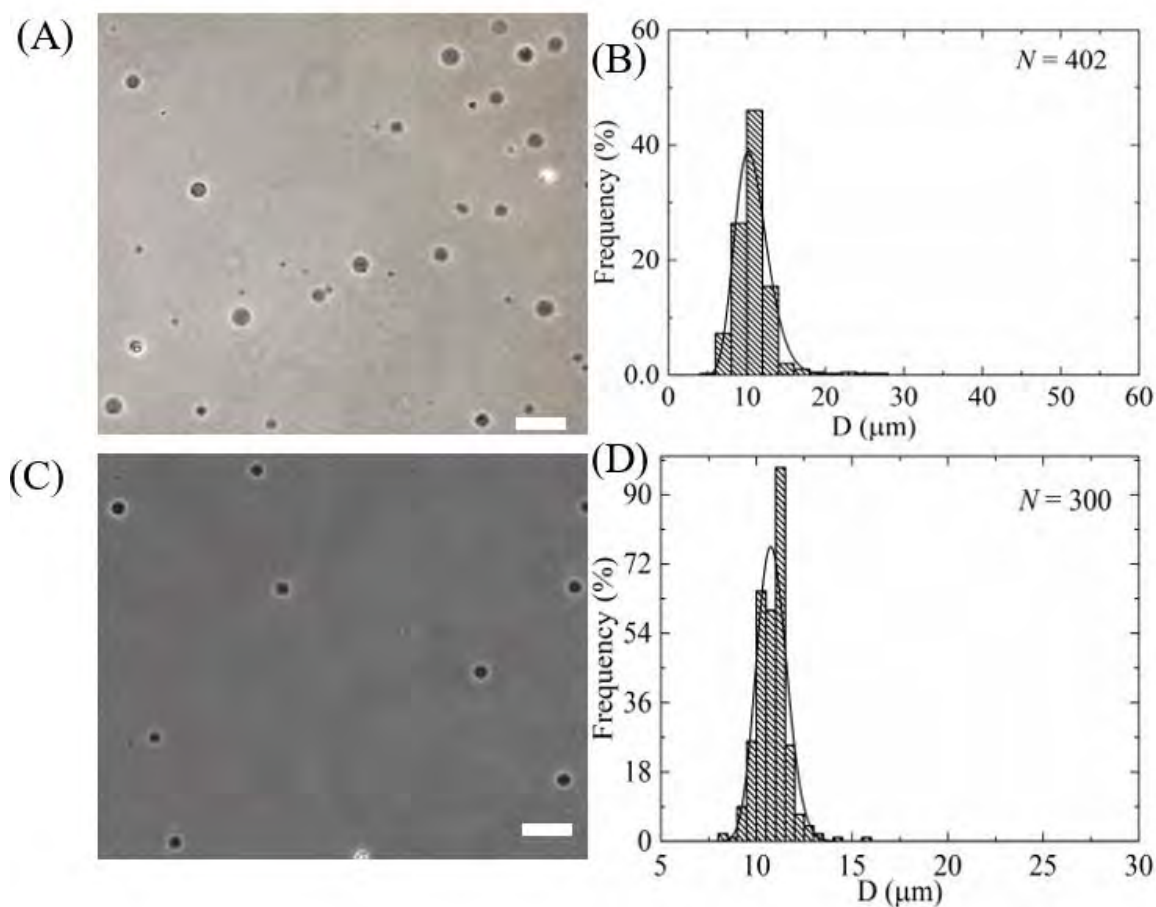


Fig. 4.13 Effects of repeated purification on the 40%DOPG/60% DOPC-GUVs (for case (i), second independent experiment). The purification was performed at a flow rate of 1 mL/min for 1 h. (A) and (B) represent the phase contrast image and the corresponding size distribution histogram of GUVs in filter holder 2 after the first purification. (C) and (D) show the phase contrast image and the corresponding size distribution histogram of GUVs in filter holder 2 after the second purification. The bar in the images (A, C) corresponds to a length of 20 μm .

The average sizes of GUVs were 10.9 ± 0.2 and 13.0 ± 0.5 μm ($n = 2$) while the values of average skewness were 0.58 ± 0.04 and 0.23 ± 0.02 for the first and second purification, respectively. The corresponding values of mode were 10.4 ± 0.3 and 10.8 ± 0.03 μm for the first and second purification, respectively. The value of skewness became lesser after the

second purification, indicating the higher number of similar sizes GUVs in filter holder 2. In addition, the value of mode in the second purification was higher compared to the first purification, indicating also the higher number of similar sizes GUVs in filter holder 2. Moreover, the fraction of required sized GUVs under filter holder 2 compared to the total number of GUVs before filtration for case (i) was $(83 \pm 1)\%$ after the second purification, while it was $(49 \pm 2)\%$ in the first purification as shown in Table 4.2. The corresponding values for case (ii) and case (iii) are also presented in Table 4.2. These investigations clearly indicate that if we need more similar size GUVs, it is necessary to perform purification more than once.

By repeating the dual filtration twice, a higher fraction of required size GUVs was obtained. The reason was that initially, the presence of many smaller vesicles hinders the passage of GUVs through the pores, those vesicles were less in the purified GUV suspension. The hindrance became negligible in the second purification as the purified suspension was used. Moreover, a new set of polycarbonate membranes was used in the filter holders before repeating the experiment. The skewness was much smaller (0.23 ± 0.02) in second purification compared to first purification (0.58 ± 0.04) (Figs. 4.12(B), (D); 4.13(B), (D)). For case (i) such as for the combination of 10 μm and 12 μm pores polycarbonate membranes, the fraction of required size GUVs under filter holder 2 compared to the total number of GUVs before filtration was 49% for purification once, while the corresponding value was 83% for purification twice. Therefore, the required sized vesicles contain $\sim 49\%$ of the total volume of the original population for purification once, while the corresponding value was $\sim 83\%$ for purification twice. The remaining amount of lipids was lost. These values varied for other combinations of polycarbonate membrane as presented in Table 4.2. To get a concentrated similar size of GUVs, the second purification is an important choice though it would require double-time duration compared to the first purification using dual filtration.

4.9 Purification of GUVs Using an Extra Filtration with Dual Filtration

The effects of the purification of GUVs using an extra filtration with dual filtration as shown in Fig. 4.14. Here, polycarbonate membranes of 12, 10, and 8 μm pores were used in filter

holders 1, 2, and 3, respectively. Fig. 4.14(B) and (C) show the size distribution histograms of GUVs in filter holder 2 and filter holder 3, respectively. The solid line of Fig. 4.14(B) and C corresponds to the fitting with Eq 4.1. These size distributions were very similar to that obtained in dual filtration for case (i) and case (iii) (Figs. 4.1(F), 4.2 (F), 4.5 (D), and 4.6 (D)). The average value and the skewness of the distribution of GUVs in filter holder 2 were $11.5 \mu\text{m}$ and 0.59 , respectively. The corresponding values were $9.1 \mu\text{m}$ and 0.84 under filter holder 3. The average size of GUVs and skewness of distribution under filter holder 2 were $11.2 \pm 0.4 \mu\text{m}$ and 0.82 ± 0.06 , respectively ($n = 2$), while corresponding values were $8.8 \pm 0.2 \mu\text{m}$ and 0.46 ± 0.07 under filter holder 3.

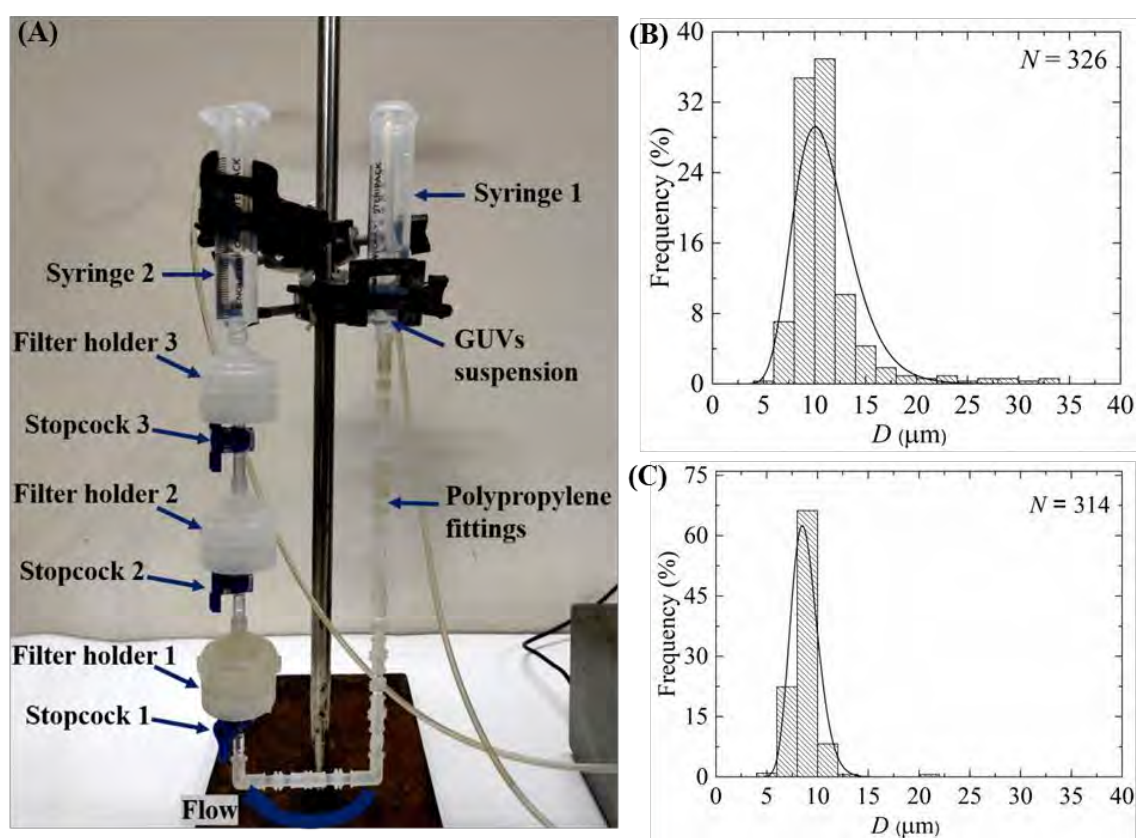


Fig. 4.14 (A) Experimental set-up for the Purification of GUVs using an extra filtration with dual filtration technique. (B) and (C) represent the size distribution histograms of GUVs under filter holders 2 and 3 respectively. The purification was performed at a flow rate of 1 mL/min for 1 h.

When an extra filtration with dual filtration was used, we obtained two different size distributions of GUVs (Fig. 4.14 (B), (C)). One of the main advantages of using these arrangements was that it provided two different size distributions of GUVs at a time in a single purification. However, more experiments are needed to check its performance.

After discussing the above results, we can say that the proposed technique purifies the GUVs by removing the smaller vesicles and water-soluble fluorescent probe (i.e., calcein) from the GUV suspension. It gives a narrower size distribution of GUVs compared to single filtration. In the dual filtration technique, we used three combinations [(case (i), case (ii), and case (iii))] with higher pores of polycarbonate membrane was used in filter holder 1 compared to filter holder 2. Different size distribution of purified GUV suspension was obtained for different combinations of polycarbonate membranes. The flow rate dependent average size of GUVs were investigated and observed that the size of vesicles became slightly higher at flow rate 1.0–2.0 mL/min than 0.75 mL/min (Fig. 4.11). As stated above, GUVs can change their shape at higher pressure [12, 99], and therefore, at flow rate 1.0 mL/min and higher values, some GUVs with diameters greater than the pore sizes were able to pass through. The extrusion-dialysis method [35] was developed for preparing the monodisperse vesicles. This work was similar to the dual filtration technique. In their work, at first, a large pore-sized (i.e., 5 μm diameter pores) polycarbonate membrane was used for extrusion, and then for dialysis smaller pore sized (i.e., 3 μm diameter pores) polycarbonate membrane was used for removing the smaller vesicles. As a result, they obtained an oleate vesicle population between 3–5 μm in diameter. In the same way, POPC vesicles of a range of 0.8–1.0 μm were obtained using a different arrangement of polycarbonate membranes. This method integrated two individual methods; one was extrusion (which was generally used for preparing the large unilamellar vesicles-LUVs) and another was dialysis. In the first step of dialysis, it was taken about 1 h (i.e., 5–6 rounds of 5–10 min each) for removing the dye from the vesicle suspension. In the following step, it was taken about 12 h (i.e., at least 6 rounds of minimum 2 h each) for removing the smaller vesicles. The author reported that the overall duration of the process required ~ 24 h [34]. In their work, they prepared

multilamellar vesicles (MLVs) by extrusion, and therefore, the resulting vesicles in suspension were also multilamellar. In the dual filtration technique, the GUVs were prepared by using the well-known natural swelling method [21], and the target was to get the similar-sized GUVs having a size range higher than that obtained in the extrusion-dialysis method. For example, in the proposed dual filtration technique, using a combination of 12 μm and 10 μm pores in diameter polycarbonate membranes, it was obtained the GUVs with an average size of $\sim 11 \mu\text{m}$. In addition, three different combinations of polycarbonate membranes were used for understanding the performance of purification. In this case, the time duration for purification was about 1 h, while the extrusion-dialysis method required ~ 24 h. Hence, a longer time period is required for getting the purified vesicle suspension in the extrusion-dialysis method, which would be hampered the stability of spherical-shaped vesicles.

The size of an animal cell is 10-30 μm and the size of plant cells is generally 10-100 μm [101]. So, the specific size of GUVs which are considered as the mimic of a biological cell is the most important parameter for the various study regarding GUVs. This dual filtration technique delivered us that specific size of GUVs.

CHAPTER 5

CONCLUSIONS

A dual filtration technique has been developed for the purification of GUVs in which a combination of polycarbonate membranes of different sizes of pores was used. Here, 12, 10, and 8 μm pores of polycarbonate membrane filter papers were used for the purification of GUVs. This technique would effectively provide a specific and narrow range size distribution of GUVs. Three combinations of polycarbonate membrane filter paper were inserted in filter holder 1 and filter 2.

For case (i), 12 μm pores polycarbonate membrane filter paper was used in filter holder 1 and 10 μm pores polycarbonate membrane was used in filter holder 2. For case (ii), in the filter holder 1, 12 μm pores polycarbonate membrane was used and in the filter holder 2, 8 μm pores polycarbonate membrane was used. For case (ii), the polycarbonate membrane of 10 μm pores was used in filter holder 1 and 8 μm pores filter paper was used in filter holder 2. In each case, the higher pores of polycarbonate membrane were utilized in filter holder 1 and the smaller pores of filter paper were in filter holder 2. The average size of the GUVs, the skewness, and the mode under filter holder 1 and 2 was calculated. The size distribution was fitted by the well-known lognormal distribution. The purification was performed at a flow rate of 1 mL/min for 1 h for all three cases.

For several independent experiments of the case (i), i.e., for the combination of 12 and 10 μm polycarbonate pores filter paper, the arithmetic mean of the average values of the distribution were obtained $10.5 \pm 0.8 \mu\text{m}$ for unpurified GUVs, $23.0 \pm 1.5 \mu\text{m}$ for purified GUVs under filter holder 1, and $11.5 \pm 1.0 \mu\text{m}$ for purified GUVs under filter holder 2, where \pm indicates standard deviation. The average values of skewness were obtained 1.73 ± 0.25 for unpurified GUVs, 1.21 ± 0.15 for purified GUVs under filter holder 1 and 0.94 ± 0.60 for purified GUVs under filter holder 2. The average values of mode were obtained $7.3 \pm 0.8 \mu\text{m}$ for unpurified GUVs, $18.7 \pm 0.5 \mu\text{m}$ for purified GUVs under filter holder 1 and $9.9 \pm 0.8 \mu\text{m}$ for purified GUVs under filter holder 2. The asymmetry became less for the samples collected from filter holder 2, i.e., the probability of finding similar size GUVs was

higher. The range of size of GUVs under filter holder 1 was 9.2-45.0 μm and under filter holder 2 was 6.6-26.2 μm . For case (ii), the average size of GUVs under filter holder 2 was $11.5 \pm 0.02 \mu\text{m}$, the average skewness was 1.64 ± 0.6 and the average mode was $8.3 \pm 1.5 \mu\text{m}$, and the size range of GUVs is 4.4-32.4 μm . The average size of GUVs for case (iii) was $9.0 \pm 0.03 \mu\text{m}$, the average value of skewness was 0.81 ± 0.01 , the average value of mode was $8.1 \pm 0.01 \mu\text{m}$, and the size range of GUVs is 4.4-30.7 μm .

Experiment with single filtration (with 12 μm pores polycarbonate membrane) was also performed and compared the average values attained from the experiment with the average values of GUVs collected under filter holder 1 in dual filtration. After performing several independent experiments, the range of size of purified GUVs is obtained 6-59 μm . The average value of GUVs was $12.3 \pm 2.6 \mu\text{m}$, the average value of skewness was 1.65 ± 0.15 and the average value of mode was $8.7 \pm 1.4 \mu\text{m}$ for unpurified GUVs. For purified GUVs, the average value of GUVs was obtained $22.8 \pm 1.3 \mu\text{m}$, and the average value of skewness and mode was 1.21 ± 0.12 and $18.5 \pm 0.5 \mu\text{m}$ respectively.

As expected, the values obtained in single filtration were very similar to those obtained from filter holder 1 in dual filtration since the pore sizes of the filters were the same. It has been seen that the average size of GUVs, skewness, and mode was much higher in single filtration as compared to that obtained in the dual filtration technique.

The developed technique also removed the water-soluble fluorescence probe from the suspension of GUVs. Before purification, the GUV suspension contained a strong green color because of 1 mM calcein. After purification, it has been seen that the suspension becomes colorless, which indicates calcein-free GUV suspension. Thus, we can say that this technique completely eliminates the water-soluble fluorescent probe from the suspension. This purification was performed using 12 μm pores polycarbonate membrane in filter folder 1 and 10 μm pores polycarbonate membrane in filter holder 2. The average size of GUVs and the corresponding skewness was $13.0 \pm 0.5 \mu\text{m}$ and 1.24 ± 0.60 ; which were very similar to that obtained in case (i).

It has been seen that the average size of GUVs increased at least 10% at a flow rate of 1.0–2.0 mL/min than that at 0.75 mL/min. As the average size for 1.0–2.0 mL/min became the same within the experimental error, those flow rates were considered suitable for the

dual filtration technique. By repeating the filtration, one can obtain an even higher number of similar sized GUVs. If the GUV suspension could be purified twice, the probability of obtaining the required sized GUVs became twice.

Extra filtration was also used with this dual filtration technique, i.e., 3 filter holders were used. 12 μm pores polycarbonate membrane was used in filter holder 1, 10 μm pores of polycarbonate membrane was in filter holder 2 and 8 μm pores polycarbonate membrane was in filter holder 3. The average size of GUVs and skewness of distribution under the filter holder 2 were $11.2 \pm 0.4 \mu\text{m}$ and 0.82 ± 0.06 , respectively, while corresponding values were $8.8 \pm 0.2 \mu\text{m}$ and 0.46 ± 0.07 under the filter holder 3. These size distributions were very similar to that obtained in dual filtration for case (i) and case (iii). Thus, two different size distributions can be obtained from a single experiment at a time.

This novel purification technique is successfully developed and validated. It might be a promising tool for getting similar-sized vesicles which will be useful in various experiments.

REFERENCES

- [1] Murate, M., Kobayashi, T., "Revisiting transbilayer distribution of lipids in the plasma membrane," *Chem. Phys. Lipids*, vol. 194, pp. 58-71, 2016.
- [2] Ohvo-Rekilä, H., Ramstedt, B., Leppimäki, P., Slotte, J. P., "Cholesterol interactions with phospholipids in membranes," *Prog. Lipid Res.*, vol. 41(1), pp. 66-97, 2002.
- [3] Pautot, S., Frisken, B. J., Weitz, D. A., "Production of unilamellar vesicles using an inverted emulsion," *Langmuir*, vol. 19(7), pp. 2870-2879, 2003.
- [4] Spector, A. A., Yorek, M. A., "Membrane lipid composition and cellular function," *J. Lipid Res.*, vol. 26(9), pp. 1015-1035, 1985.
- [5] Divecha, N., Irvine, R. F., "Phospholipid signaling," *Cell*, vol. 80(2), pp. 269-278, 1995.
- [6] Lingwood, D., and Simons, K., "Lipid rafts as a membrane-organizing principle," *Science*, vol. 327(5961), pp. 46-50, 2010.
- [7] Rosoff, V. M., "Vesicles", Surfactant Science Series, vol. 62, Marcel Dekker, New York, 1996.
- [8] Lian, T., Ho, R. J., "Trends and developments in liposome drug delivery systems," *J. Pharma. Sci.*, vol. 90(6), pp. 667-680, 2001.
- [9] Malam, Y., Loizidou, M., Seifalian, A. M., "Liposomes and nanoparticles: nanosized vehicles for drug delivery in cancer," *Trends Pharma. Sci.*, vol. 30(11), pp. 592-599, 2009.
- [10] Allen, T. M., Cullis, P. R., "Liposomal drug delivery systems: from concept to clinical applications," *Adv. Drug Deliv. Rev.*, vol. 65(1), pp. 36-48, 2013.
- [11] Evans, E., Smith, B. A., "Kinetics of hole nucleation in biomembrane rupture," *New J. Phys.*, vol. 13(9), pp. 095010, 2011.
- [12] Yamashita, Y., Masum, S. M., Tanaka, T., Yamazaki, M., "Shape changes of giant unilamellar vesicles of phosphatidylcholine induced by a de novo designed peptide interacting with their membrane interface," *Langmuir*, vol. 18(25), pp. 9638-9641, 2002.

- [13] Yu, Y., Granick, S., "Pearling of lipid vesicles induced by nanoparticles," *J. Am. Chem. Soc.*, vol. 131(40), pp. 14158-14159, 2009.
- [14] Shigematsu, T., Koshiyama, K., Wada, S., "Effects of stretching speed on mechanical rupture of phospholipid/cholesterol bilayers: molecular dynamics simulation," *Sci. Rep.*, vol. 5(1), pp. 1-10, 2015.
- [15] Karal, M. A. S., Ahamed, M. K., Rahman, M., Ahmed, M., Shakil, M. M., Rabbani, K. S., "Effects of electrically-induced constant tension on giant unilamellar vesicles using irreversible electroporation," *Eur. Biophys. J.*, vol. 48(8), pp. 731-741, 2019.
- [16] Dhand, R., "New frontiers in aerosol delivery during mechanical ventilation," *Respiratory care*, vol. 49(6), pp. 667, 2004.
- [17] Edwards, D. A., Ben-Jebria, A., Langer, R., "Recent advances in pulmonary drug delivery using large, porous inhaled particles," *J. App. Physiol.*, vol. 85(2), pp. 379-385, 1998.
- [18] Verschraegen, C. F., Gilbert, B. E., Loyer, E., Huaringa, A., Walsh, G., Newman, R. A., Knight, V., "Clinical evaluation of the delivery and safety of aerosolized liposomal 9-nitro-20 (s)-camptothecin in patients with advanced pulmonary malignancies," *Clin. Cancer Res.*, vol. 10(7), pp. 2319-2326, 2004.
- [19] Islam, M. Z., Alam, J. M., Tamba, Y., Karal, M. A. S., Yamazaki, M., "The single GUV method for revealing the functions of antimicrobial, pore-forming toxin, and cell-penetrating peptides or proteins," *Phys. Chem. Chem. Phys.*, vol. 16(30), pp. 15752-15767, 2014.
- [20] Karal, M. A. S., Ahammed, S., Levadny, V., Belaya, M., Ahamed, M. K., Ahmed, M., Mahbub, Z. B., Ullah, A. A., "Deformation and poration of giant unilamellar vesicles induced by anionic nanoparticles," *Chem. Phys. Lipids*, vol. 230, pp. 104916, 2020.
- [21] Reeves, J. P., Dowben, R. M., "Formation and properties of thin-walled phospholipid vesicles," *J. Cell. Physiol.*, vol. 73(1), pp. 49-60, 1969.
- [22] Angelova, M. I., Dimitrov, D. S., "Liposome electroformation," *Faraday Dis. Chem. Soc.*, vol. 81, pp. 303-311, 1986.
- [23] Sugiura, S., Kuroiwa, T., Kagota, T., Nakajima, M., Sato, S., Mukataka, S., Walde, P., Ichikawa, S., "Novel method for obtaining homogeneous giant vesicles from a

- monodisperse water-in-oil emulsion prepared with a microfluidic device,” *Langmuir*, vol. 24(9), pp. 4581-4588, 2008.
- [24] Oku, N., MacDonald, R. C., “Differential effects of alkali metal chlorides on formation of giant liposomes by freezing and thawing and by dialysis,” *Biochemistry*, vol. 22(4), pp. 855-863, 1983.
- [25] Shum, H. C., Lee, D., Yoon, I., Kodger, T., Weitz, D. A., “Double emulsion templated monodisperse phospholipid vesicles,” *Langmuir*, vol. 24(15), pp. 7651-7653, 2008.
- [26] Suzuki, H., Tabata, K. V., Noji, H., Takeuchi, S., “Highly reproducible method of planar lipid bilayer reconstitution in polymethyl methacrylate microfluidic chip,” *Langmuir*, vol. 22(4), pp. 1937-1942, 2006.
- [27] Walde, P., Cosentino, K., Engel, H., Stano, P., “Giant vesicles: preparations and applications,” *ChemBioChem*, vol. 11(7), pp. 848-865, 2010.
- [28] Tamba, Y., & Yamazaki, M., “Single giant unilamellar vesicle method reveals effect of antimicrobial peptide magainin 2 on membrane permeability,” *Biochemistry*, vol. 44(48), pp. 15823-15833, 2005.
- [29] Tamba, Y., Terashima, H., Yamazaki, M., “A membrane filtering method for the purification of giant unilamellar vesicles,” *Chem. Phys. Lipids*, vol. 164(5), pp. 351-358, 2011.
- [30] Tamba, Y., Yamazaki, M., “Magainin 2-induced pore formation in the lipid membranes depends on its concentration in the membrane interface,” *J. Phys. Chem. B*, vol. 113(14), pp. 4846-4852, 2009.
- [31] Baker R. W., *Membrane technology and applications*. New York: McGraw-Hill; 2000.
- [32] Fanti, A., Gammuto, L., Mavelli, F., Stano, P., Marangoni, R., “Do protocells preferentially retain macromolecular solutes upon division/fragmentation? A study based on the extrusion of POPC giant vesicles,” *Integr. Bio.*, vol. 10(1), pp. 6-17, 2018.
- [33] Fayolle, D., Fiore, M., Stano, P., Strazewski, P. “Rapid purification of giant lipid vesicles by microfiltration,” *Plos One*, vol. 13(2), pp. e0192975, 2018.
- [34] Karal, M. A. S., Rahman, M., Ahamed, M. K., Shibly, S. U. A., Ahmed, M., Shakil,

- M. M., "Low cost non-electromechanical technique for the purification of giant unilamellar vesicles," *Eur. Biophys. J.*, vol. 48(4), pp. 349-359, 2019.
- [35] Zhu, T. F., Szostak, J. W., "Preparation of large monodisperse vesicles," *Plos One*, vol. 4(4), pp. e5009, 2009.
- [36] Klymchenko, A. S., Oncul, S., Didier, P., Schaub, E., Bagatolli, L., Duportail, G., Mély, Y., "Visualization of lipid domains in giant unilamellar vesicles using an environment-sensitive membrane probe based on 3-hydroxyflavone," *Biochim. Biophys. Acta. (BBA)-Biomembranes*, vol. 1788(2), pp. 495-499, 2009.
- [37] Gudheti, M. V., Mlodzianoski, M., Hess, S. T., "Imaging and shape analysis of GUVs as model plasma membranes: effect of trans DOPC on membrane properties," *Biophys. J.*, vol. 93(6), pp. 2011-2023, 2007.
- [38] Portet, T., Febrer, F. C., Escoffre, J. M., Favard, C., Rols, M. P., Dean, D. S., "Visualization of membrane loss during the shrinkage of giant vesicles under electropulsation," *Biophys. J.*, vol. 96(10), pp. 4109-4121, 2009.
- [39] Tamba, Y., Ariyama, H., Levadny, V., Yamazaki, M., "Kinetic pathway of antimicrobial peptide magainin 2-induced pore formation in lipid membranes," *J. Phys. Chem. B*, vol. 114(37), pp. 12018-12026, 2010.
- [40] Yamazaki, M., "The single GUV method to reveal elementary processes of leakage of internal contents from liposomes induced by antimicrobial substances," *Advances in Planar Lipid Bilayers and Liposomes*, vol. 7, pp. 121-142, 2008.
- [41] Ahamed, M. K., Karal, M. A. S., Ahmed, M., Ahammed, S., "Kinetics of irreversible pore formation under constant electrical tension in giant unilamellar vesicles," *Eur. Biophys. J.*, vol. 49(5), pp. 371-381, 2020.
- [42] Tanaka, T., Sano, R., Yamashita, Y., Yamazaki, M., "Shape changes and vesicle fission of giant unilamellar vesicles of liquid-ordered phase membrane induced by lysophosphatidylcholine," *Langmuir*, vol. 20(22), pp. 9526-9534, 2004.
- [43] Yu, Y., Vroman, J. A., Bae, S. C., Granick, S., "Vesicle budding induced by a pore-forming peptide," *J. Am. Chem. Soc.*, vol. 132(1), pp. 195-201, 2010.
- [44] Rawicz, W., Olbrich, K. C., McIntosh, T., Needham, D., Evans, E., "Effect of chain length and unsaturation on elasticity of lipid bilayers," *Biophys. J.*, vol. 79(1), pp. 328-339, 2000.

- [45] Karal, M. A. S., Yamazaki, M., "Communication: Activation energy of tension-induced pore formation in lipid membranes," *J. Chem. Phys.*, vol. 143(8), 08B402_1, 2015.
- [46] Baumgart, T., Hess, S. T., Webb, W. W., "Imaging coexisting fluid domains in biomembrane models coupling curvature and line tension," *Nature*, vol. 425(6960), pp. 821-824, 2003.
- [47] Nomura, S. I. M., Tsumoto, K., Hamada, T., Akiyoshi, K., Nakatani, Y., Yoshikawa, K., "Gene expression within cell-sized lipid vesicles," *ChemBioChem*, vol. 4(11), pp. 1172-1175, 2003.
- [48] Tsumoto, K., Matsuo, H., Tomita, M., Yoshimura, T., "Efficient formation of giant liposomes through the gentle hydration of phosphatidylcholine films doped with sugar," *Coll. Surf. B: Biointerf.*, vol. 68(1), pp. 98-105, 2009.
- [49] Hishida, M., Seto, H., Yamada, N. L., Yoshikawa, K., "Hydration process of multi-stacked phospholipid bilayers to form giant vesicles," *Chem. Phys. Lett.*, vol. 455(4-6), pp. 297-302, 2008.
- [50] Shimanouchi, T., Umakoshi, H., Kuboi, R., "Kinetic study on giant vesicle formation with electroformation method," *Langmuir*, vol. 25(9), pp. 4835-4840, 2009.
- [51] Pott, T., Bouvrais, H., Méléard, P., "Giant unilamellar vesicle formation under physiologically relevant conditions," *Chem. Phys. Lipids*, vol. 154(2), pp. 115-119, 2008.
- [52] Mertins, O., da Silveira, N. P., Pohlmann, A. R., Schröder, A. P., Marques, C. M., "Electroformation of giant vesicles from an inverse phase precursor," *Biophys. J.*, vol. 96(7), pp. 2719-2726, 2009.
- [53] Vitkova, V., Mader, M., Podgorski, T., "Deformation of vesicles flowing through capillaries," *EPL (Europhys. Letters)*, vol. 68(3), pp. 398, 2004.
- [54] García-Sáez, A. J., Schwille, P., "Fluorescence correlation spectroscopy for the study of membrane dynamics and protein/lipid interactions," *Methods*, vol. 46(2), pp. 116-122, 2008.
- [55] Ariola, F. S., Li, Z., Cornejo, C., Bittman, R., Heikal, A. A., "Membrane fluidity and lipid order in ternary giant unilamellar vesicles using a new bodipy-cholesterol

- derivative,” *Biophys. J.*, vol. 96(7), pp. 2696-2708, 2009.
- [56] Tan, Y. C., Hettiarachchi, K., Siu, M., Pan, Y. R., Lee, A.P., “Controlled microfluidic encapsulation of cells, proteins, and microbeads in lipid vesicles,” *J. Am. Chem. Soc.*, vol. 128(17), pp. 5656-5658, 2006.
- [57] Chiu, H. C., Lin, Y.W., Huang, Y. F., Chuang, C. K., Chern, C. S., “Polymer vesicles containing small vesicles within interior aqueous compartments and pH-responsive transmembrane channels,” *Angewandte Chemie Int. Ed.*, vol. 47(10), pp. 1875-1878, 2008.
- [58] Morigaki, K., Walde, P., “Giant vesicle formation from oleic acid/sodium oleate on glass surfaces induced by adsorbed hydrocarbon molecules,” *Langmuir*, vol. 18(26), pp. 10509-10511, 2002.
- [59] Funakoshi, K., Suzuki, H., Takeuchi, S., “Formation of giant lipid vesiclelike compartments from a planar lipid membrane by a pulsed jet flow,” *J. Am. Chem. Soc.*, vol. 129(42), pp. 12608-12609, 2007.
- [60] Walde, P., *Encyclopedia of nanoscience and nanotechnology*, vol. 1, A-Ch. American Scientific publishers, pp. 43-79, 2004.
- [61] Schubert, R., “Liposome Preparation by Detergent Removal,” *Methods Enzymol.*, vol. 367, pp. 46-70, 2003.
- [62] Moscho, A., Orwar, O., Chiu, D. T., Modi, B. P., Zare, R. N., “Rapid preparation of giant unilamellar vesicles,” *PNAS*, vol. 93(21), pp. 11443-11447, 1996.
- [63] Kulin, S., Kishore, R., Helmerson, K., Locascio, L., “Optical manipulation and fusion of liposomes as microreactors,” *Langmuir*, vol. 19(20), pp. 8206-8210, 2003.
- [64] Johnson, N. L., Kotz, S., Balakrishnan, N., “*Continuous univariate distributions volume 2*,” vol. 289, John Wiley & sons, 1995.
- [65] Ahmed, M., Karal, M. A. S., Ahamed, M. K., Ullah, M. S., “Analysis of purification of charged giant vesicles in a buffer using their size distribution,” *Eur. Physical J. E*, vol. 44(4), pp. 1-8, 2021.
- [66] Johnson, N. L., Kotz, S. I., Balakrishnan, N., “Beta distributions,” *Continuous univariate distributions*. 2nd ed. New York, NY: John Wiley and Sons, pp. 221-235, 1994.
- [67] Olson, F., Hunt, C. A., Szoka, F. C., Vail, W. J., Papahadjopoulos, D., “Preparation

- of liposomes of defined size distribution by extrusion through polycarbonate membranes,” *Biochim. Biophys. Acta. (BBA)-Biomembranes*, vol. 557(1), 9-23, 1979.
- [68] Al-Kattan, A., Dufour, P., Drouet, C., “Purification of biomimetic apatite-based hybrid colloids intended for biomedical applications: A dialysis study,” *Coll. Surf. B: Biointerf.*, vol. 82(2), pp. 378-384, 2011.
- [69] Rubenstein, J. L., Fine, R. E., Luskey, B. D., Rothman, J. E., “Purification of coated vesicles by agarose gel electrophoresis,” *J. cell Bio.*, vol. 89(2), pp. 357-361, 1981.
- [70] Blitz, A. L., Fine, R. E., Toselli, P. A., “Evidence that coated vesicles isolated from brain are calcium-sequestering organelles resembling sarcoplasmic reticulum,” *J. Cell Bio.*, vol. 75(1), pp. 135-147, 1977.
- [71] Shimanouchi, T., Walde, P., Gardiner, J., Mahajan, Y. R., Seebach, D., Thoma, A., Kramer, S. D., Voser, M., Kuboi, R., “Permeation of a β -heptapeptide derivative across phospholipid bilayers,” *Biochim. Biophys. Acta. (BBA)-Biomembranes*, vol. 1768(11), pp. 2726-2736, 2007.
- [72] Peterlin, P., Arrigler, V., Kogej, K., Svetina, S., Walde, P., “Growth and shape transformations of giant phospholipid vesicles upon interaction with an aqueous oleic acid suspension,” *Chem. Phys. Lipids*, vol. 159(2), pp. 67-76, 2009.
- [73] Riske, K. A., Sudbrack, T. P., Archilha, N. L., Uchoa, A. F., Schroder, A. P., Marques, C. M., Baptista, M. S., Itri, R., “Giant vesicles under oxidative stress induced by a membrane-anchored photosensitizer,” *Biophys. J.*, vol. 97(5), pp. 1362-1370, 2009.
- [74] Ramundo-Orlando, A., Longo, G., Cappelli, M., Girasole, M., Tarricone, L., Beneduci, A., Massa, R., “The response of giant phospholipid vesicles to millimeter waves radiation,” *Biochim. Biophys. Acta. (BBA)-Biomembranes*, vol. 1788(7), pp. 1497-1507, 2009.
- [75] Mally, M., Majhenc, J., Svetina, S., Žekš, B., “Mechanisms of equinatoxin II-induced transport through the membrane of a giant phospholipid vesicle,” *Biophys. J.*, vol. 83(2), pp. 944-953, 2002.
- [76] Ewers, H., Römer, W., Smith, A. E., Bacia, K., Dmitrieff, S., Chai, W., Mancini, R., Kartenbeck, J., Chambon, V., Berland, L., Oppenheim, A., Schwarzmann, G.,

- Feizi, T., Schwille, P., Sens, P., Helenius, A., Johannes, L., "GM1 structure determines SV40-induced membrane invagination and infection," *Nat. Cell Bio.*, vol. 12(1), pp. 11-18, 2010.
- [77] Claessens, M. M. A. E., Leermakers, F. A. M., Hoekstra, F. A., Stuart, M. C., "Osmotic shrinkage and reswelling of giant vesicles composed of dioleoylphosphatidylglycerol and cholesterol," *Biochim. Biophys. Acta. (BBA)-Biomembranes*, vol. 1778(4), pp. 890-895, 2008.
- [78] Chaize, B., Nguyen, M., Ruyschaert, T., le Berre, V., Trévisiol, E., Caminade, A.M., Majoral, J. P., Pratviel, G., Meunier, B., Winterhalter, M., Fournier, D., "Microstructured liposome array," *Bioconjugate Chem*, vol. 17(1), pp. 245-247, 2006.
- [79] Kalyankar, N. D., Sharma, M. K., Vaidya, S. V., Calhoun, D., Maldarelli, C., Couzis, A., Gilchrist, L., "Arraying of intact liposomes into chemically functionalized microwells," *Langmuir*, pp. 22(12), pp. 5403-5411, 2006.
- [80] Zhao, J., Jedlicka, S. S., Lannu, J. D., Bhunia, A. K., Rickus, J. L., "Liposome-Doped Nanocomposites as Artificial-Cell-Based Biosensors: Detection of Listeriolysin O," *Biotechnol. Prog.*, vol. 22(1), pp. 32-37, 2006.
- [81] Kim, H. J., Bennetto, H. P., Halablab, M. A., Choi, C., Yoon, S., "Performance of an electrochemical sensor with different types of liposomal mediators for the detection of hemolytic bacteria," *Sen. Actuat. B: Chem.*, vol. 119(1), pp. 143-149, 2006.
- [82] Zepik, H. H., Walde, P., Kostoryz, E. L., Code, J., Yourtee, D. M., "Lipid vesicles as membrane models for toxicological assessment of xenobiotics," *Crit. Rev. Toxicol.*, vol. 38(1), pp. 1-11, 2008.
- [83] Cans, A. S., Andes-Koback, M., Keating, C. D., "Positioning lipid membrane domains in giant vesicles by micro-organization of aqueous cytoplasm mimic," *J. Am. Chem. Soc.*, vol. 130(23), pp. 7400-7406, 2008.
- [84] Khalifat, N., Puff, N., Bonneau, S., Fournier, J. B., Angelova, M. I., "Membrane deformation under local pH gradient: mimicking mitochondrial cristae dynamics," *Biophys. J.*, vol. 95(10), pp. 4924-4933, 2008.
- [85] Merkle, D., Kahya, N., Schwille, P., "Reconstitution and anchoring of cytoskeleton

- inside giant unilamellar vesicles,” *ChemBioChem*, vol. 9(16), pp. 2673-2681, 2008.
- [86] Long, M. S., Jones, C. D., Helfrich, M. R., Mangeney-Slavin, L. K., Keating, C. D., “Dynamic microcompartmentation in synthetic cells,” *PNAS*, vol. 102(17), pp. 5920-5925, 2005.
- [87] Girard, P., Pécréaux, J., Lenoir, G., Falson, P., Rigaud, J. L., Bassereau, P., “A new method for the reconstitution of membrane proteins into giant unilamellar vesicles,” *Biophys. J.*, vol. 87(1), pp. 419-429, 2004.
- [88] Cans, A. S., Wittenberg, N., Karlsson, R., Sombers, L., Karlsson, M., Orwar, O., Ewing, A., “Artificial cells: unique insights into exocytosis using liposomes and lipid nanotubes,” *PNAS*, vol. 100(2), pp. 400-404, 2003.
- [89] Karlsson, A., Karlsson, R., Karlsson, M., Cans, A. S., Strömberg, A., Ryttsén, F., Orwar, O., “Networks of nanotubes and containers,” *Nature*, vol. 409(6817), pp. 150-152, 2001.
- [90] Holopainen, J. M., Angelova, M. I., Kinnunen, P. K., “Vectorial budding of vesicles by asymmetrical enzymatic formation of ceramide in giant liposomes,” *Biophys. J.*, vol. 78(2), pp. 830-838, 2000.
- [91] Chiu, D. T., Wilson, C. F., Ryttsén, F., Strömberg, A., Farre, C., Karlsson, A., Nordholm, S., Gaggar, A., Modi, B. P., Moscho, A., Garza-Lopez, R. A., Orwar, O., Zare, R.N., “Chemical transformations in individual ultrasmall biomimetic containers,” *Science*, vol. 283(5409), pp. 1892-1895, 1999.
- [92] Hsin, T. M., Yeung, E. S., “Single-Molecule Reactions in Liposomes,” *Angewandte Chemie Int. Ed.*, vol. 46(42), pp. 8032-8035, 2007.
- [93] Nič, M., Jirát, J., Košata, B., Jenkins, A., McNaught, A., “IUPAC compendium of chemical terminology,” *IUPAC, Research Triangle Park, NC*, 2009.
- [94] Kagan, B. L., Selsted, M. E., Ganz, T., Lehrer, R. I., “Antimicrobial defensin peptides form voltage-dependent ion-permeable channels in planar lipid bilayer membranes,” *PNAS*, vol. 87(1), pp. 210-214, 1990.
- [95] R. Gibrat, "Une loi des reparations economiques: l'effect proportionnel" *Bull. Statist. Gen. Fr.*19, pp. 469, 1930.
- [96] Mitzenmacher, M., "A Brief History of Generative Models for Power Law and Lognormal Distributions", *Internet Math.* 1, pp. 226–251, 2004.

- [97] Leipnik, R. B. "On lognormal random variables: I-the characteristic function," *J. Aust. Math. Soc. Ser. B Appl. Math.*, vol. 32, pp. 327–347, 1991.
- [98] Karal, M. A. S., Ahmed, M., Levadny, V., Belaya, M., Ahamed, M. K., Rahman, M., Shakil, M. M., "Electrostatic interaction effects on the size distribution of self-assembled giant unilamellar vesicles," *Phys. Rev. E*, vol. 101(1), pp. 012404, 2020.
- [99] Tanaka, T., Tamba, Y., Masum, S. M., Yamashita, Y., Yamazaki, M., "La³⁺ and Gd³⁺ induce shape change of giant unilamellar vesicles of phosphatidylcholine," *Biochim. Biophys. Acta. (BBA)-Biomembranes*, vol. 1564(1), pp. 173-182, 2002.
- [100] Yoshida, N., Tamura, M., Kinjo, M., "Fluorescence correlation spectroscopy: a new tool for probing the microenvironment of the internal space of organelles," *Single Molecules*, vol. 1(4), pp. 279-283, 2000.
- [101] Rideau, E., Dimova, R., Schwille, P., Wurm, F. R., & Landfester, K., "Liposomes and polymersomes: a comparative review towards cell mimicking," *Chem. Soc. Rev.*, vol. 47(23), pp. 8572-8610, 2018.

APPENDIX

PUBLICATIONS

Published Journal:

A new purification technique to obtain specific size distribution of giant lipid vesicles using dual filtration

Authors (Joint first author): Mohammad Abu Sayem Karal, **Tawfika Nasrin**, Marzuk Ahmed, Md. Kabir Ahamed, Shareef Ahammed, Salma Akter, Sharif Hasan, Zaid Bin Mahbub.

Journal: *PLOS ONE*, vol. 16(7), e2054930, 2021 (I. F. 3.24, Q1 Ranked)

Conference Presentations:

1. Tawfika Nasrin, Salma Akter, Shareef Ahammed, Marzuk Ahmed, Md. Kabir Ahamed, and Mohammad Abu Sayem Karal; Dual Filtration in Purification Controls the Size Distribution of Giant Vesicles (SMM-06), 6th Conference (Virtual) of BAC, Dhaka, Bangladesh, 15-16 January, 2021, (Oral Presentation), page. 107.

2. Tawfika Nasrin and Mohammad Abu Sayem Karal: A New Purification Technique to Obtain Specific Size Distribution of Giant Lipid Vesicles Using Dual Filtration (MP-06), National Conference on Physics, Virtual, Organized by BPS, Dhaka, Bangladesh, 06-07 August, 2021 (Oral Presentation), Zoom Online Platform.

RESEARCH ARTICLE

A new purification technique to obtain specific size distribution of giant lipid vesicles using dual filtration

Mohammad Abu Sayem Karal^{1*}, Tawfika Nasrin¹, Marzuk Ahmed¹, Md. Kabir Ahamed¹, Shareef Ahammed¹, Salma Akter¹, Sharif Hasan¹, Zaid Bin Mahbub²

1 Department of Physics, Bangladesh University of Engineering and Technology, Dhaka, Bangladesh, **2** Department of Mathematics and Physics, North South University, Dhaka, Bangladesh

* These authors contributed equally to this work.

* asayem221@phy.buet.ac.bd



OPEN ACCESS

Citation: Karal MAS, Nasrin T, Ahmed M, Ahamed M.K, Ahammed S, Akter S, et al. (2021) A new purification technique to obtain specific size distribution of giant lipid vesicles using dual filtration. PLoS ONE 16(7): e0254930. <https://doi.org/10.1371/journal.pone.0254930>

Editor: Ghulam Md Ashraf, King Abdulaziz University, SAUDI ARABIA

Received: May 19, 2021

Accepted: July 7, 2021

Published: July 29, 2021

Copyright: © 2021 Karal et al. This is an open access article distributed under the terms of the [Creative Commons Attribution License](https://creativecommons.org/licenses/by/4.0/), which permits unrestricted use, distribution, and reproduction in any medium, provided the original author and source are credited.

Data Availability Statement: All relevant data are within the paper.

Funding: This study was supported by the Ministry of Science and Technology, Bangladesh (No. 39.00.0000.009.06.024.19-12), Ministry of Education, Bangladesh (No. 37.20.0000.004.033.020.2016), Information and Communication Technology Division (ICTD), Ministry of Posts, Telecommunications and Information Technology, Bangladesh (No. 56.00.0000.028.33.105.18-05), and Committee for

Abstract

A new purification technique is developed for obtaining distribution of giant unilamellar vesicles (GUVs) within a specific range of sizes using dual filtration. The GUVs were prepared using well known natural swelling method. For filtration, different combinations of polycarbonate membranes were implemented in filter holders. In our experiment, the combinations of membranes were selected with corresponding pore sizes—(i) 12 and 10 μm , (ii) 12 and 8 μm , and (iii) 10 and 8 μm . By these filtration arrangements, obtained GUVs size distribution were in the ranges of 6–26 μm , 5–38 μm and 5–30 μm , respectively. In comparison, the size distribution range was much higher for single filtration technique, for example, 6–59 μm GUVs found for a membrane with 12 μm pores. Using this technique, the water-soluble fluorescent probe, calcein, can be removed from the suspension of GUVs successfully. The size distributions were analyzed with lognormal distribution. The skewness became smaller (narrow size distribution) when a dual filtration was used instead of single filtration. The mode of the size distribution obtained in dual filtration was also smaller to that of single filtration. By continuing this process of purification for a second time, the GUVs size distribution became even narrower. After using an extra filtration with dual filtration, two different size distributions of GUVs were obtained at a time. This experimental observation suggests that different size specific distributions of GUVs can be obtained easily, even if GUVs are prepared by different other methods.

1. Introduction

Vesicles are model of cells, which are used for studying the function of complex biomembranes [1]. These vesicles are considered as a promising tool for their wide range of industrial and medical applications [2–4]. The cell size vesicles such as giant unilamellar vesicles (GUVs) have been widely used to investigate the elasticity of membranes [5], deformation [6, 7] and poration [8, 9] of vesicles. Although intravenous drug delivery generally uses vesicles with sizes